Spinal Cord Grey Matter Pathology in Multiple Sclerosis

Thesis submitted to the University of Nottingham

For the degree of Doctorate of Medicine

June 2008 by

Christopher Patrick Gilmore

BMedSci, BMBS, MRCP (UK)

Table of Contents

Figures and Tables

Abstract

Background:

Traditionally, Multiple Sclerosis (MS) has been considered to be a predominantly white matter (WM) disease. More recent studies have revealed considerable grey matter (GM) involvement in the brain. However there is a paucity of literature examining GM pathology in the spinal cord.

Objectives and methods:

We use human post-mortem material to explore various aspects of spinal cord GM pathology in MS including (i) the extent and pattern of spinal cord demyelination, (ii) the relative contributions of GM and WM volume loss to spinal cord atrophy, (iii) the extent of neuronal pathology within the spinal cord and (iv) the sensitivity of post-mortem MRI for detecting spinal cord GM plaques.

Results:

Within the spinal cord, GM demyelination is more extensive than WM demyelination with many lesions showing a novel morphological pattern whereby the plaque borders maintain a strict respect for the GM/WM boundary. Demyelination is more extensive in the spinal cord GM than in other brain regions examined. Post-mortem MR imaging at 4.7 Tesla is highly sensitive for detecting the spinal cord GM plaques.

We demonstrate substantial neuronal loss in the spinal cord in MS, observing reductions in both interneuron and motoneuron numbers. This neuronal loss occurs predominantly within GM plaques. We also observe reductions in interneuron size, both within plaques and in the myelinated GM. Despite this, we find no evidence of spinal cord GM atrophy.

Conclusions:

This study represents the first detailed examination of spinal cord GM involvement in MS. We demonstrate substantial GM pathology in the spinal cord, further challenging the concept that MS is a predominantly WM disease. A greater understanding of this pathology may provide important insights into MS pathogenesis and mechanisms of disability in the disease.

Publications and presentations related to thesis

Publications

Regional variations in the extent and pattern of grey matter demyelination in Multiple Sclerosis: a comparison between the cerebral cortex, cerebellar cortex, deep grey matter nuclei and the spinal cord

Gilmore CP, Donaldson I, Bö L, Owens T, Lowe J, and Evangelou N

Accepted for publication, JNNP 2008

Spinal cord gray matter demyelination in multiple sclerosis-a novel pattern of residual plaque morphology

Gilmore CP, Bö L, Owens T, Lowe J, Esiri MM and Evangelou N

Brain Pathol. 2006 Jul;16(3):202-8

Spinal cord atrophy in multiple sclerosis due to white matter volume loss

Gilmore CP, DeLuca GC, Bö L, Owens T, Lowe J, Esiri MM and Evangelou N

Original Contribution, Archives of Neurology, 2005; 62: 1859-1862

Prizes

Spinal cord grey matter is a predilection site for demyelination in Multiple Sclerosis

Gilmore CP, Bö L, Owens T, Lowe J, Esiri MM and Evangelou N

ABN Spring Meeting, Brighton, 20th April 2006 - Charles Symonds Prize for best platform presentation by a trainee

Spinal cord grey matter demyelination in multiple sclerosis

Gilmore CP, Bö L, Owens T, Lowe J, Esiri MM and Evangelou N

Institute of Neurology Annual Poster Event, University of Nottingham, 2nd November 2005 - Postgraduate poster prize winner

4.7 Tesla MRI is highly sensitive for detecting spinal cord grey matter demyelination in MS
Gilmore CP, Geurts JJG, Evangelou N, Bot JCJ, van Schijndel RA, Pouwels PJW, Barkhof F and Bö L
European Committee for Treatment and Research in Multiple Sclerosis (ECTRIMS), Thessaloniki, Greece, 1st October 2005 - Platform presentation as 4th place in poster prize competition

Spinal cord atrophy in multiple sclerosis is due to white matter volume loss
Gilmore CP, DeLuca GC, Bö L, Owens T, Lowe J, Esiri MM, Evangelou N
Platform presentation as 2nd place in poster prize competition
MS Society Annual Meeting, 26th May 2005, Heriot Watt, Edinburgh

Spinal cord atrophy in multiple sclerosis: relative contributions of white matter and grey matter tissue loss
Gilmore CP, DeLuca GC, Bö L, Owens T, Lowe J, Esiri MM and Evangelou N
Institute of Neurology Annual Poster Event, University of Nottingham, November 3rd 2004 – Postgraduate poster prize winner

Other Platform Presentations

Evidence of substantial spinal cord neuronal pathology in multiple sclerosis
Gilmore CP, Bö L, Owens T, DeLuca GC, Lowe J, Esiri MM, Evangelou N
ECTRIMS, Madrid, 27th September 2006

Spinal cord atrophy in multiple sclerosis is due to white matter volume loss
Gilmore CP, DeLuca GC, Bö L, Owens T, Lowe J, Esiri MM, Evangelou N
ABN Spring Meeting Queens University, Belfast, 1st April 2005

Spinal cord atrophy: it's all in the white matter
Gilmore CP, DeLuca GC, Bö L, Owens T, Lowe J, Esiri MM, Evangelou N
ECTRIMS, Vienna, 9th October 2004

Other Oral Presentations

Spinal cord grey matter pathology in Multiple Sclerosis

Department of Neuroinflammation Seminar Series, Thursday 14th September. Invited talk, Gilliat Lecture Theatre, Institute of Neurology, Queen's Square, 14th September 2006

Grey matter pathology in Multiple Sclerosis

Institute of Neuroscience Neuroprotection and Neurodegeneration Research Meeting, University of Nottingham, 5th May 2006

Poster Presentations

Spinal cord neuronal pathology in Multiple Sclerosis

Gilmore CP, Bö L, Owens T, DeLuca GC, Lowe J, Esiri MM, Evangelou N

Presented at

- ABN Autumn Meeting, London, 5th October 2006

AND

- Institute of Neurology Annual Poster Event, University of Nottingham, 15th November 2005

Regional variation in the extent and pattern of grey matter demyelination in multiple sclerosis: a pathological comparison between the cerebral cortex, cerebellar cortex, thalamus and spinal cord

Gilmore CP, Donaldson I, Bö L, Owens T, Lowe J, Evangelou N

Presented at

- ECTRIMS, Madrid, 27th September 2006

AND

- Institute of Neurology Annual Poster Event , University of Nottingham, 15th November 2005

AND

- ABN Spring Meeting, Homerton College, Cambridge, 13th April 2007

Spinal cord gray matter is a predilection site for demyelination in multiple sclerosis
Gilmore CP, Bö L, Owens T, Lowe J, Esiri MM and Evangelou N
American Academy of Neurology, San Diego, April 2006

Spinal cord grey matter demyelination in multiple sclerosis
Gilmore CP, Bö L, Owens T, Lowe J, Esiri MM and Evangelou N
ECTRIMS, Thessaloniki, Greece. September 2005

4.7 Tesla MRI is highly sensitive for detecting spinal cord grey matter demyelination in MS
Gilmore CP, Geurts JJG, Evangelou N, Bot JCJ, van Schijndel RA, Pouwels PJW, Barkhof F and Bö L
ABN Autumn Meeting, Torquay, September 2005

Abbreviations

AChE	Acetylcholinesterase
BBB	Blood Brain Barrier
ChAT	Choline Acetyltransferase
CNP	2'3'-cyclic nucleotide 3'-phosphodiesterase
CNS	Central Nervous System
CSF	Cerebrospinal Fluid
DAB	Diaminobenzidine
EAE	Experimental Autoimmune Encephalomyelitis
FLAIR	Fast Fluid-Attenuated Inversion Recovery
GFAP	Glial Fibrillary Acidic Protein
GM	Grey Matter
HLA	Human Leucocyte Antigen
HRP	Horse Radish Peroxidase
IFN-γ	Interferon gamma
IHC	Immunohistochemistry
IL-1β	Interleukin-1 Beta
LC	Lower Cervical
LFB	Luxol Fast Blue
LGN	Lateral Geniculate Nucleus
LT	Lower Thoracic
Lum	Lumber
MAG	Myelin-Associated Glycoprotein
MBP	Myelin Basic Protein
MHC	Major Histocompatibility Complex
MMPs	Matrix Metalloproteinases
MOG	Myelin-Oligodendrocyte Glycoprotein
MRI	Magnetic Resonance Imaging
MRS	Magnetic Resonance Spectroscopy
MS	Multiple Sclerosis
NAA	N-acetylaspartate
NO	Nitric Oxide

PBS	Phosphate-Buffered Saline
PD	Proton Density
PLP	Proteolipid Protein
PP	Primary Progressive
RR	Relapsing Remitting
SP	Secondary Progressive
T	Tesla
TNFα	Tissue Necrosis Factor Alpha
TRAIL	Tumour Necrosis Factor-Related Apoptosis-Inducing Ligand
UC	Upper Cervical
UT	Upper Thoracic
WM	White Matter

Acknowledgments

The work presented in this thesis was performed in the Departments of (i) Histopathology and (ii) Clinical Neurology, Queens Medical Centre, Nottingham University Hospitals NHS Trust with the exception of Chapter 6, which was completed at the VU Medical Centre, Amsterdam under the supervision of Dr Lars Bö (LB), Professor Frederik Barkhof and Jeroen J.G. Geurts (JJGG).

I am deeply indebted to Dr Nikos Evangelou (Division of Clinical Neurology, Queens Medical Centre) for his enthusiasm, guidance and supervision throughout the research period. I have also received invaluable support from Dr Lars Bö (Department of Neuropathology, VU Medical Centre, Amsterdam), Professor Margaret Esiri (Department of Neuropathology, Oxford Radcliffe NHS Trust), Professor James Lowe (Department of Neuropathology, Queens Medical Centre) and Professor Cris Constantinescu (Division of Clinical Neurology, Queens Medical Centre).

In addition I would like to acknowledge the work of Dr Trudy Owens (Department of Economics, Queens Medical Centre) who performed the statistical analyses, Ian Donaldson (ID) who - under my supervision - performed the measurements used in Chapter 2 as part of a BMedSci thesis, Neil Hand and Howard Coleman who performed the immunohistochemistry staining, Lianne Finnerty and Denise Morgan who cut the tissue sections, Trevor Gray and Chris Tench for their I.T. advice, Anne Kane for her help with the figures, and Evgenia Theodorakopoulou for her assistance with the reproducibility study in Chapter 5.

I would also like to thank Abhi Vora of the UK MS Brain Bank and Dr Rivka Ravid, co-ordinator of the Netherlands MS Brain Bank, for providing the autopsy material used in Chapters 2 and 6 respectively. The autopsy material used in the remainder of the study was provided by Professor Esiri, Oxford Radcliffe Hospital.

The study was funded by a grant from the MS Society of Great Britain and Northern Ireland (grant number 801/03, N.E.).

Chapter 1: Introduction

1.1 Overview

Multiple Sclerosis (MS) is a chronic inflammatory disease of the Central Nervous System (CNS) characterised by multifocal demyelinated sclerotic plaques. MS is the most common chronically disabling neurological condition affecting young adults in the UK, where it affects approximately 90,000 people[1].

1.1.1 Epidemiology

The prevalence of MS varies considerably, being highest in northern Europe, southern Australia and North America[2]. There is a latitudinal gradient in prevalence, independent of genetic factors, with rates increasing as one moves away from the equator[2]. Migration studies demonstrate that those who emigrate from an area of low-prevalence to an area of high-prevalence remain at low risk if they move after 15 years of age[3]. Latitudinal gradients are even described within the UK, with the highest rates being observed in Scotland and Northern Ireland. The overall prevalence in the UK is 100-150/100,000 with an annual incidence of approximately 7/100, 000[4]. Overall MS affects twice as many women as men. The disease usually presents in the third or forth decade of life; presentation before adolescence and beyond the age of 60 is uncommon.

1.1.2 Genetic Studies

Family studies reveal that MS has a concordance rate of 31% among monozygotic twins, in comparison to 5% in dizygotic twins, highlighting a substantial influence of genetic factors[5]. Genetic studies demonstrate weak associations with multiple genes including certain Human Leucocyte Antigen (HLA) haplotypes (reviewed by Dyment et al[6]) and polymorphisms in two non-HLA genes, the interleukin-2 receptor α gene and the interleukin-7 receptor α gene[298].

1.1.3 Aetiology

The aetiology of MS remains unknown. Several lines of evidence suggest it is an immune-mediated disorder. These include observations related to genetic studies, animal studies, immunosuppressive medications and histological assessments of MS plaques[7]. It is hypothesised that the activation of $CD4^+$ Th1 cells - sensitised to a self-antigen in the

CNS - is an important early step in the disease process[476]. The oligodendrocyte-myelin complex appears to be the principal target of this immune attack[7]. A single oligodendrocyte can myelinate up to 30–40 axons[8]; each myelin sheath consists of layers of specialised oligodendrocyte plasma membrane wrapped in a spiral around the axon. This multilamellar myelin sheath is composed of lipids and a number of myelin proteins including MBP (myelin basic protein), PLP (proteolipid protein), MAG (myelin-associated glycoprotein), MOG (myelin-oligodendrocyte glycoprotein) and CNP (2'3'-cyclic nucleotide 3'-phosphodiesterase)[8]. It is speculated that one of these proteins, or some other CNS antigen, may be targeted by the immune system in MS. One proposed mechanism for this loss of immunological tolerance is "molecular mimicry", whereby exposure to an environmental agent containing epitopes similar to self-antigens results in the generation of activated, auto-reactive T cells. Candidate agents include the infections Ebstein Barr Virus, Chlamydia Pneumonia and Human Herpes Virus 6[9].

It is suggested that these auto-reactive T cells then migrate into the CNS parenchyma through a disrupted Blood Brain Barrier (BBB) where they recognise their target antigen, processed by Antigen Presenting Cells such as macrophages and microglia. Lymphocytes and macrophages subsequently secrete a range of substances which mediate tissue damage and further propagate the inflammatory response. However, it is important to note that recent studies argue against a primary role for $CD4^+$ T cells in the initiation of demyelination, reporting that these cells are scarce in very early MS lesions[10, 11].

1.1.4 Clinical Course

80% of MS patients present with relapsing remitting (RR) symptoms[12]. The clinical features of the relapse reflect the anatomical location of the demyelinated plaque, with symptoms frequently resulting from plaques in the anterior visual pathway, the brainstem and cerebellum, and the spinal cord. The degree of functional recovery following a relapse is variable. Complete clinical recovery is frequently seen early in the disease course, while at later stages there is often a persistent neurological deficit. In general, relapse frequency declines over time. However, the majority of patients (approximately 80% after 20 years) enter a "secondary progressive" (SP) phase of disease, characterised by a gradual accumulation of disability with or without superimposed relapses[13]. Even a substantial proportion of patients labelled as having a "benign" disease course after 10

years, will eventually develop progressive disability[13, 14]. 20% of patients present with Primary Progressive MS (PPMS), characterised by a progressive course from onset without relapses. In contrast to relapsing disease, PPMS usually presents with a chronic progressive myelopathy, affects males and females equally and has an older mean age of onset. Fixed disability in MS can therefore be acquired by two mechanisms; incomplete recovery from relapse and disease progression. Overall 50% of MS patients require a walking aid within 15 years of disease onset[13].

1.1.5 Diagnosis and Management

The diagnosis of MS is made on clinical grounds, often supported by paraclinical investigations such as Magnetic Resonance Imaging (MRI), evoked potential studies and cerebrospinal fluid (CSF) examination. The diagnosis hinges on the ability to demonstrate the dissemination of lesions in both time and space; that is to establish that two or more episodes of demyelination have affected separate sites within the CNS at separate times. Over 95% of MS cases have hyperintense lesions on T2 weighted MRI. Imaging can also provide evidence of dissemination of lesions in space and time and is useful in excluding conditions which mimic MS[15]. In over 90% of cases CSF examination demonstrates oligoclonal IgG bands or increased IgG levels, providing evidence of intrathecal synthesis of immunoglobulins. Visual and somatosensory evoked potential studies frequently provide neurophysiological evidence of dysfunction of the optic nerves and sensory pathways.

The mainstay of management remains symptomatic treatment for sensory disturbance, spasticity, sphincter disturbance, fatigue and depression. Corticosteroids, for example intra-venous methyl prednisolone, are frequently used to hasten recovery following a disabling relapse although they do not significantly alter the ultimate recovery from an attack[16]. “Disease modifying” immunomodulatory therapies (Interferon β and glatiramir acetate) result in a substantial reduction in the development of new gadolinium-enhancing MRI lesions and reduce relapse frequency by approximately 30%, but appear to have little impact on the progressive phase of the disease[17]. More powerful therapeutic options include Natalizumab (an α4-integrin antagonist), Alemtuzumab (Campath-1H, an anti-CD52 monoclonal antibody) and Mitoxantrone which are more efficacious but have less favourable side-effect and safety profiles[18-20].

1.2 The Pathology of MS – the White Matter plaque

The pathological hallmark of MS is the demyelinated white matter (WM) plaque, a sharply demarcated oval-shaped lesion which may reach several centimetres in diameter. The initial event in the formation of the demyelinated plaque is unknown, as are the factors governing plaque topography. They may occur anywhere in the CNS with predilection sites including the periventricular WM, optic nerves, cerebellum, cervical cord, brainstem and leucocortical junction[21-25]. Plaques are generally centred on one or more small veins or venules, sometimes displaying finger-like projections (Dawson's fingers) along the course of the vessel[21, 25]. At the histological level the WM plaque is characterised by BBB breakdown and inflammatory cell infiltration, demyelination and variable degrees of remyelination, astroglial scar tissue, and axonal loss:

1.2.1 Inflammatory cell infiltration

Under healthy conditions immune cell invasion across the BBB is highly restricted, with only a small proportion of leukocytes participating in "immunological surveillance" within the CNS[477, 478]. However, post-mortem studies reveal extra-vascular deposition of serum proteins within MS plaques, indicating BBB breakdown in the disease state[26, 27]. A number of molecules are involved in effecting BBB breakdown and the recruitment of inflammatory cells to the MS plaque. For example T cell migration is facilitated by (i) the up-regulation of adhesion molecules on the luminal surface of cerebral blood vessels as a result of inflammatory mediators activating endothelial cells[28], (ii) chemokines which promote macrophage trafficking[29], and (iii) matrix metalloproteinases (MMPs, produced by macrophages) which degrade the extracellular matrix, further aiding entry of inflammatory cells into the brain tissue[30].

Macrophages make up the majority of inflammatory cells in the WM plaque[25]. A proportion of macrophages are derived from blood-borne monocytes, while others stem from resident microglia. Under non-pathological conditions microglia are incapable of acting as Antigen Presenting Cells. However, during CNS inflammation they become activated, expressing MHC class II and co-stimulatory molecules essential for optimal antigen presentation to T cells, and may also adopt a macrophagic morphology.

The inflammatory activity of lesions can be categorised according to the extent and distribution of MHC class II-expressing cells (i.e. activated microglia and macrophages)[31]. "Active" lesions contain an abundance of activated macrophages (both in the brain parenchyma and the perivascular spaces of blood vessels), a variable number of activated T lymphocytes (predominantly perivascular $CD4^+$ and $CD8^+$ T cells) and a smaller number of B cells. A proportion of active plaques show evidence of ongoing demyelinating activity, identified by the presence of myelin degradation products within macrophages; the frequency of these plaques is low in patients with chronic MS[32]. The most commonly encountered lesions at autopsy are "chronic inactive", which contain smaller numbers of inflammatory cells. Other lesions are described as "chronic active", with the plaque borber demonstrating a prominent inflammatory infiltrate, while there is a paucity of inflammatory cells in the centre.

The inflammatory process in MS is not restricted to the demyelinated plaques. A range of pathological abnormalities have also been described in the non-demyelinated, macroscopically "normal-appearing" WM[25, 33]. Changes include gliosis, inflammatory cell infiltration, microglial activation, axonal loss, thickening of blood vessel walls, perivascular deposits of lipofuscin, the expression of inflammatory mediators and subtle BBB changes (e.g. abnormal tight junction proteins on vascular endothelia with evidence of extravascular fibrinogen leakage)[30, 34-39]. One study reported some degree of histological abnormality in 72% of the macrocopically "normal appearing" WM examined[34]. Meningeal inflammation is also well recognised in MS[40, 41].

1.2.2 Demyelination and oligodendrocyte pathology

Injury to the myelin-oligodendrocyte complex is likely to occur via a number of mechanisms, although the relative importance of these processes is poorly understood. MHC class II-restricted interactions between $CD4^+$ T cells and antigen-presenting macrophages are likely to be important in inducing the inflammatory reaction which ultimately results in oligodendrocyte damage[25]. T cells and macrophages secrete numerous cytotoxic products which have been implicated in oligodendrocyte injury; $CD8^+$ T cells release perforin[42] and lymphotoxin[43, 44] while macrophages produce reactive oxygen[45] and nitrogen species[46, 47], proteases, excitatory amino acids[48] and cytokines (e.g. TNFα and IFNγ[49, 50]). Oligodendrocyte apoptosis may also be mediated via the Fas-

Fas ligand pathway, which involves interaction between the molecules Fas (expressed by the oligodendrocyte) and Fas ligand (on macrophages and $CD8^+$ T cells) [51-53].

The role of B cells and autoantibodies in MS is uncertain[54, 479]. B cells and plasma cells are observed in the perivascular spaces and meninges, with parenchymal infiltration being less common. Actively demyelinating plaques may contain immunoglobulins (mainly IgG) and complement components which are either produced locally (by B cells and macrophages / microglia respectively) or enter through the "leaky" BBB. Antibody-mediated processes may contribute to demyelination, with antibody-opsonized myelin being destroyed by activated macrophages or through complement activation[54, 55, 479].

1.2.3 Evidence of Heterogeneity in MS lesions

It has been suggested that active MS plaques can be classified into one of four types[56, 57]. All four patterns show T cell and macrophage infiltration. Demyelination in type I lesions appears to be T cell mediated, while type II lesions also contain prominent deposition of immunoglobulin and activated complement. Type III lesions show degenerative changes in the distal processes of the oligodendrocyte with preferential loss of the myelin protein MAG, and nuclear changes consistent with oligodendrocyte apoptosis. It has been suggested that this pattern may occur secondary to viral or toxin-induced oligodendrocyte injury. Type IV lesions show primary oligodendrocyte degeneration followed by myelin destruction. Only small numbers of type IV lesions have been described to date, all in PPMS. Despite this inter-individual heterogeneity there appears to be homogeneity within individual patients; that is, all active plaques within a particular patient appear to exhibit the same pattern, although it is unclear if new lesions that develop over time also follow this pattern.

More recent studies have challenged this concept of lesion heterogeneity[10, 11]. Barnett and Prineas have proposed that extensive oligodendrocyte apoptosis is the initial event in the formation of the MS plaque, with the dying oligodendrocyte inciting a secondary inflammatory response[10]. Studying cases of early MS who died of rapidly worsening disease, they observed oligodendrocyte apoptosis in areas with only mild reductions in myelin density and an absence of macrophages and T cells, suggesting that oligodendrocyte pathology actually precedes leukocyte infiltration.

1.2.4 Gliosis

Astrocytes become activated by a variety of pathological processes including CNS inflammation. This process of reactive gliosis is characterised by astrocyte proliferation, upregulation of intermediate filament proteins including glial fibrillary acidic protein (GFAP) and morphological changes including cellular hypertrophy and the emission of processes (stellation). The degree of gliosis is variable - in some plaques astroglial processes occupy most of the space created by myelin loss, while in others there is marked expansion of the extracellular space[58]. It is unclear whether gliosis is protective or detrimental; astrocytes produce various neurotrophic factors and cytokines which may contribute to remyelination and neurite outgrowth[59]. Alternatively the astroglial scar may mechanically impede these processes[60]. In vitro, astrocytes have the ability to express MHC class I and II, but whether they present antigen in vivo is controversial[61, 62].

1.2.5 Remyelination

Remyelination is well recognised in MS. There is some evidence that early in the disease course plaques contain high numbers of oligodendrocytes and show pronounced remyelination[32], while in later stages few oligodendrocytes are found and remyelination is either absent or restricted to the lesion border[63]. In contrast Patrikios et al report extensive remyelination in a subset of patients with chronic MS[64].

There is much debate as to whether remyelinating cells are derived from oligodendrocytes that survive the demyelinating attack, or if they are recruited from a pool of glial progenitors[32, 65, 66]. Several studies suggest that oligodendrocytes which survive in the vicinity of a demyelinated area do not divide and are incapable of forming new myelin sheaths[67], while glial progenitors are able to divide and migrate to repopulate a demyelinated region[68, 69]. The myelin sheaths in remyelinated lesions are uniformly thin and have shorter internodes[70], showing reduced staining intensity with myelin stains. Lesions which show complete remyelination are termed “shadow plaques”.

1.2.6 Axonal loss

Post-mortem studies demonstrate extensive axonal loss in MS, not only in WM plaques but also the peri-plaque WM and the so-called “normal appearing” WM[71-73]. Further evidence for axonal loss comes from Magnetic Resonance Spectroscopy (MRS) studies. MRS provides quantitative indices of several tissue metabolites including N-

acetylaspartate (NAA), a putative index for axonal injury or loss in vivo, and significant reductions in NAA have been reported both within MS plaques[74] and in the "normal appearing" WM[75].

Axonal degeneration occurs early in the disease course[73, 76]. Small calibre axons appear to be more susceptible to injury than larger fibres which are relatively well preserved[77-79]. The mechanisms of axonal loss remain speculative[80]. Axonal damage is greatest in areas of high inflammatory content with lesser degrees of injury being observed in inactive lesions and the peri-plaque WM[71, 73, 81-83]. In particular, acute axonal injury correlates with the number of $CD8^+$ T cells and activated macrophages, suggesting a role for these cells[73, 83]. $CD8^+$ T cells have been shown to transect axons in vitro[84-86] while macrophage products such as Nitric Oxide[87], TNFα[88, 89] and proteases[90] may also induce axonal injury. Autoantibodies against neuronal proteins have been identified in sera and CSF from MS patients, raising the possibility of antibody-mediated axonal injury [91-94]. The demyelinated axon may be particularly vulnerable to immune-mediated injury, while remyelination may afford some protection against axonal degeneration, with less axonal damage being observed in remyelinated lesions in comparison to demyelinated plaques[71, 73].

It has been proposed that axonal degeneration in chronic inactive plaques occurs secondary to a mismatch between energy supply and demand (i.e. a state of "virtual hypoxia") [80, 95]. Rather than being restricted to the nodes of Ranvier, Na^+ channels become distributed diffusely along the chronically demyelinated axon, increasing Na^+ influx. However, mitochondrial function may be compromised in MS[96, 97], impairing the ATP-dependant Na^+/K^+ pump which normally restores this ion gradient. Instead, the energy-independent Na^+/Ca^{2+} pump exchanges Na^+ for extracellular Ca^{2+}, disrupting Ca^{2+} homeostasis and activating Ca^{2+}-dependant proteases which degrade the axon cytoskeleton. Low levels of inflammatory mediators and the removal of neurotrophic support (i.e. normally provided by the myelinating oligodendrocytes) may also contribute to axonal loss in chronic plaques[53, 71, 98, 99].

Following axonal transection in an MS plaque, the distal portion of the axon undergoes Wallerian degeneration and is phagocytosed by macrophages[100]. Retrograde degeneration of the proximal axon may also occur. These processes are generally considered to account for the extensive axonal loss reported in the "normal appearing"

WM, although evidence is somewhat conflicting[72, 101]. Evangelou et al reported a strong correlation between lesion loads in the cerebrum and axonal number in the corresponding area of the corpus callosum[72]. In contrast DeLuca et al found little correlation between plaque loads and axonal loss in the spinal cord, suggesting a neurodegenerative process, independent of inflammatory / demyelinating activity, may contribute to axonal loss in MS[101].

1.3 The pathological substrate of clinical disability in MS

The symptoms of an MS relapse are believed to predominantly reflect inflammation and demyelination. The axons' ability to conduct nerve impulses in the normal saltatory manner is compromised in the demyelinated state, leading to slowing or blockade of conduction[102]. Functional impairment will occur if a significant proportion of nerve fibres in a clinically eloquent site are affected. The anatomical site of the lesion determines symptomatology, although the majority of lesions cannot be linked to clinical symptoms[4]. Demyelinated axons may also discharge spontaneously and show increased mechanical sensitivity leading to paroxysmal symptoms including Lhermitte's phenomenon (sensory disturbance travelling down the spine on neck flexion). Incomplete demyelination may result in intermittent conduction block, for example conduction failure in association with a rise in temperature (Uhtoff's phenomenon). Animal studies suggest that disability can result from inflammation in the absence of demyelination[480, 481]. This may partly reflect Nitric Oxide production, which potentially contributes to conduction block[103].

Axonal degeneration has been proposed as a major cause of irreversible and progressive neurological disability in MS patients[53]. Axonal loss occurs in the very early stages of disease[76, 104], but may not cause clinical symptoms due to a functional reserve of axons and other compensatory mechanisms. However when axonal loss in a clinically eloquent tract reaches a threshold, it leads to permanent disability. This "axonal hypothesis" is supported by MRS studies suggesting that NAA levels are a better predictor of clinical disability than conventional MRI lesion loads[75, 105, 106]. Imaging studies also demonstrate significant atrophy in various CNS structures in MS[107-110], even in the early stages of disease[111-113]. Although direct evidence is lacking, this tissue loss is assumed to mainly reflect axonal loss. Importantly, several studies report that atrophy rates correlate with the accumulation of disability[110, 114-120].

Several mechanisms are likely to contribute to functional recovery following relapse. In the early stages removal of inflammatory mediators such as nitric oxide may reverse conduction block, while the resolution of oedema may relieve mechanical pressure on fibre tracts. Electrical conduction may be restored by both remyelination and by the insertion of voltage-gated Na^+ channels along the internodal membrane of the denuded axon[121, 122]. Compensatory adaptive changes in the cerebral cortex may further facilitate recovery[123]. Failure of these mechanisms with time (e.g. exhaustion of the oligodendrocyte progenitor pool) may explain the observation that recovery from relapse tends to be incomplete in the later stages of the disease. Cumulative axonal loss - following repeated inflammatory attacks – and gliotic scarring are also likely to contribute to incomplete remission.

1.4 GM Pathology in MS

CNS tissue can be divided into WM and grey matter (GM). The WM consists of axonal tracts, with the high proportion of myelinated axons giving the WM its colour, while the GM - where the neuronal cell bodies reside - appears grey on account of the high density of neuronal nuclei. In comparison with WM, the myelin content of GM is reduced. However, although the dendritic tree and the neuronal cell body is unmyelinated, many myelinated fibres do enter and leave the GM and many regions of GM contain large numbers of myelinating oligodendrocytes[124, 125]. A proportion of oligodendrocytes within GM - so-called satellite or perineuronal oligodendrocytes - lie opposed to the perikarya of neurons and are believed to play an important role in maintaining neuronal homeostasis[125, 126].

MS is traditionally described as a disease of WM. While it was acknowledged that the pathological process was not limited to the WM, only a modest degree of GM involvement was recognised[21-23]. However this has been called into question over recent years with the realisation that GM demyelination is grossly underestimated by conventional staining and imaging techniques[127-129]. In light of this, it is essential that GM pathology in MS is re-assessed.

Several post-mortem studies – using more sensitive staining techniques – have identified the cerebral cortex as a predilection site for demyelination[127, 130-134]. Like WM plaques,

cortical lesions are characterised by sharply demarcated areas of complete myelin loss associated with substantial neuronal/axonal injury[130, 132]. However they show a number of striking differences in comparison with their WM counterparts, for example they contain minimal inflammation and gliosis, and often display a distinct morphology which is not "perivenous" in distribution[127, 130, 132, 135-137]. Furthermore the extent of cortical demyelination correlates poorly with the degree of WM demyelination suggesting that different pathological processes may be responsible for myelin loss in the two different tissue compartments[129, 133] .

Numerous MRI studies demonstrate significant GM atrophy in the brain[138-140]. Several other studies report abnormalities in quantitative MRI parameters in GM brain structures related to Magnetisation Transfer[141-145], Diffusivity and Fractional Anisotropy[144, 146-149], T1 Relaxation time[150-152] and MRS[153-159]. While the precise pathological correlate of these imaging changes are poorly understood they indicate the presence of tissue damage beyond the resolution of conventional MRI, and further support the notion that there is substantial GM pathology in MS.

1.4.1 GM pathology may be an important contributor to clinical disability in MS

It has been suggested that GM pathology contributes to fatigue, depression and cognitive problems in MS[134, 152, 160]. All of these symptoms are common, frequently manifesting early in the disease course and causing substantial morbidity[161]:

- Fatigue has been reported to occur in 78% of MS patients[162], with one study suggesting that fatigue was the earliest symptom in 31% of patients and the most troublesome symptom in 28%[163].

- The lifetime prevalence of depression approaches 50% in the MS population, with major depression occurring in over 25%[164, 165]. While a "reactive" depression may represent a psychological reaction to chronic disability, there is growing evidence that MS-related depression has an "organic" component, for example reflecting pathology in the frontal lobes. Both fatigue and depression are predictors of impaired quality of life in MS, independent of physical disability[166, 167]. There is also an increased risk of other psychiatric disorders including bipolar affective

disorder, euphoria and psychotic symptoms, which have even been described at disease onset[168, 169].

- Cognitive impairment affects approximately 40% of MS pateints[170]. Typically the dementia is of a subcortical pattern, with prominent defects in attention and executive function, although a smaller number demonstrate neuropsychological deficits typical of cortical dementia such as dysphasia, dysgraphia and dyslexia[171]. A minority of patients may even present with ''cortical MS'', characterised by predominantly neuropsychological or cognitive deficits or distinct syndromes (anomia, agraphia, aphasia, alexia, alien hand) consistent with cortical dysfunction [171, 172]

- The prevalence of epilepsy in MS is estimated to be increased three- to six-fold in comparison with the general population[173]

"Juxtacortical" lesion load has been correlated with a number of clinical features including physical disability, epilepsy, cognitive dysfunction and depression[174-180]. However MRI does not detect the vast majority of GM plaques so the pathological substrate of these symptoms - including the relative importance of GM and WM pathology - is unclear. Imaging studies suggest that cognitive dysfunction and mood disturbance in MS may be related to GM brain atrophy[180-185], and fatigue has been linked to subcortical GM pathology, as evidenced by studies using both quantitative MRI, functional MRI and 18F-fluorodeoxyglucose Positron Emission Tomography[152, 160, 186, 187]. Cortical demyelination - particularly within the cingulated gyrus, insular cortex and temporobasal cortex - may result in cognitive deficits[134]. However it has also been suggested that WM lesions may cause disruption of (i) subcortical U fibers and other intra- and interhemispheric connections between different cortical areas and (ii) cortico-subcortical circuits, linking the cortex with the basal ganglia and the thalamus, leading to fatigue, depression and cognitive impairment[160, 170, 172, 175-177, 188, 189 , 190].

GM pathology may also contribute to a number of symptoms classically attributed to WM disease, including motor disability, sensory symptoms and ataxia. Extensive cortical demyelination may be an important pathologic correlate of irreversible disability in progressive forms of MS[133]. Indeed the failure of conventional MRI to adequately detect

GM pathology is likely to contribute to the clinico-radiological paradox, that is the poor correlation between MRI lesion load measures (i.e. which will largely reflect WM disease) and disability. In contrast several groups have noted correlations between measures of physical disability and both GM atrophy[191-196] and quantitative MRI measurments related to GM[141, 197-199].

1.4.2 The spinal cord is ideally suited for quantitative post-mortem studies

The spinal cord resides in the spinal canal of the vertebral column, extending from the medulla caudally to the level of the lower thoracic or upper lumbar vertebrae. It is suspended by the denticulate ligaments (which attach to the lateral surfaces of the cord) and is separated from the CSF-filled subarachnoid space by the Pia mater, the innermost meningeal layer that adheres to the cord surface. The average length of the adult cord is 45cm in males and 42cm in females[200]. The cord is divided into 8 cervical, 12 thoracic, 5 lumbar, 5 sacral and 1 coccygeal segmental levels, corresponding to the attachment of 31 pairs of spinal nerves and it is thickest at the cervical and lumbosacral enlargements (C4-T1 and L2-S3 respectively).

The cord is composed of a central core of GM, surrounded by WM (**figure 1.1**). The relative proportion of GM to WM varies between levels[200]. The WM consists of three columns or funiculi – the ventral, lateral (containing the descending corticosinal tracts) and dorsal columns. The GM is butterfly-shaped in transverse section and has a distinctive configuration at each spinal level, with the cross-sectional area being greatest in the cervical and lumbosacral enlargements. Rexed divided the spinal GM into 10 zones or laminae on the basis of cytoarchitectonic features, although it is often not possible to identify these laminae on human post-mortem material[201]. The GM is composed of a pair of dorsal (posterior) and ventral (anterior) horns - primarily concerned with sensory and motor function respectively - linked by the GM commissure, which contains the central canal. In the thoracic and upper lumbar segments there are small lateral horns, which contain sympathetic efferent neurons.

Few post-mortem studies have assessed GM pathology outside of the cerebral cortex in MS. There is a particularly striking paucity of literature examining GM pathology in the spinal cord. The spinal cord is well suited for post-mortem examination on account of its well characterised, relatively simple anatomy with readily identifiable structures[202]. The

cord is an extremely relevant site to study MS pathology, for a number of reasons: Firstly, MS plaques commonly affect the spinal cord[21, 24, 79, 203]; one autopsy series reported spinal cord plaques in 48 out of 59 MS cases (81.4%), periventricular lesions surrounding the lateral ventricles in 98 out of 126 (77.7%), and optic nerve lesions in 11 out of 20 (55%)[204]. Secondly, these plaques frequently result in clinical symptoms[205, 206]. Characteristically spinal cord lesions cause a partial myelitis, with patchy, asymmetric motor and sensory symptoms, and often bladder involvement. More rarely a complete cord syndrome (i.e. transverse myelitis) is observed[207]. In a cross-sectional population-based study of 301 MS patients in South Glamorgan physical examination revealed sensory, motor or reflex changes consistent with a spinal cord lesion in 74% of cases[208]. In comparison 92% of patients had visual pathway involvement, 55% had brainstem or cerebellar dysfunction and 40% had evidence of cerebral impairment. Cord involvement is also prevalant in African and asian populations, where optico-spinal MS is the predominant disease phenotype[209]. Finally, substantial axonal loss occurs in the spinal cord, both within WM plaques and myelinated WM[76-79, 210] and may be an important contributor to clinical disability in SP and PP disease, both of which are typically characterised by a progressive myelopathy[110, 203, 205, 210-218].

Due to its small cross-sectional area, the resolution of current MRI scanners is not sufficiently high to study the spinal cord GM *in vivo*. Post-mortem examination is therefore essential, although a number of factors require consideration when interpreting autopsy studies. Firstly, in contrast to imaging studies, post-mortem examinations only provide a "snap-shot" at a single time-point, and do not allow us to study the temporal evolution of pathology. Secondly, the great majority of MS plaques found at autopsy are longstanding. Acute lesions are rarely fatal and so examination of the initial stages of the disease process is rarely possible. Biopsy material is enriched in early lesions, but is virtually exclusively sampled from the brain rather than the spinal cord. Thirdly, severe, disabling, long-standing MS cases are likely to be over-represented in an autopsy series[25]. Cases with short disease durations that come to autopsy tend to be particularly aggressive; whether the histopathological features of these "atypical" cases are fully representative of MS is questionable[36]. Finally, detailed clinical information is rarely available at or shortly before the time of death, so it is difficult to investigate the functional significance of pathological changes.

1.5 Thesis Outline

Only a small number of post-mortem studies have examined GM involvement in MS, with the majority of these focusing on the cerebral cortex. To our knowledge this study represents the first detailed examination of spinal cord GM involvement in MS. A greater understanding of GM pathology in this clinically eloquent site may provide insight into the pathophysiology of MS and mechanisms of disability in the disease. We use post-mortem material to explore various aspects of spinal cord GM pathology in MS. The specific aims of the study are as follows:

1. To compare the extent of GM and WM demyelination between different regions of the CNS by examining tissue from the cerebral cortex, cerebellar cortex, thalamus and spinal cord, assessing the proportion of WM that is demyelinated and the proportion of GM that is demyelinated in each area.

2. To assess the extent and pattern of GM and WM demyelination in the spinal cord, surveying the cord at multiple levels.

3. To examine the relative contributions of GM and WM volume loss to spinal cord atrophy in MS.

4. To assess the extent of neuronal pathology – changes in both neuronal number and neuronal size – within the spinal cord GM, both in relation to demyelinated plaques and the myelinated GM.

5. To assess the sensitivity of post-mortem MRI for detecting spinal cord GM plaques.

These aims are addressed in chapters 2-6, respectively. The autopsy material is derived from a number of sources: the Netherlands Brain Bank, the UK Multiple Sclerosis Brain Bank and the neuropathology department, Oxford Radcliffe NHS Trust, which we believe to be the largest collection of spinal cord autopsy material in MS. The local research ethics committee approved the study.

Figures

Figure 1.1

*Palmgren silver-stained transverse sections of the spinal cord at the upper cervical (**A**), lower cervical (**B**), upper thoracic (**C**), lower thoracic (**D**) and lumbar levels (**E**) (Palmgren silver stain). The butterfly-shaped grey matter (GM) has a distinctive morphology at each spinal level, with the GM cross-sectional area being greatest in the lower cervical and lumbosacral regions. The white matter (WM) consists of three columns – the anterior, lateral and dorsal columns (AC, LC and DC respectively). The GM is composed of a pair of dorsal horns (DH) and anterior horns (AH) linked by the GM commissure (GMC), which contains the central canal (CC). In the thoracic segments there are small lateral horns (LH). DR – Dorsal root.*

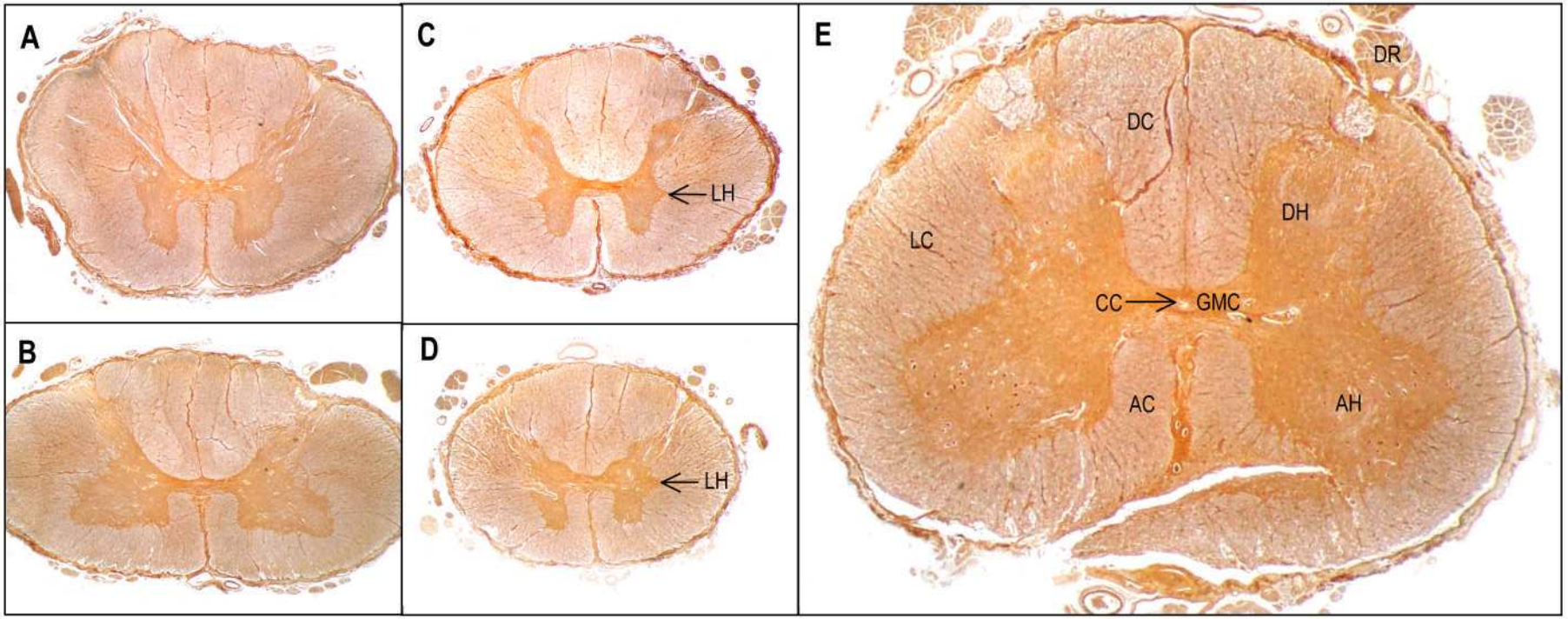
A
B
C
LH
D
LH
E
DR
DC
DH
LC
CC
GMC
AC
AH

Chapter 2: Regional variations in the extent and pattern of grey matter demyelination in Multiple Sclerosis - a comparison between the cerebral cortex, cerebellar cortex, deep grey matter nuclei and the spinal cord

2.1 Introduction

The factors influencing plaque topography in MS are not fully understood. MS plaques may appear anywhere in the CNS but particular sites are preferentially involved. Studies using conventional myelin staining techniques indicate that the majority of WM plaques occur in a perivenular distribution[21, 23, 219-221], with areas containing a high density of small veins and venules - such as the periventricular WM, leucocortical junction and the WM tracts of the brainstem and spinal cord - showing a preponderance for demyelination[22, 23, 25, 222]. The perivenular distribution of plaques has also been demonstrated in vivo by MR venography[223]. A smaller proportion of WM plaques do not show a perivenous distribution, indicating that additional factors influence plaque morphology[21, 25, 57, 95, 219, 224].

Several observations suggest that the perivascular space (also known as the Virchow-Robin space) is the focus of the MS plaque, rather than the blood vessel per se[225]. This space - which is continuous with the "potential" subpial space - is lined internally by the outer surface of the blood vessel and externally by the basement membrane of the glia limitans, extending as far as the capillaries on both the arterial and venular sides of the vascular tree[226]. The Virchow-Robin space is an important site for immunological reactions to take place. It contains resident perivascular macophages which can present antigen to blood-derived lymphocytes; the space may subsequently become engorged with inflammatory cells which then migrate into the brain parenchyma[226]. Cuffs of inflammatory cells in Virchow-Robin spaces are prominent features of acute MS plaques[226]. Interestingly lymphoproliferative tumours that propagate within perivascular spaces show a similar topography to MS plaques with the subependymal region and the corpus callosum being frequently affected[227].

Several groups have used conventional myelin staining techniques to assess the frequency of MS plaques in the cerebral cortex[22, 23, 222]. These studies suggest that the

majority of GM lesions involve the leucocortical junction[22, 23, 222]. Brownell and Hughes described the distribution of macroscopically visible lesions in 22 MS brains, reporting that 17% of these plaques affected the leucocortical junction while only 5% of plaques were restricted to the cortex alone[22]. Similarly Kidd et al, who assessed cortical pathology in 12 MS brains using Luxol Fast Blue (LFB) and Heidenhein's myelin stain, observed that 76% of cortical lesions involved the subcortical WM, while 24% exclusively involved the cortex[222]. 7 distinct patterns of cortical lesions were described, the majority of which arose within the territory of a principal cortical veins or one of its branches[222].

A number of histochemical staining techniques are available for detecting myelin, each with its relative merits and pitfalls[228]. LFB has an affinity for the phospholipids in myelin[229] and is a particularly popular stain because - in contrast to many traditional myelin staining methods (e.g. Weigert's[230], Weil's[231] and Heidanhain's stains[232]) - it can be applied to formalin fixed tissues without requiring the use of a mordant (i.e. a substance used to set the stain). LFB is frequently used in conjunction with Cresyl Violet[233], a counter-stain that binds the nuclei, the Nissl substance and the LFB anions present in the myelin. Additional techniques are available to demonstrate degenerated myelin on frozen sections, including Marchi's stain[234] and oil-soluble dyes such as Oil Red O[235] which stains degraded myelin within macrophages.

While conventional staining techniques such as LFB are satisfactory for identifying MS lesions within the heavily myelinated WM, they are suboptimal for visualising the fine myelinated fibres of the cerebral cortex[127, 129, 228]. The poor sensitivity of LFB for detecting cortical demyelination is in part due to the practice of de-staining the sections (i.e. washing the sections in a mixture of 70% ethanol and lithium carbonate to remove non-specific "background" staining) until the "normal" cortex is no longer blue[130, 236], although a considerable proportion of plaques remain undetected when this step is omitted (personal communication, Lars Bö). Therefore previous studies are limited by the techniques used to identify cortical plaques, which are likely to have grossly underestimated the extent of GM demyelination.

The current "gold standard" technique for detecting GM demyelination is myelin protein immunohistochemistry (IHC), using antibodies against myelin components such as MBP, PLP, MAG, MOG and CNP[127, 132, 237, 238]. In contrast to conventional myelin stains (e.g.

LFB and Heidenhain's stain), this technique is highly sensitive for detecting GM demyelination[127, 132].

A number of studies have used myelin protein IHC to demonstrate that substantial cortical demyelination occurs in MS[127, 130-134]. Indeed Bö et al reported demyelination was more extensive in the cerebral cortex (mean 26.5% demyelinated, median 14%) than in the subcortical WM (mean 6.5%, median 0%)[127].

Bö et al described four patterns of cortical plaque[127]: Type I lesions are located at the leucocortical junction, extending across both WM and GM. Type II lesions lie completely within the cortex and do not extend to the pial surface of the brain or the subcortical WM. Type III and IV lesions extend from the pial surface of the brain into the cortex; type III lesions extend partly into the cortex, often reaching cortical layer 3 or 4, while type IV lesions extend through the full width of the cortex, without involvement of the subcortical WM. In contrast to type I and II plaques, subpial lesions (i.e. type III and IV lesions) do not appear to occur in a perivenous distribution, frequently spanning extensive areas of cortex, sometimes affecting multiple adjacent gyri. Overall subpial lesions accounted for 67% of the cortical lesions, and 84% of the demyelinated cortical area[127]. 5 of the 20 MS cases examined by Bö et al exhibited extensive subpial demyelination in widely spaced cortical areas, suggesting that a pattern of "general cortical subpial demyelination" occurs in a subgroup of cases. In these cases 57% of the cortex was demyelinated in comparison with only 2.2% of the subcortical WM[127]. Subpial lesions have also been described in animal models of MS[239, 240]. Merkler et al injected the pro-inflammatory cytokines TNFα and INFγ into the cerebral cortex of MOG-immunised Lewis rats producing areas of demyelination with a striking similarity to MS lesions, with extensive subpial plaques accounting for 90% of the demyelinated cortex[240]. Similarly Pomeroy et al reported that subpial plaques accounted for 88% of the demyelinated cortical area in marmosets with MOG-induced Experimental Autoimmune Encephalomyelitis (EAE)[239].

Fewer studies have examined demyelination in the deep GM structures of the brain. Brownell and Hughes estimated that 4% of MS plaques in the brain affect the central GM[22]. Lumsden reported that 6.8% of plaques were located within the Basal Ganglia, and 2% were in the Thalamus[23]. Adams examined deep GM structures in 63 MS cases, identifying plaques in the caudate, thalamus and putamen in 10 cases, 6 cases and 8

cases respectively[204]. Deep GM pathology has not been assessed in detail using myelin protein IHC; Vercellino et al detected deep GM plaques in 3 out of 6 MS cases[132], while Geurts et al examined 9 cases of chronic MS, observing only 8 deep GM plaques in comparison with 70 WM and 90 cortical lesions[128]. Huitinga et al used LFB-staining to identify hypothalamic lesions in 15 out of 16 MS cases[241]. The authors suggest such lesions may be clinically significant, impairing activation of the corticotrophin releasing hormone system – and the subsequent production of endogenous corticosteroids - in response to an MS relapse. To our knowledge, only one study has used myelin protein IHC to assess demyelination in the cerebellar cortex, while no study has quantified GM demyelination in the spinal cord[242].

A number of studies have compared the frequency of MS plaques within different CNS regions[22, 23, 204, 243]. However the myelin staining techniques employed in these studies are recognised as being insensitive for detecting GM demyelination[127, 132]. Therefore it is unclear whether GM demyelination is more prominent in the spinal cord, the cerebral cortex or other GM structures. In this study we use myelin protein IHC to make within-subject comparisons of the extent of WM and GM demyelination in the cerebral cortex, cerebellum, spinal cord and thalamus, allowing us to explore the relationship between pathology at these different sites. We have therefore included areas where MS lesions frequently result in neurological deficits (e.g. the spinal cord and the cerebellum), areas where neuronal loss and GM atrophy has been demonstrated (i.e. the cerebral cortex and the thalamus), and areas previously considered to be predilection sites for WM and GM lesions. We hypothesise that subpial areas (i.e. the cerebral cortex and the cerebellar cortex) will show a preponderance for GM demyelination, while the thalamus and the spinal cord will contain a relative paucity of lesions.

2.2 Materials and methods

2.2.1 Clinical material

Autopsy material was obtained from 14 pathologically confirmed MS cases and 3 controls. This material was aquired from the Multiple Sclerosis Brain Bank, London. The MS patients (1 male, 13 female) were aged 44-81 years (mean 56.6 years, median 56 years) with disease durations of 6-32 years (mean 23.7 years, median 22 years). 11 cases had SPMS, 2 had PPMS and 1 had RR disease. The controls (2 females aged 69 and 73, 1 male aged 35) had no clinical or pathological evidence of neurological disease. The

material was fixed in 4% paraformaldehyde for 2 - 3 weeks before being embedded in paraffin.

2.2.2 Preparation of the sections

5µm sections were taken from 7 predetermined areas of the CNS, irrespective of macroscopic appearance; the motor cortex, cingulated gyrus, cerebellar cortex (cut in the plane of the dentate nucleus), thalamus and spinal cord (transverse sections from the cervical, thoracic and lumbar levels).

2.2.3 Immunohistochemistry

Sections were stained for Proteolipid Protein (PLP) using the EnVision method (DAKO EnVision kit, MCA839G, Dako, Denmark), a system based on a Horse Radish Peroxidase (HRP)-labelled polymer conjugated to secondary antibodies. Sections were deparaffinated in a series of xylene, 100%alcohol, 96%alcohol, 70%alcohol and water, washed with phosphate-buffered saline (PBS). Endogenous peroxidase activity was quenched by treating the specimens for 5 minutes with DAKO Peroxidase Block before incubation with the primary antibody for 60 minutes at room temperature. After washing in PBS the sections were incubated for 30 minutes with the pre-diluted Envision-HRP complex and washed again in PBS. The sections were then developed for 10 minutes with diaminobenzidine (DAB, dilution 1:50), washed in tap water, dehydrated in alcohol 70% to 100%, and xylene and finally stained for 1 minute with haematoxylin and washed in tap water until the nuclei stained blue. The primary antibody used was mouse anti-Myelin PLP (IgG2a, clone number plpc1, dilution 1:3000, MCA839G, Serotec).

2.2.4 Assessment of GM and WM lesions

The PLP-stained sections were scanned in a slide scanner (Nikon Super Coolscan 4000, Nikon UK Ltd., Kingston upon Thames, UK) to produce a digital image on which the MS lesions and the GM/WM boundary were manually outlined using image analysis software ("AnalySIS Pro" running SIS software, Olympus UK Ltd., Southall, UK). The PLP-stained sections, examined via microscopy (10x, Leitz Dialux 20EB microscope), were used as a reference to aid the identification of these regions, and the control cases was used to establish the normal regional variations in myelin staining density between the different CNS structures.

The number of demyelinated plaques in each region was counted, with areas of WM and GM demyelination being scored separately. Plaques in the cerebral cortex were classified as type I, II, III or IV lesions according to the system of Bö et al, as described above[127]. Outside of the cerebral cortex, plaques were scored as pure WM lesions, pure GM lesions or mixed GM/WM lesions. By measuring the total GM area, total WM area and the cross-sectional area of plaques, the proportion of GM that was demyelinated (P_{GMd}) and the proportion of WM that was demyelinated (P_{WMd}) was calculated.

Material from the control cases was used to establish the normal regional variations in myelin staining density between the different CNS structures. In control cases the myelin staining density is low in the superficial layers of the cerebral cortex (layers I-III), the cerebellar cortex and the GM commissure and Substantia Gelatinosa of the spinal cord (**figure 2.1A, 2.2A, 2.3F**). Within these structures lesions were defined as sharply demarcated areas showing a complete loss of myelin. In the remaining regions, where the density of myelin is usually much higher, lesions were defined as sharply demarcated areas, characterised by either complete myelin loss or markedly reduced myelin density on the PLP-stained sections.

GM structures were identified by the presence of neurons and by the reduced myelin staining intensity in comparison with the WM. Additional morphological characteristics were used to identify the GM / WM boundary more precisely, particularly in the demyelinated state:

Cerebral Cortex; radially orientated myelinated fibres are seen within the normal cerebral cortex, running perpendicular to the cortical surface. These fibres are clearly visible to the point where they reach the leucocortical junction, allowing the GM/WM boundary to be identified (**figure 2.1D**). Type I cortical lesions are generally small and do not interfere with reliable identification of the GM/WM boundary.

Cerebellar Cortex; the cerebellar cortex has three layers; an outermost molecular layer, a middle Purkinje layer and an innermost granular layer (**figure 2.2A-D**). The molecular layer is devoid of myelin, even in control cases, consisting of the extensive dendritic tree of the Purkinje cells and the unmyelinated axons of the granule cells. The middle layer, which contains the large Purkinje cells, is a single cell thick and contains only small

amounts of myelin. In view of the paucity of myelin in these two outermost layers, measurements of P_{GMd} were restricted to the granular layer. The GM/WM boundary in the cerebellum is readily identified - both in the myelinated and demyelinated state - on account of the distinctive appearance of the dense network of granule cells whose round nuclei appear blue on the haematoxylin counterstained sections.

Thalamus; the thalamic nuclei are interspersed with large amounts of WM and the myelin staining intensity is similar in the GM and WM, so the GM/WM boundary is not striking (**figure 2.3A**). The sections were therefore examined at high magnification and the tissue classified as GM if neurons were visible. In general the WM of the thalamus was seen to be composed of anisotropically arranged fibre bundles, aiding identification of the GM/WM boundary.

Spinal Cord; when the transverse sections are examined by microscopy – even in the demyelinated state – the axons of the WM tracts are readily identified running perpendicular to the plane of section.

2.2.5 Statistical analysis

Paired t tests were used to compare P_{GMd} with P_{WMd}. Correlations between P_{GMd} and P_{WMd} were assessed using Spearman's ranked test. Multiple regression analyses were used to examine the influence of age, anatomical location and disease duration on P_{GMd} and P_{WMd} ("Stata" version 9, StataCorp, Texas USA). As the sample contained only 2 PP and 1 RR case, and only 1 male case, MS subtype and gender were not included in the regression analysis.

2.2.6 Reproducibility of measurements

To evaluate intra-observer reproducibility 16 sections (4 cerebral cortex, 4 thalamus, 4 cerebellar cortex, 4 spinal cord) were selected at random and P_{GMd} and P_{WMd} were measured by an observer (ID) on two separate occasions, with a one month interval between measurements (coefficient of variation for GM measures = 4.7%; 6.8% for WM measures). These measurements were repeated by a second observer (CPG) in order to assess the inter-observer reproducibility (coefficient of variation for GM measures = 3.2%; 1.5% for WM measures).

2.3 Results

2.3.1 Lesion counts and morphology

The number of areas of GM and WM demyelination in each of the CNS areas is shown in **table 2.1**. Within the cerebral cortex and the thalamus the majority of GM plaques (95.8% and 87.5% respectively) were restricted to the GM and did not impinge on the WM. In the cerebellum 51% of areas of GM demyelination were restricted to the GM. In contrast only 16.7% of spinal cord GM plaques involved the GM exclusively.

Cerebral Cortex (figure 2.1); In the sections from the cingulate gyrus 20 areas of demyelination were detected in the GM (1 type I, 3 type II, 15 type III, 1 type IV) while the motor cortex contained 27 GM lesions (9 type II, 18 type III). Therefore we observed a total of 47 GM lesions in the cerebral cortex (1 type I, 12 type II, 33 type III, 1 type IV). The majority of cortical lesions were subpial (i.e. type III and IV) in location (72% by number, 96% by area). In several cases these involved extensive lengths of the cortical ribbon.

Cerebellar Cortex (figure 2.2); All of the pure GM lesions within the cerebellar cortex involved the full thickness of the granular cell layer, with apparent sparing of the digital WM, and frequently extended over multiple folia. While we restricted our assessment of P_{GMd} to the innermost granule cell layer of the cerebellar cortex, we note that demyelination in the granular cell layer was invariably accompanied by myelin loss in the purkinje cell layer. Similarly it was extremely rare to see loss of myelin in the purkinje cell layer with preserved myelin in the granular layer.

Thalamus (figure 2.3 A - D); the borders of MS plaques within the deep GM structures did not appear to show any respect for the GM/WM boundary. A number of periventricular plaques were observed within the GM of the Thalamus. In some cases these lesions appear to extend from the ventricular ependyma, into the thalamic GM to a relatively constant depth.

Spinal cord (figure 2.3 E - G); In a number of cases a proportion of the border of the GM plaque maintains a strict respect for the GM/WM boundary. This pattern of plaque morphology is examined in detail in **Chapter 3**.

2.3.2 Demyelination is more extensive in the GM than the WM

Overall, P_{GMd} (mean 28.8%) was significantly greater than P_{WMd} (15.6%) ($p < 0.001$). There was a significant correlation between P_{GMd} and P_{WMd} ($r = 0.7621$, $p < 0.001$).

P_{GMd} was greater than P_{WMd} in the motor cortex (3.9% versus 0.5%, $p = 0.0128$), cerebellar cortex (43.7% versus 8.7%, $p = 0.0055$), cervical cord (44.2% versus 35.3%, $p = 0.0464$) and thoracic cord (55.5% versus 38.0%, $p = 0.0082$). There was not a statistically significant difference between P_{GMd} and P_{WMd} in the lumbar cord (40.8% versus 29.3%, $p = 0.0693$), the cingulate cortex (16.0% versus 6.5%, $p = 0.1185$) and the deep GM nuclei (7.1% versus 4.0%, $p = 0.3885$). These results are summarised in **figure 2.4**.

2.3.3 Regional differences in the extent of demyelination

To examine for regional differences in the extent of GM demyelination, P_{GMd} was regressed on anatomical location controlling for age and disease duration. In comparison with the cervical cord, P_{GMd} was significantly reduced in the motor cortex (coefficient of regression = -0.4703, $p < 0.001$, that is, controlling for other variables, P_{GMd} was on average 47% greater in the cervical cord than the motor cortex), the cingulate (coefficient of regression = -0.3220, $p = 0.001$) and the thalamus (coefficient of regression = -0.4449, $p < 0.001$). P_{GMd} was not significantly different in the cerebellum (coefficient of regression = -0.0217, $p = 0.875$), thoracic cord (coefficient of regression = 0.0984, $p = 0.416$) or lumbar cord (coefficient of regression = -0.0829, $p = 0.538$) in comparison with the cervical cord. P_{GMd} was greater in the cingulate gyrus (mean 16.0%, median 11.4%) than in the motor cortex (mean 3.9%, median 2.0%) ($p = 0.013$).

The correlation between P_{GMd} and P_{WMd} varied between the different anatomical sites, being greatest in the spinal cord (e.g. thoracic cord; $r = 0.908$, $p < 0.001$) and thalamus ($r = 0.569$, $p = 0.042$). In contrast, the two variables did not correlate in the cerebral cortex (e.g. cingulate gyrus; $r = 0.161$, $p = 0.6$). The correlation approached statistical significance in the cerebellum ($r = 0.534$, $p = 0.060$). P_{GMd} in the cingulate cortex correlated significantly with P_{GMd} in the cerebellar cortex ($r = 0.745$, $p = 0.003$), but not with P_{GMd} in the spinal cord (e.g. thoracic cord; $r = 0.407$, $p = 0.214$).

P_{GMd} was significantly greater in the cerebellar cortex than in the cingulate gyrus (p = 0.01). However when we compared the proportion of the surface of the cingulate gyrus that was demyelinated (mean 36.1%) with the proportion of the surface of the cerebellar granular layer that was demyelinated (mean 43.6%) there was no significant difference (p = 0.491).

In comparison with the lumbar cord, P_{WMd} was reduced in the WM adjacent to the motor cortex (coefficient of regression = -0.2975, p = 0.003), cingulate (coefficient of regression = -0.2499, p = 0.014), thalamus (coefficient of regression = -0.2548, p = 0.021) and cerebellum (coefficient of regression = -0.1982, p = 0.053). P_{WMd} was not significantly different in the cervical (coefficient of regression = -0.0829, p = 0.538) or thoracic cord (coefficient of regression = 0.0984, p = 0.416) in comparison with the lumbar cord. The extent of demyelination – for each of the regions examined – is summarised on a case-by-case basis in **table 2.2**.

2.3.4 Influence of age and disease duration on extent of demyelination

Age (coefficient of regression = -0.0134, p = 0.004) appeared to have a significant influence on P_{GMd}, with younger patients having greater GM demyelination. Disease duration did not appear to influence P_{GMd} (coefficient of regression = 0.0091, p = 0.179).

Both age (coefficient of regression = -0.0100, p = 0.003) and disease duration (coefficient of regression = 0.0092, p = 0.049) appeared to have a significant influence on P_{WMd} with more extensive demyelination being observed in younger patients and those with longer disease durations.

We were unable to examine the influence of gender on the extent of demyelination as the MS cohort only contained 1 male patient.

2.4 Discussion

Numerous studies have examined the distribution of MS plaques within the CNS using histochemical myelin stains[21-23]. This work suggests that MS is predominantly a disease of WM, although it has long been recognised that it may also involve GM structures[21-24, 204, 222, 241]. However, these studies are likely to have substantially underestimated the

extent of GM pathology due to limitations in the staining techniques employed[127, 129, 132]. In light of this, it is essential that the extent and pattern of demyelination in MS be re-evaluated using more sensitive methods of lesion detection.

Previous studies have used myelin protein IHC, the "gold standard" technique for detecting GM demyelination, to demonstrate substantial cortical involvement in MS[127, 131-133]. In contrast, GM pathology in the spinal cord, cerebellar cortex and thalamus has received relatively little attention[132, 242]. Our current study is the first to compare the extent and pattern of GM demyelination between these four regions within the same patient group. Rather than simply reporting the absolute numbers of plaques in each site - which provides a rather crude measure of the extent of demyelination - we have calculated the proportion of GM and WM tissue that is demyelinated in each region.

We have defined MS plaques as sharply demarcated areas, characterised by either complete myelin loss or markedly reduced myelin density on sections stained with the anti-PLP antibody. PLP, a component of compact myelin, links the exoplasmic surfaces of the multi-lamellar myelin sheath[8]. However we stress that the pattern of myelin loss that we observe is not unique to this particular myelin antibody; identical results are produced with anti-MBP, -MAG, -MOG and -CNP antibodies (personal communication, Lars Bö).

Interestingly McNally and Peters report that DAB may be used to stain myelin on tissue sections that have been treated with horse serum[244]. The resulting myelin staining is faint but can be enhanced using a silver intensification procedure and is said to be particularly useful for examining myelinated fibres in GM. The mechanisms of binding of the horse serum to the myelin and the subsequent deposition of DAB at the binding sites are unclear. However the method could not be used on paraffin-embedded material. Furthermore the specificity of the PLP IHC was checked in the current study by omitting the primary antibody; when the tissue was exposed to DAB in the presence of the secondary antibody, but not the anti-PLP antibody, staining was blank.

Lucchinetti et al reported four distinct subtypes of active MS plaques[57, 95]. In the early stages of plaque development, type 3 lesions show a preferential loss of MAG, while other myelin proteins (including PLP, MBP and CNP) persisted within the partly damaged myelin sheaths. It is therefore feasible that PLP IHC may fail to detect a small number of

MS plaques. However, actively demyelinating plaques make up a small proportion of lesions in chronic MS[32], and in patients with disease durations greater than one year, type 3 lesions only make up a small proportion of actively demyelinating lesions (2 out of 27 actively demyelinating lesions examined by Lucchinetti et al)[57]. It should also be noted that selective loss of MAG has yet to be confirmed by other groups[245].

Perhaps surprisingly, few studies of MS have compared the extent of demyelination - either GM or WM demyelination - in intracranial structures with that in the spinal cord[204, 243]. None of these studies have assessed GM demyelination in detail. Numerous other groups have examined pathology in the brain *or* the cord but comparisons between studies are likely to be confounded by differences in MS subtype, disease course, disease duration, age, gender etc. Examining 70 MS cases, Ikuta et al reported extensive demyelinated plaques within the spinal cord, cerebrum and cerebellum in 53%, 51% and 19% of cases respectively[243]. In another large study Adams observed periventricular plaques in 78% of cases, while 22% contained plaques in the cerebral cortex and 81% contained spinal cord plaques[204]. Spinal cord GM plaques were reported in only 3.4% of cases, further highlighting the limitations of conventional staining techniques. Neither study provides detailed information on the extent or pattern of demyelination in these sites. In the current study we observe a striking preponderance for WM demyelination in the spinal cord in comparison with the other WM structures examined. GM demyelination is also much greater in the spinal cord than in the cerebral cortex and deep GM structures. However, in contrast to the situation in the WM, the extent of GM demyelination in the cerebellar cortex is comparable to that in the cord. Interestingly we find that P_{GMd} is greater than P_{WMd} in all of the regions studied; these differences are statistically significant in the motor cortex, cerebellar cortex and throughout the spinal cord.

Plaques which cause particularly disabling symptoms – such as brainstem, cerebellar and the spinal cord plaques - are likely to be over-represented in an autopsy series[25]. Therefore, while anatomical factors – such as a high density of post-capillary venules – may indeed predispose to MS plaques in these areas, this may be exaggerated somewhat in autopsy studies. This potential source of sampling bias must be considered when interpreting our results. We also acknowledge that our sampling regimen is by no means exhaustive. Several WM areas have not been sampled, most notably the

periventricular region, brainstem and optic nerves; therefore we cannot conclusively state that demyelination is more extensive in the GM than in the WM. In a study of 6 MS cases, Vercellino et al quantified demyelination in a single coronal section of the brain - cut in the plane of the thalamus and basal ganglia, but also including the periventricular WM - reporting greater demyelination in the WM than the GM (mean 21.75%, median 11% versus mean 14.8%, median 3.25%)[132]. However it is important to note that we have included material from the spinal cord, the subcortical WM, the corpus callosum (present on all of the cingulate gyrus sections) and the cerebellum, all of which are considered to be predilection sites for WM plaques[25].

2.4.1 Demyelination in the cerebral cortex

We report that the majority of plaques in the cerebral cortex (72% by number, 96% by area) are subpial in location. Previous studies also indicate that cortical demyelination predominantly occurs in a subpial distribution[127, 129, 131-134]. Consistent with Kutzeligg et al[133], we find no correlation between P_{GMd} and P_{WMd} in the cerebral cortex, suggesting that cortical demyelination – in particular subpial demyelination – occurs by an independent mechanism to WM demyelination.

It has been suggested that subpial demyelination is mediated by a soluble factor, diffusing inward from the surface of the brain[41, 127, 130, 134]. Such a myelinotoxic factor may spread from remote areas of the CNS via the CSF or be generated by meningeal inflammation. The CSF in MS often contains raised number of inflammatory cells, particularly in acute disease[246]. The majority of these cells are T lymphocytes, some of which are specific for putative myelin autoantigens[247-250]. B cells secreting IgG antibodies against the myelin proteins MOG[249, 251], PLP [248, 252], MBP[253, 254] and MAG[255] have also been detected in the CSF in MS. Although the pathogenic role of autoreactive B cells is unclear[246], several lines of evidence suggest that antibody-mediated processes contribute to demyelination in MS[57, 256, 479] and EAE[257]. Other CSF factors may contribute to subpial demyelination including TNFα and IFNγ, both of which may be raised in the CSF in MS[247, 258, 259]. IFNγ augments antibody-mediated demyelination when injected into the CSF of rats in combination with anti-MOG antibodies[257], while TNFα has been shown to induce oligodendrocyte apoptosis in vitro[43, 260].

Meningeal inflammation is well recognised in MS and may be important in mediating subpial demyelination[40, 41]. Kutzelnigg et al reported that T cells, B cells and plasma cell infiltrates are invariably seen in the meninges overlying subial plaques[134]. Similarly Pomeroy et al observed increased numbers of B cells, T cells and macrophages in the pia mater overlying subpial plaques in an animal model of MS[239]. [239]. Lymphoid follicle-like structures have been described in the leptomeninges of both MS patients and mice with EAE[41, 261]. These structures contained proliferating B-cells, in addition to T-cells, plasma cells and a network of follicular dendritic cells, suggesting that they represent ectopic B-cell follicles with germinal centres, sites where activated B cells undergo clonal expansion and selection to differentiate into plasma cells secreting high affinity antibodies. In keeping with this hypothesis, B cells at various stages of maturation have been identified in the CSF of MS patients, including centroblasts, cells that are exclusively found inside secondary lymphoid organs[262].

Previous work has suggested that there is considerable regional variability in the degree of demyelination in the cerebral cortex[127, 132-134]. Several studies demonstrate that the cingulate gyrus is a predilection site for cortical demyelination, both in MS and EAE[127, 132, 134, 239]. For example Bö et al observed more extensive demyelination in the cingulate in comparison with other cortical areas (mean 43.8%, median 49.4% versus mean 11.5%, median 2.2% in the parietal lobe)[127]. Likewise we find greater demyelination in the cingulate than the motor strip. The mean 16% demyelination that we observe in the cingulate is similar to the 19.4% reported by Vercellino et al[132]. Kutzelnigg et al found subpial demyelination to be most pronounced within the bases of sulci and within deep invaginations of the cortex, notably the cingulate gyrus, insular cortex and temporobasal cortex[134]. The preponderance for these areas may reflect regional differences in CSF flow, with extensive demyelination occurring in areas of CSF stasis[134, 239] .

2.4.2 Cerebellar Demyelination

Few studies have examined GM demyelination in the cerebellar cortex in MS[204, 242]. Using conventional staining techniques Adams assessed cerebellar pathology in 102 MS cases, detecting cortical demyelination in only a single case[204]. Considering the low myelin density within the "healthy" granular cortex (**figure 2.2, A-D**), it is perhaps not surprising that demyelination in this area is not detected with histochemical stains. However myelin protein IHC reveals that the cerebellar cortex is actually a predilection site for

demyelination in MS, with P_{GMd} exceeding 70% in 6 of the 13 cases examined in the current study. The cerebellum also showed the greatest difference between P_{GMd} (mean 43.7%) and P_{WMd} (mean 8.7%). Our findings are consistent with a recently published study by Kutzelnigg et al who examined cerebellar pathology in 40 MS cases and 8 controls, demonstrating extensive demyelination of the cerebellar cortex affecting all cortical layers in a band-like manner[242]. This pattern of demyelination was exclusive to MS subjects and was not observed in non-MS controls, including cases with cerebellar hypoxia.

We are confident that the *sharply* demarcated areas of *complete* myelin loss that we observe in the cerebellar cortex do indeed represent MS lesions, rather than Wallerian degeneration. Tract degeneration would be expected to result in *poorly* demarcated areas of *incomplete* myelin loss[64]. Furthermore, the efferent projections of the purkinje cells - which pass through the granular layer - are myelinated, as are their recurrent collateral branches; tract degeneration within the afferent connections of the cerebellum would not result in a loss of this myelin[263].

While demyelination in the cerebellar GM consistently involves the full thickness of the cortex, the great majority of cerebral subpial plaques are limited to the superficial cortical layers; therefore a greater proportion of the cerebellar cortex is demyelinated (43.7% versus 16% in the cingulate gyrus). Interestingly, when we analysed the proportion of the cortical surface that was demyelinated, the cerebellum and the cingulate showed similar degrees of involvement (43.7% versus 36.1%). We note that Kutzelnigg et al occasionally observed demyelination of the cerebellar cortex both (i) in a perivenous distribution and (ii) extending a variable depth into the granular layer[242], patterns of demyelination that we did not detect (i.e. lesions invariably affected the full thickness of the cerebellar cortex in our study). Like the subpial plaques of the cerebral cortex, the subpial GM lesions in the cerebellum are extensive, typically involving long stretches of cortex so that multiple folia may be completely demyelinated. P_{GMd} in the cingulate cortex correlated significantly with P_{GMd} in the cerebellar cortex (further supporting the work of Kutzelnigg et al who found a correlation between cortical demyelination in the cerebellum and the forebrain[242]), but not with P_{GMd} in the spinal cord, further suggesting that subpial demyelination occurs by a different mechanism to demyelination in other sites. Kutzelnigg et al found no correlation between GM and WM demyelination in the cerebellum, while we find a trend towards

significance[242]. However, in agreement with their findings, we do observe some subjects with extensive cerebellar cortical demyelination in the near absence of WM lesions.

2.4.3 Spinal Cord Demyelination

It is important to note that despite our speculations that subpial demyelination is mediated by a factor related to the CSF, GM demyelination is even more extensive in the spinal cord where the GM is surrounded by WM. Animal studies indicate that there are marked differences between the GM of the brain and spinal cord in terms of their response to injury, with inflammation being more pronounced in the spinal cord GM in comparison to the striatum following either traumatic injury or the injection of pro-inflammatory cytokines[264, 265]. Similar differences between sites may result in regional differences in the extent of GM demyelination.

While the subpial WM of the spinal cord is a predilection site for lesions in particular models of EAE[266], this is not the case in MS where the subpial WM does not appear to be any more susceptible to demyelination than the deeper tissue. Indeed areas of extensive demyelination are frequently observed with sparing of a narrow rim of preserved myelin in the subpial margin of the cord (see **figure 3.4H**, **figure 3.8A, I** and **figure 3.9K** from **Chapter 3** for examples)[204]. We occasionally observe demyelination limited to the subpial WM of the spinal cord, but this is an infrequent finding (**figure 2.3G**). Although we frequently see demyelination in the central portion of the spinal cord, this does not appear to be centred on the central canal per se, but rather involves the GM commissure - sometimes selectively, with sparing of the adjacent WM tracts (see **figure 3.4H-K** and **figure 3.9K-L**). Such a pattern of demyelination is unlikely to be mediated by a myelinotoxic factor in the CSF. The lumen of the central canal remains patent, allowing the flow of CSF, in newborns and young children, but often closes in later life. Yasui et al examined the anatomy of the central canal using autopsy material from 158 autopsy cases ranging in age from only 1 week to 116 years[267]. While the patency rate under 1 year of age was almost 100%, cases in which the canal was occluded at all segmental levels appeared in the second decade, with their number increasing with advancing age. By the fourth decade the majority of cases were occluded at all cord levels.

A proportion of GM plaques in the spinal cord show a strict respect for the GM/WM boundary. In this respect they show similarity to the subpial lesions in the cerebellar

cortex and the type IV plaques which involve the full-thickness of the cerebral cortex, but do not impinge on the subcortical WM. Only a single type IV cortical lesion was observed in the current study, most likely reflecting the fact that we have examined relatively small areas of cortex, but more gross examples are well described in the literature[127, 132]. It is possible that these three lesion patterns - which clearly challenge our current understanding of the factors that determine plaque morphology - share a common pathogenic mechanism. This concept is explored in detail in **Chapter 3**. We note that the converse pattern of demyelination (i.e. demyelinated WM, with sparing of the adjacent GM) was not observed in any of the regions.

2.4.4 Thalamic Demyelination

Consistent with previous studies[128, 132] we detect a modest degree of demyelination in the thalamus, observing thalamic plaques in 9 out of 13 MS cases, with a mean 7.1% being demyelinated. The nuclei of the thalamus are interspersed with a substantial amount of WM and we did not observe lesions respecting the GM/WM boundary. Although the ependymal surface was not identifiable on all of the sections, subependymal GM plaques were present in a number of cases, sometimes extending over a relatively large area (**figure 2.3C, D**).

It is well recognised that the periventricular WM is a predilection site for MS plaques. It is unclear whether subependymal thalamic plaques share a common pathogenic mechanism with these lesions. Adams et al examined the periventricular region in 129 MS cases, observing periventricular plaques in 82% of these[224]. In the majority of cases the plaque topography was most consistent with a perivenular origin[224]. Furthermore 84% of active periventricular lesions showed a discrete perivenular distribution in comparison to 53% of chronic lesions, suggesting that over time discrete perivenular lesions coalesce to form the characteristic pattern of periventricular demyelination. However, a smaller number of periventricular WM plaques appear to arise from the ependymal surface of the ventricle itself[25, 224].

It has been suggested that inflammatory cells or a demyelinating factor within the ventricular system may contribute to periventricular demyelination[25, 268]. Like the outer pial surface of the brain, the inner ependymal surface is permeable, potentially permitting the diffusion of a myelinotoxic agent from the ventricular CSF into the periventricular tissue[269,

[270]. In guinea-pigs with chronic relapsing EAE, a proportion of plaques appear to be primarily related to the ventricular surface[268]. Numerous supraependymal macrophages and lymphocytes overlie these lesions, suggesting that inflammatory cells within the ventricular system may mediate periventricular demyelination[268]. Further work is required to examine the relationship between periventricular GM plaques and subependymal veins in MS and to compare the extent of periventricular demyelination between GM and WM structures.

2.4.5 Influence of disease duration and MS subtype

In agreement with previous work, we find no correlation between disease duration and the extent of GM demyelination[127, 133, 242]. However, disease duration was less than 10 years in only one subject, indicating that studies on patients with shorter disease durations are required to determine whether GM demyelination is an early or late event.

Bö et al found no statistical difference in the degree of demyelination in the cerebral cortex between MS subtypes, although there was a trend towards more extensive demyelination in progressive disease forms (16% in RR, 23% in SP, 37% in PP)[127]. A large post-mortem study of 52 MS cases reported greater cortical demyelination in patients with PP or SPMS (median 13% of cortex demyelinated) than in acute or RR cases (0% and 3% respectively), suggesting that a high degree of cortical demyelination may be a pathological correlate of disease progression[133]. WM lesion loads were similar in the different clinical subgroups. Similarly Kutzelnigg et al reported that cortical demyelination in the cerebellum was extensive in progressive MS, but sparse in acute and RR disease[242].

Due to a paucity of PP and RR cases in our study we have been unable to investigate the influence of MS subtype on the extent of demyelination in the cerebral cortex and other GM structures. We note that, in the single RR case (case 6, **table 2.2**) 18.7% of the cingulate cortex was demyelinated, suggesting that extensive cortical demyelination is not exclusively a feature of progressive disease. Interestingly no cerebral cortical plaques were detected in the two PPMS cases (cases 11 and 14), while two of the cases of progressive MS (cases 5 and 14) showed no demyelination of the cerebellar cortex. However we acknowledge that, in comparison with other studies, we have examined smaller areas of cortex.

Due to a lack of detailed clinical information we are unable to explore the functional consequences of GM plaques. It has been suggested that GM plaques in the cerebral cortex may play a role in mood disturbance, cognitive impairment, fatigue and – less commonly – seizures in MS[129, 132, 134, 271]. Similarly lesions in the cerebellar cortex and the spinal cord may be relevant clinically. It is not uncommon to observe striking cerebellar ataxia in the absence of prominent MRI changes[272], a phenotype that could potentially reflect extensive demyelination in the GM of the cerebellum, with relative sparing of the WM. More sophisticated in vivo imaging techniques are required in order to explore the clinical correlates of these GM lesions in more detail.

2.5 Conclusion

We demonstrate substantial variation in the extent of both GM and WM demyelination between different regions of the CNS. Of the areas examined, GM demyelination was most extensive in the spinal cord and cerebellum, while WM demyelination was most prominent in the spinal cord. Demyelination was greater in the GM than in the WM at each of the anatomical sites. Further work is required to better characterise these GM plaques in order to understand both the factors that influence lesion topography and the apparent preponderance for GM demyelination in MS.

Figures

Figure 2.1

*Paraffin sections from control (**A, C**) and MS cerebral cortex (**B, D-F**), immunohistochemically stained with anti-Proteolipid Protein antibodies. **A, C** - Myelin staining in the motor cortex of a control; staining is reduced in the cortical grey matter (GM) in comparison to the subcortical white matter (WM), particularly in the superficial cortical layers, seen more clearly at higher magnification (**C**). **B** – Type III subpial lesion extending over the majority of the cingulate gyrus (open arrows indicate lesion border). **D** – A different type III plaque at high magnification demonstrating complete myelin loss in the subpial tissue. In comparison to subpial lesions, type I (**E**) and type II (**F**) lesions are generally smaller and often perivenular in distribution. The dashed lines represent the GM/WM boundaries. Scale bars (**C-F**) represent 500µm.*

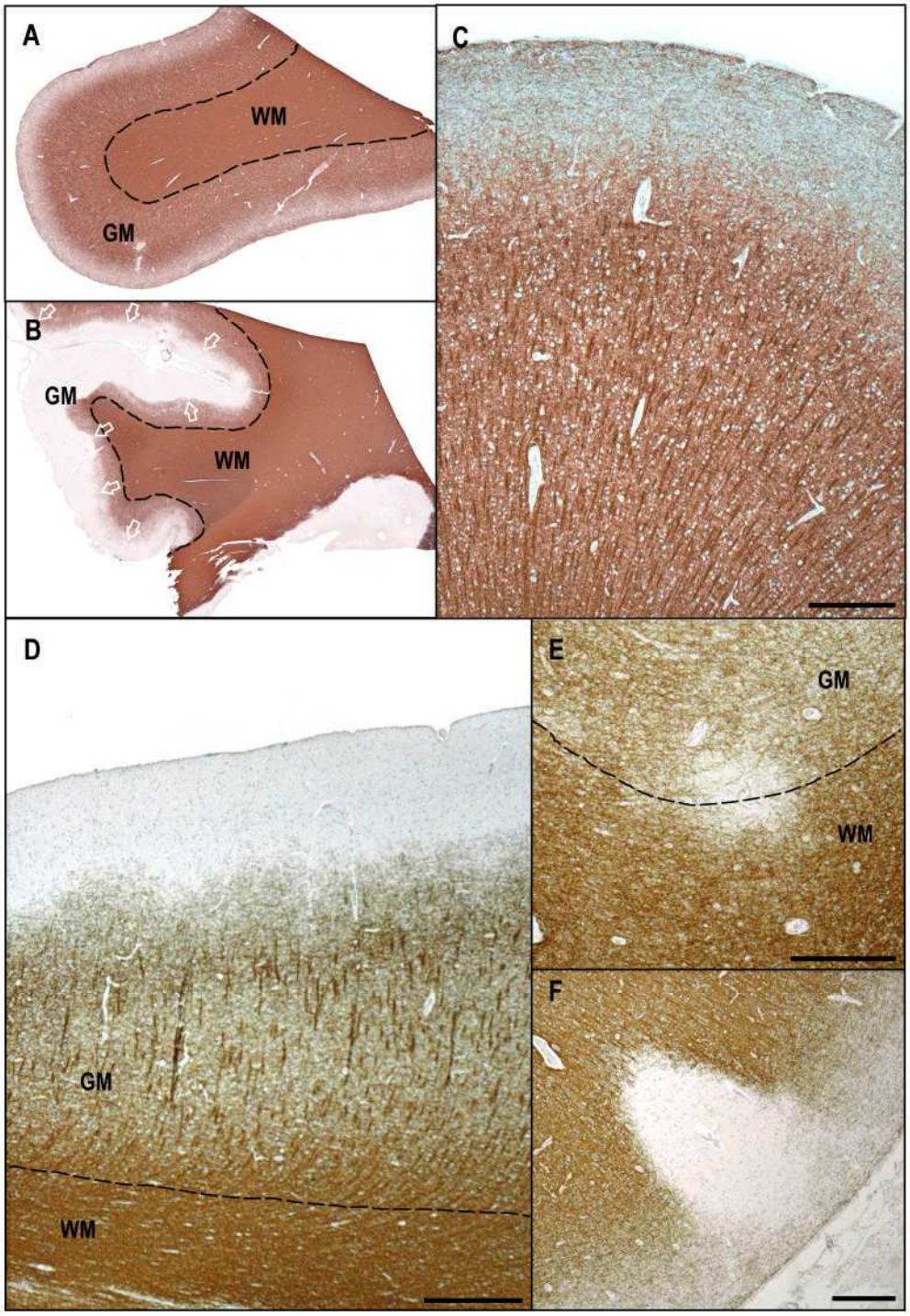
A
WM
GM
B
GM
WM
C
D
GM
WM
E
GM
WM
F

Figure 2.2

*Paraffin sections from control (**A - D**) and MS cerebellar cortex (**E - I**), immunohistochemically stained with anti-Proteolipid Protein antibodies. **A, B** - Myelin staining in a control case; in comparison with the white matter (WM) of the cerebellum, there is a relative paucity of myelin within the granular cell (Gr) and purkinje (Pu) layers of the cerebellar cortex, while the outermost molecular (Mo) layer is devoid of myelin, even in the non-diseased state. **C, D** – Myelin staining density in the Pu (**C**) and Gr (**D**) layers at higher magnification. **E** – Mixed grey matter (GM) / WM lesions in the cerebellar cortex of an MS case; a similar plaque viewed at higher magnification (**F**) shows demyelination of both the digital WM and the cortical GM of a folia. **G, H** – A proportion of cerebellar plaques are characterised by a complete loss of myelin within the cortex, with sparing of the adjacent subcortical WM, so that the lesion boundary shows a strict respect for the GM/WM boundary. **I** – demyelination in the Gr layer is invariably accompanied by myelin loss in the Pu layer, and vice-versa. The scale bars in **B, F** and **G** represent 500μm; in **C, D, H** and **I** they represent 50μm.*

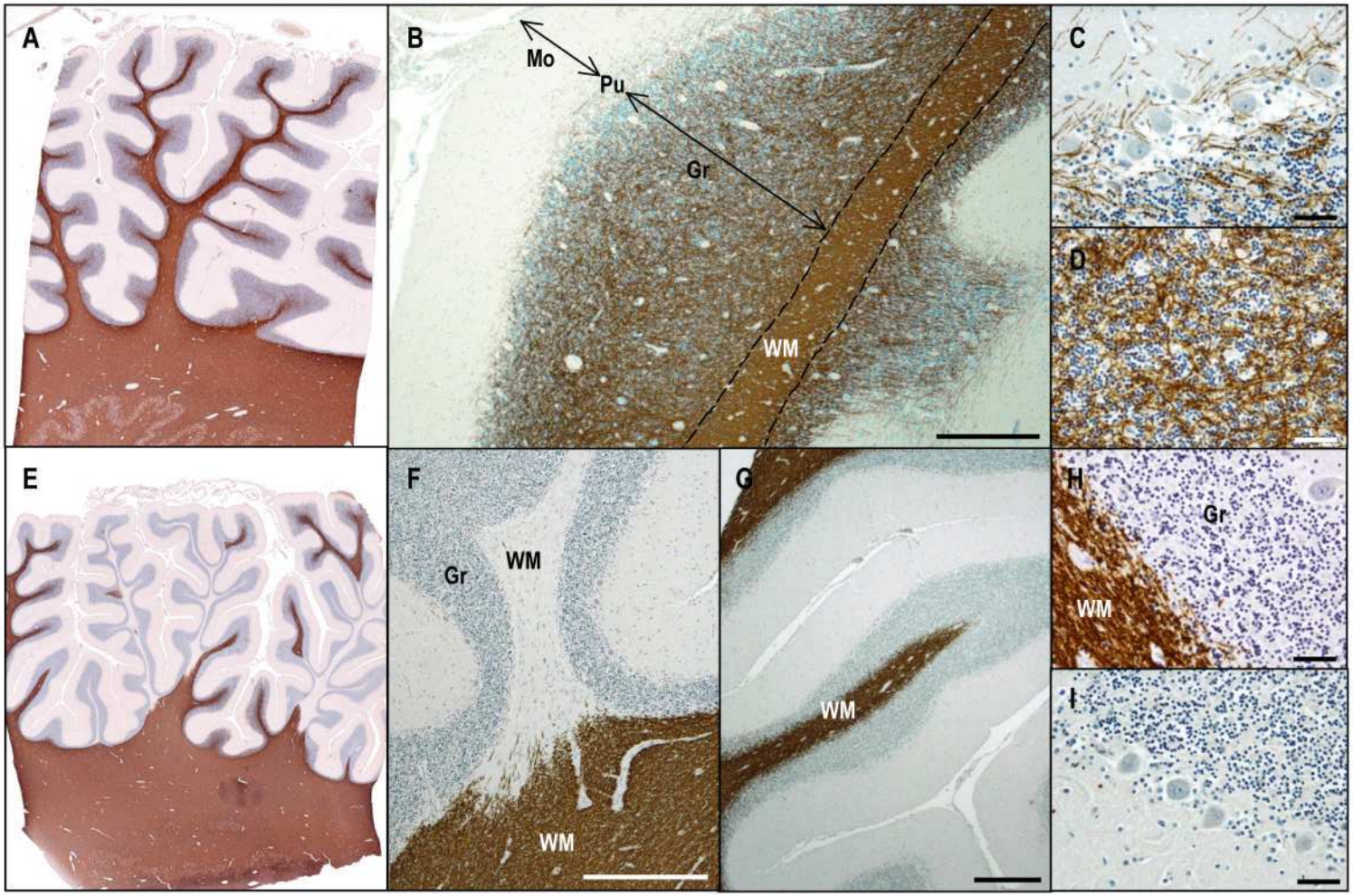
A
B
Mo
Pu
Gr
WM
C
D
E
F
Gr
WM
WM
G
WM
H
Gr
WM
I

Figure 2.3

*Paraffin sections from the thalamus (**A – D**) and the spinal cord (**E – G**) stained with anti-Proteolipid Protein antibodies. **A** – Control case, showing gray matter (GM) nuclei interspersed with white matter (WM). **B – G** MS cases. **B** – multiple demyelinated plaques, largely within the GM. **C** – subependymal periventricular plaque lying within the GM, also seen at higher magnification (**D**); the morphology is somewhat reminiscent of the type III cortical plaques. **E** – two mixed GM/WM plaques in the cervical cord, both display a complete disregard for the GM/WM boundary. There is a paucity of myelin staining within the Substantia Gelatinosa, which is also observed in the non-diseased state (not shown). **F, G -** A proportion of plaques within the spinal cord maintain a strict respect for the GM/WM boundary. At higher magnification (**G**) a thin layer of demyelination is seen affecting the subpial WM at the periphery of the cord (open arrows). The dashed lines represent the GM/WM boundaries. Scale bars (**D, G**) represent 500μm.*

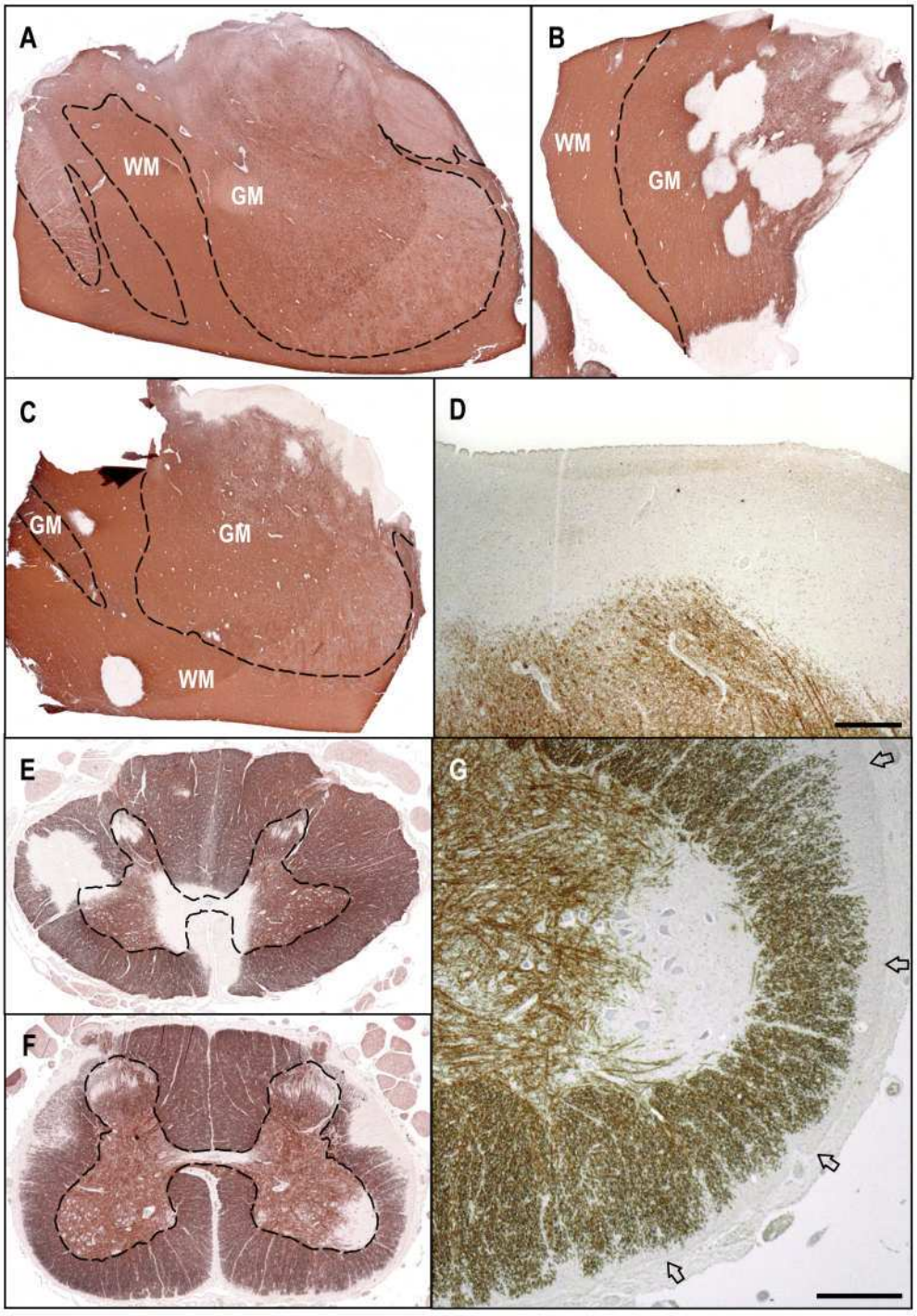
A
WM
GM
B
WM
GM
C
GM
GM
WM
D
E
F
G

Figure 2.4

Bar chart illustrating the proportion of grey matter (GM) that is demyelinated and the proportion of white matter (WM) that is demyelinated at the different CNS sites. Values represent mean ± standard error. Spinal cord values represent the pooled results from the three cord levels.

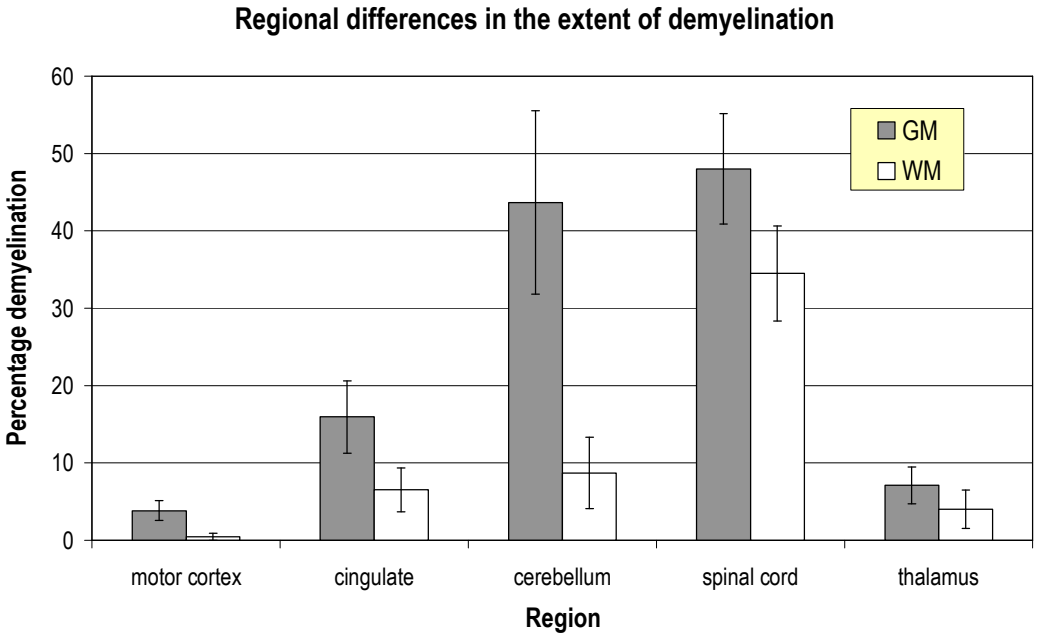

Table 2.1

*Frequency of lesions in the five anatomical regions. Spinal cord values represent the pooled results from the three cord levels. *Pure GM lesions; i.e. lesions that are restricted to the GM and do not impinge on the adjacent WM. **Tissue sections consist of cerebral cortex and subcortical WM. GM = grey matter, WM = white matter.*

Location	**Tissue sections examined**	**Areas of GM demyelination**		**Areas of WM demyelination**	
		Number	**Proportion that are pure GM lesions***	**Number**	**Proportion that are pure WM lesions**
Cingulate**	13	20	90%	9	77.8%
Motor cortex**	12	28	100%	2	100%
Deep GM	13	36	87.5%	13	61.5%
Cerebellum	13	79	50.6%	41	56.1%
Spinal Cord	37	42	16.7%	70	14.3%

Case	Age	Gender	Disease Duration	MS Subtype	Motor cortex % Demyelinated Area		Cingulate % Demyelinated Area		Cerebellum % Demyelinated Area		Thalamus % Demyelinated Area		Spinal cord % Demyelinated Area	
					GM	WM	GM	WM	GM	WM	GM	WM	GM	WM
1	62	F	22	SP	11.5	0	11.4	14.0	23.6	2.2	NA	NA	26.1	32.7
2	81	F	37	SP	NA	NA	8.8	9.1	7.4	0	0	0	25.9	15.6
3	56	F	25	SP	5.0	0	34.4	0	90.2	2.6	14.1	0	49.3	26.8
4	45	F	16	SP	8.9	0	24.3	0.1	100	59.1	6.0	0	NA	NA
5	58	F	22	SP	0	0	0	0	0	0	0	0	49.9	21.5
6	46	F	6	RR	0	0	18.7	0	0	0	18.1	0	NA	NA
7	59	F	20	SP	0	0	0	0	74.8	8.3	0.4	0	13.6	2.2
8	70	F	26	SP	6.0	0	41.7	0	77.2	1.9	11	21.0	52.7	30.0
9	44	F	18	SP	1.6	0	20.8	12.4	85.3	24.1	27.0	26.7	70.6	48.7
10	71	F	32	SP	2.4	0.2	0.5	0	12.0	12.1	0.6	0	0	0
11	56	F	33	PP	0	0	0	0	2.7	3.2	0	0	100	94.6
12	48	F	32	SP	NA	NA	NA	NA	NA	NA	0	0	90.4	53.3
13	44	M	19	SP	10.9	5.5	46.8	15.7	94.5	0	10.7	4.7	72.6	70.1
14	53	F	NA	PP	0	0	0	33.7	0	0	4.7	0	0	0

Table 2.2

The proportion of GM that is demyelinated and the proportion of WM that is demyelinated in each region in the 14 MS cases examined. Spinal cord values represent the pooled results from the three cord levels. GM = grey matter, WM = white matter, SP = secondary progressive, RR = relapsing remitting, PP = primary progressive, NA = information not available.

Chapter 3: The extent and pattern of Grey Matter demyelination in the spinal cord in Multiple Sclerosis

3.1 Introduction

The spinal cord is a predilection site for demyelination in MS[21, 24, 204, 243]. For example, in an MRI study of 80 MS patients, 74% were found to have spinal cord lesions[205]. Furthermore, the cord is a common site for MS relapses, with lesions more frequently resulting in clinical symptoms than brain lesions[206]. Involvement of this clinically eloquent area also contributes substantially to motor, sensory and sphincter disturbance in progressive forms of the disease.

The topographic distribution of MS plaques in the spinal cord has been examined in detail using histochemical staining techniques[21, 24]. These studies suggest that plaques occur throughout the length of the cord, particularly at the cervical level[24]. Fog described three characteristic patterns of plaque corresponding to the three WM columns[21] (**figure 3.1**). Posterior column lesions typically involved the central portion of the WM, with sparing of the lateral portions of the tract and the cord surface. The dorsal region of the lateral column was also reported to be a predilection site for plaques, where lesions often had a wedge-shaped outline in transverse section and extended to the pial surface of cord, involving the pyramidal tracts. Oppenheimer hypothesised that these plaques may be precipitated by mechanical stresses, transmitted to small vessels of the cord through the dendiculate ligaments[24]. Involvement of the anterior WM tracts was relatively infrequent with the exception of symmetrical areas of demyelination on either side of the anterior median fissure[21].

According to Fog, many spinal cord plaques arose on the course of small veins and venules[21]. At the point of maximal cross-sectional area plaques typically surrounded a radial vein, involving both WM and GM. From here the plaque followed the ascending and descending tributaries of the vein which coursed vertically within the WM; as it extended in cranial and caudal directions the plaque tapered and became limited to the WM. Therefore, while plaques predominantly affected the WM, they often impinged on the GM, displaying a total disregard for anatomical boundaries, including the GM / WM boundary[21, 24, 204]. However spinal cord GM demyelination was not examined in detail.

We have previously demonstrated that the spinal cord GM is a predilection site for demyelination in MS, suggesting that the conventional myelin staining techniques used in previous studies substantially underestimated GM involvement. In this much larger study we perform a more extensive and detailed assessment of spinal cord pathology in MS, using PLP IHC to assess the extent and pattern of GM demyelination at five different cord levels. We hypothesise that GM involvement parallels WM involvement, with the cervical cord showing preferential involvement. Furthermore, we compare the utility of LFB staining with myelin protein IHC in detecting myelin loss in this area.

3.2 Materials and methods

3.2.1 Clinical material

Human autopsy material was obtained from 36 pathologically confirmed cases of MS and 12 controls. This material was derived from the neuropathology department, Oxford Radcliffe NHS Trust. The cases were selected at random from a collection of 55 MS cases and 33 controls studied previously[79, 101, 203]. The MS patients (16 male, 20 female) were aged 32-79 years (mean 59, median 58) with disease durations of 2-43 years (mean16, median 15). The controls (6 male, 6 female), aged 33-77 years (mean 59, median 63), had no clinical or pathological evidence of neurological disease.

3.2.2 Preparation of the sections

For each of the MS and control cases 6µm formalin-fixed paraffin-embedded transverse sections were taken from 5 predetermined levels of the spinal cord, irrespective of macroscopic appearance (upper cervical, lower cervical, upper thoracic, lower thoracic and lumbar levels).

3.2.3 Immunohistochemistry

Sections were stained using the EnVision method as described in **Chapter 2.2.3**. The primary antibodies used were mouse anti-Myelin Proteolipid Protein (IgG2a, clone number plpc1, dilution 1:3000, MCA839G, Serotec) and rabbit anti-human GFAP (dilution 1:4000, Z0334, DAKO).

3.2.4 Histochemical Staining

In order to compare LFB- and PLP-staining for detecting GM demyelination in the spinal cord, 30 sections were stained with LFB Cresyl Violet using a protocol described previously[273].

3.2.5 Measurement of GM and WM lesions

The PLP-stained sections were scanned in a slide scanner (Nikon Super Coolscan 4000) to produce a digital image. Using these images the MS lesions were manually outlined using image analysis software ("AnalySIS Pro" running SIS software). Lesions were defined as sharply demarcated areas, characterised by either complete myelin loss or markedly reduced myelin density on the PLP-stained sections (**figure 3.2**). Areas of demyelinated GM and WM were measured separately (**figure 3.3**). In addition, the cross-sectional areas of the spinal cords and the cross-sectional GM areas were measured in order to calculate the proportion of GM that was demyelinated (P_{GMd}) and the proportion of WM that was demyelinated (P_{WMd}). The PLP-stained sections, examined via microscopy (10x, Leitz Dialux 20EB microscope), were used as a reference to help identify the MS lesions and the GM boundaries.

3.2.6 Statistical analysis

Paired t tests were used to compare P_{GMd} with P_{WMd}. Correlations between P_{GMd} and P_{WMd} were assessed using Spearman's ranked test. Multiple regression analyses were used to examine the influence of age, sex, cord location and disease duration on P_{GMd} and P_{WMd} ("Stata" version 9, StataCorp, Texas USA).

3.3 Results

3.3.1 PLP Immunohistochemistry

The distribution of myelin in the GM of the non-diseased human spinal cord has been described using histochemical staining[274]. Consistent with this study we found considerable regional variation in myelin density within the GM, with a paucity of myelinated fibres in the Substantia Gelatinosa of the dorsal horns, the GM commissure and – in the thoracic cord – the lateral GM column (**figure 3.4 A-G**). Between controls there was a degree of inter-individual variability, particularly within the GM commissure (**figure 3.4 B, G**).

3.3.2 Lesion counts

In the 150 sections studied from the 36 MS cases, 262 areas of demyelination were detected in the WM and 194 areas were detected in the GM. 86 of the 262 WM lesions (33%) were restricted to the WM and did not impinge on the GM. 43 of the 194 GM lesions (22%) were restricted to the GM and did not involve the WM. It has previously been reported that the vast majority of lesions in this spinal cord material are inactive[101]. In keeping with this we observed evidence of ongoing demyelination (i.e. macrophages containing LFB- or PLP-inclusions) in only four lesions (two WM lesions and two mixed WM/GM lesions).

3.3.3 Demyelination is more extensive in the GM than the WM of the spinal cord

Overall, P_{GMd} (mean 33.3%) was significantly greater than P_{WMd} (19.7%) ($p < 0.0001$). Similarly, when the 5 cord levels were analysed separately, P_{GMd} was greater than P_{WMd} at the upper cervical ($p = 0.0247$), upper thoracic ($p = 0.0001$), lower thoracic ($p = 0.0003$) and lumbar ($p = 0.0021$) levels (**figure 3.5**). The difference did not reach statistical significance at the lower cervical level ($p = 0.0751$). There was a significant correlation between P_{GMd} and P_{WMd} ($r = 0.8316$, $p < 0.0001$).

P_{WMd} was highest at the upper cervical level (31.8%). To examine this further P_{WMd} was regressed on the cord level controlling for age, sex and disease duration. In comparison with the upper cervical level, P_{WMd} was significantly reduced at the lower thoracic (coefficient of regression = -0.1514, $p = 0.036$, that is, controlling for other variables, P_{WMd} was on average 15% greater at the upper cervical than the lower thoracic level) and lumbar (coefficient of regression = -0.2163, $p = 0.001$) levels. In addition there was a trend towards significant reductions at the lower cervical ($p = 0.054$) and upper thoracic ($p = 0.053$) levels.

In comparison to the upper cervical cord, and controlling for other variables, cord level did not appear to have a significant influence on P_{GMd} (lower cervical $p = 0.079$, upper thoracic $p = 0.759$, lower thoracic $p = 0.471$, lumbar $p = 0.198$).

Similar results were obtained when we considered only the areas of complete demyelination (i.e. when areas of markedly reduced myelin density were excluded from the statistical analysis). The proportion of completely demyelinated GM (28.4%) was greater than the proportion of completely demyelinated WM (17.5%) ($p < 0.001$). When the 5 cord levels were analysed separately, the proportion of completely demyelinated GM was greater at the upper

cervical (p = 0.0275), upper thoracic (p = 0.0001), lower thoracic (p = 0.0018) and lumbar (p = 0.0034) levels (**figure 3.6**). The difference did not reach statistical significance at the lower cervical level (p = 0.1856).

There is considerable variation in both the total cross-sectional area and the WM:GM ratio between the different levels of the spinal cord[275]. We have controlled for this variation by assessing the proportion of the tissue that is demyelinated, rather than the absolute area. We note that the absolute area of demyelinated WM is greater than the area of demyelinated GM, simply reflecting the substantially greater volume of WM in the cord.

3.3.4 Influence of age, sex and disease duration on extent of demyelination

Age (coefficient of regression = -0.0095, $p < 0.001$) appeared to have a significant influence on P_{WMd}, with younger patients having greater WM demyelination. There was a trend for gender to influence P_{WMd}, with demyelination being more extensive in males (coefficient of regression = 0.08695, p = 0.055). Disease duration did not significantly influence P_{WMd} (p = 0.140).

Both age (coefficient of regression = -0.0087, p = 0.001) and gender (coefficient of regression = 0.1326, p = 0.043) appeared to have a significant influence on P_{GMd}, while disease duration did not (p = 0.225).

3.3.5 Lesion morphology

A large number of WM lesions show a similar morphology to those described previously using conventional staining techniques[21, 24]. Predilection sites include the central portion of the posterior columns and the lateral columns, where the plaques frequently have a wedge-shaped outline in transverse section and impinge on the GM (**figure 3.7**).

Within the GM, plaques showed no obvious preponderance for any particular region; lesions frequently involved the anterior horns, posterior horns and the GM commissure, often in combination. In a number of cases a proportion of the border of the GM plaque maintains a strict respect for the GM/WM boundary. This pattern of residual plaque morphology, which has not been described previously, was observed in both mixed GM/WM lesions and pure GM lesions (**figure 3.8, A-H** and **figure 3.9, K-L**). The myelin content of the WM immediately adjacent to these demyelinated areas of GM appeared normal using both LFB- and PLP-

staining, even when examined at high magnification. Conversely, we did not observe areas of demyelinated WM with sparing of the adjacent GM.

In a number of other cases, completely demyelinated areas of GM were observed adjacent to areas of WM with an obvious reduction in myelin staining density with PLP and LFB-staining (**figure 3.8, I-K**). Overall, out of the 105 sections that contained at least one GM plaque, 55 contained a GM plaque where a proportion of the plaque border maintained a strict respect for the GM/WM boundary. Such plaques were observed in 22 of the 36 cases, with disease durations ranging from 5 years to 34 years.

3.3.6 GFAP expression within GM and WM plaques

GFAP staining within demyelinated areas is highly variable. Staining density was increased in some GM and WM plaques; in other plaques staining was reduced in comparison with corresponding areas of myelinated tissue. GM plaques frequently showed evidence of astrocytic activation (**figure 3.9**). Gliosis is further discussed in **Chapter 6**.

3.3.7 The sensitivity of Luxol Fast Blue for detecting GM demyelination

For a number of the PLP-stained sections (n = 30), adjacent sections were stained with LFB to evaluate the utility of this stain for detecting GM demyelination in the spinal cord. These sections were selected to include a range of patterns of demyelination as demonstrated using the PLP staining. Lesion morphology was more readily appreciated using myelin protein IHC, which provides greater contrast between the myelinated and demyelinated tissue. However all of the areas of GM demyelination were detected by thorough examination of the LFB-stained sections at high magnification, particularly when informed by the PLP-stained sections (**figure 3.10**).

3.4 Discussion

Detailed post-mortem studies have used conventional histochemical myelin stains to examine the topology of MS plaques within the spinal cord, demonstrating that the cord is a predilection site for demyelination, which generally occurs in a "peri-venular" distribution[21, 24]. We re-evaluate pathology in this clinically eloquent site, using myelin protein IHC to assess the extent and pattern of GM demyelination. In comparison with the previous work - Fog examined 8 MS cases, while Oppenheimer studied 18 - we have used autopsy material from 36 MS cases,

examining pathology at five different cord levels. We have also studied a large number of control cases. Considerable variations in myelin density were observed in these subjects, both between individuals and between the different GM laminae, highlighting the importance of using control material to define the normal limits of myelin content.

While Oppenheimer simply reported the frequency of MS plaques at various levels of the spinal cord[24], we also evaluate the extent of WM and GM demyelination. Lesion number is a crude measure of MS pathology, particularly when comparing WM and GM involvement; simply reporting lesion number is likely to underestimate the degree of GM pathology as lesions frequently fuse in the GM, often in the vicinity of the central canal[21]. For example, using our system for counting lesions, the section in **figure 3.3C** would be scored as containing 3 WM lesions and one GM lesion.

We demonstrate that the proportion of GM that is demyelinated is greater than the proportion of WM that is demyelinated throughout the spinal cord, further challenging the view that MS is a predominantly WM disease. Although we do not have detailed clinical information regarding disability, it is possible that these GM plaques have substantial functional consequences, contributing to motor, sensory and bladder dysfunction. Animal studies demonstrate that GM-specific injuries in the spinal cord can result in substantial deficits, including paraplegia[276] and pain syndromes[277], even in the absence of damage to the WM tracts.

We have scored the material for MS plaques by visually inspecting the sections, both at low and high magnification, rather than using an automated intensity-based technique whereby an MS plaque is defined as an area with a myelin staining intensity below a particular threshold. While an automated method is likely to be less subjective and more time-efficient, there are potential limitations. As discussed previously, there are regional variations in myelin density within the GM. Furthermore, given the marked reduction in axonal density in the MS cases[79], one may expect the staining intensity of the "normal appearing" tissue to be reduced in these sections. Both of these factors should be considered when inspecting for areas of demyelination, but are difficult to accurately incorporate into a threshold-based technique. Finally it is not always possible to identify the GM/WM boundary using an intensity threshold-based technique, particularly in the demyelinated state.

We note that we occasionally observe areas of WM with more subtle reductions in myelin densities that do not fulfil our criteria for an MS plaque. These changes were extensive in several cases and were most evident on inspection of the WM at high magnification (**figure 3.2, H-K**). We have not attempted to quantify these changes, largely because they could reflect any one of a number of different pathological changes. We have previously reported a 30% reduction in corticospinal tract axonal density in this MS cohort[79]. These measurements were made outside of MS plaques[79]. Such reductions in axonal density are likely to result in secondary reductions in myelin staining density. However, numerous other pathological abnormalities are observed in the non-lesioned WM, including gliosis, inflammatory cell infiltration and oedema, all of which may result in a reduction in myelin staining density[25, 30, 33-35, 37-39, 133]. Interpretation of the staining pattern is further complicated by the fact that – as a result of axonal loss and tissue atrophy – the myelin staining density may actually "pseudo-normalise". Finally the staining intensity will not necessarily be directly proportional to the density of myelinated axons; Pistorio et al noted that myelin protein IHC saturates at a medium-to-high concentration of myelin and therefore may not be optimal for looking for subtle degrees of myelin loss outside of MS plaques[278].

In some cases these areas of reduced myelin staining may be difficult to differentiate from MS plaques with markedly reduced myelin density, which most likely represent partially remyelinated lesions. Consequently, we may have either underestimated, or overestimated, the extent of demyelination, particularly in the WM. However, in contrast to MS plaques, which have sharply demarcated borders, we would expect areas of Wallerian degeneration to appear as poorly demarcated areas of reduced myelin density with ill-defined contours[64]. Therefore we are confident that these factors have not had a significant influence on our results. We note that our measurements are highly reproducible (see "**Reproducibility of measurements**", **section 2.2.6**). Furthermore, when we consider only the areas of complete myelin loss (i.e. there is clearly less subjectivity in defining completely demyelinated lesions), we still observe a preponderance for GM - rather than WM - demyelination.

The cervical cord is often described as a predilection site for MS plaques. Oppenheimer reported that approximately 90% of sections from the upper and lower cervical cord show MS lesions, in comparison with 46% of thoracic and 41% of lumbar cord sections[24]. The cross-sectional area of the spinal cord is greatest at the lower cervical level; by correcting for this (i.e. by considering the *proportion* of demyelinated WM) our results suggests that the lower cervical

cord is no more extensively involved than other levels. The reason that the upper cervical cord is preferentially involved is unclear. One contributing factor may be that extensive plaques in this region tend to cause particularly disabling symptoms (i.e. quadraparesis) and may therefore be over-represented in an autopsy series. We find no significant difference in the extent of GM demyelination between cord levels.

Our results suggest that gender influences the extent of both WM and GM demyelination with more extensive demyelination being evident in males. There is little evidence suggesting differences in MRI lesion loads in the brain between male and female MS patients. In a study of SPMS, Li et al reported that male patients had greater T2 lesion loads than females, although females showed a greater accumulation of gadolinium-enhancing lesions over the subsequent 3 years[279]. MS tends to run a more aggressive course in male patients [280-282] and there is some evidence from post-mortem studies that axonal loss in the spinal cord is more severe in males [77]. However, interpretation of our finding is limited; owing to a lack of clinical information the multiple regression analysis does not control for MS clinical subtype, which has been reported to influence lesion loads in imaging studies[215, 283-287].

Brain MRI lesion load measures are generally lower in PPMS than in other MS phenotypes[215, 283-287]. Fewer studies have compared lesion loads in the spinal cord between different MS subtypes. Some imaging studies suggest that focal cord lesions are more frequently seen in SPMS than in PP cases[285, 288], while others report no differences between subtypes[215, 287]. Examining a cohort of 19 patients with progressive MS (10 PPMS, 9 SP disease), Kidd et al performed serial brain and spinal cord imaging over a 1 year period[215]. During this time 132 active brain lesions appeared (85% occurred in the SP group), in comparison with only 6 new cord lesions (3 in each subtype). It has been reported that, in comparison with RR and SP disease forms, PPMS patients often have extensive, diffuse MR abnormalities in the spinal cord[284, 288, 289]. Nijeholt et al suggested that these diffuse changes correspond histopathologically with areas of “partial demyelination”, but these have not been characterised further[289]. Whether there are differences in the extent of spinal cord demyelination between different MS subtypes is an important question, but one that we have been unable to address in the current study.

It is likely that MS patients who die soon after diagnosis, or at a younger age, will tend to have more aggressive disease. This may explain our observation that age appears to influence the

extent of WM and GM demyelination, whereas disease duration does not. It is less likely that spinal cord lesion load plateaus after a short time period following which disease duration has little influence on demyelinated area; longitudinal imaging studies indicate that T2 lesion load measures in the brain increase over time, even between 10 and 14 years disease duration[290]. An additional consideration when interpreting post-mortem studies is that plaques may have undergone several phases of evolution (i.e. demyelination, re-myelination and repeated demyelination)[291].

There are limitations to using single sections to examine lesion topology and it is possible that a proportion of "pure" GM lesions expand into the WM as the plaque extends in cranial and caudal directions. However, our study suggests that the majority of GM lesions in the spinal cord are mixed GM/WM lesions. In contrast the majority of cortical lesions lie entirely within GM[127, 131-134]. Consistent with these observations - and our previous study - we find a strong correlation between the degree of GM and WM demyelination in the spinal cord while there is no such correlation in the brain[133]. Spinal cord plaques may extend over a variable distance, ranging from only a few millimetres to several spinal segments in length[225]. Further studies – using either serial sections or potentially post-mortem MRI - are required to examine the three-dimensional topology of spinal cord plaques in more detail.

Many MS plaques are seen on the course of small veins and venules[21]. However we demonstrate that in many cases a proportion of the border of the GM plaque maintains a strict respect for the GM/WM boundary. This pattern of plaque morphology, which has not been described previously, does not appear to occur in a purely "perivenular" distribution. These plaques show similarities to the type IV lesions of the cerebral cortex[127] and the extensive areas of demyelination that we frequently observe in the cerebellar cortex, both of which are characterised by full-thickness cortical demyelination, with sparing of the subcortical WM. Therefore, in all three lesion patterns, a proportion of the lesion border corresponds exactly to the GM/WM boundary, suggesting a common pathogenic mechanism. Unfortunately we have little insight into plaque morphology during the early stages of lesion development, as the majority of plaques in our post-mortem series are likely to be longstanding. We observe evidence of ongoing demyelination in only two of the GM lesions; the plaque borders did not respect the GM/WM boundary in either of these lesions. It is therefore unclear whether the pattern of residual plaque morphology that we observe at autopsy reflects the morphology of

the demyelinating lesion *per se*, or demyelination with subsequent remyelination of the WM, but not the GM, portion of the lesion.

There may be differences in the glial-cell environment between GM and WM which predispose to extensive GM demyelination with sparing of the adjacent WM. There are phenotypical differences between inflammatory cells in WM lesions and those in the GM; the majority of MHC class II-positive cells in active WM plaques are macrophages, while those in cortical GM lesions have the morphology of microglia[130]. There are also phenotypical differences between astrocytes in WM and GM (the GM contains protoplasmic astrocytes while the WM contains fibrous astrocytes)[292, 293] and differences related to the oligodendrocyte-myelin complex. For example, a proportion of oligodendrocytes (so-called satellite or perineuronal oligodendrocytes) are exclusive to the GM, where they lie opposed to the perikarya of neurons[125, 126]. There is evidence that the topography of lesions in EAE is determined, in part, by the target autoantigen. T-cells that recognise MBP or PLP induce disease predominantly affecting areas with thick myelin sheaths, while MAG- or MOG-induced disease primarily involves areas containing thinner sheaths[25, 294]. Interestingly, T cells specific for GFAP or the nonmyelin autoantigen S100β, a calcium binding protein expressed and secreted by astrocytes, mediate inflammation which is more pronounced in the GM than the WM[294, 295]. Similarly, antigenic differences between the GM and WM may render the GM more vulnerable to immune-mediated attack in MS.

Bö et al suggested that demyelination in type IV lesions may be mediated by a myelinotoxic factor in the interstitial fluid (i.e. the fluid that bathes the brain parenchyma) [127]. Soluble factors can exchange between the CSF, the perivascular (Virchow Robin) spaces and the interstitial fluid via a number of pathways[269, 270, 296]. Drainage of a myelinotoxic factor along these predetermined anatomical routes may influence plaque topography in MS[240]. In the cerebral cortex interstitial fluid preferentially drains along perivascular channels to the CSF, while a substantial volume of interstitial fluid in WM also spreads diffusely through the extracellular spaces between the nerve fibres, draining into the ventricular CSF[296]. Therefore, interstitial fluid – along with any myelinotoxic factor that it may contain – may be cleared more efficiently from WM than from GM[269, 270, 296]. These differences may be further exaggerated in the diseased state as BBB breakdown and oedema – which are more prominent in WM than GM plaques[135, 136] - may facilitate the bulk flow of fluid out of the brain parenchyma[297]. Therefore GM/WM differences in the clearance of a myelinotoxic agent may be expected to produce areas of GM

demyelination with sparing of the adjacent WM, consistent with those observed in the spinal cord, cerebral cortex and cerebellar cortex. A myelinotoxic substance originating in the interstitial fluid could also potentially circulate within the Virchow-Robin space (resulting in perivenular demyelination) and the CSF (mediating subpial and periventricular demyelination)[11].

Alternatively the GM may have a poor ability to remyelinate in comparison to the WM, due to numerical or functional differences in oligodendrocyte precursors between GM and WM. The "spared" WM immediately adjacent to the GM plaques appears normal on the LFB- and PLP-stained sections (**figure 3.8, A-H**); if these areas of WM were remyelinated we may have expected the LFB-staining to demonstrate abnormally thin myelin sheaths leading to an overall reduction in myelin staining density[36]. However, we acknowledge that remyelination is more reliably assessed using more sensitive techniques[36]. Consistent with this hypothesis we observe that some plaques are characterised by completely demyelinated areas of GM adjacent to areas of WM with reduced myelin density (**figure 3.8, I-K**). It is possible that these areas of markedly reduced myelin density represent areas of remyelination, although there are other potential explanations for this pattern of staining (e.g. extensive axonal loss, oedema etc.) as discussed previously. Further work, using electron microscopy or Toluidine blue-stained resin sections, is therefore required to look for evidence of remyelination in areas of WM directly adjacent to demyelinated GM plaques which appear to respect the GM/WM boundary.

To our knowledge GM remyelinaton in MS has not been examined in detail. Merkler et al report that following cortical demyelination in a rat model of MS, demyelinated areas are repopulated with oligodendrocytes and extensive remyelination occurs within 2 weeks[240]. It is feasible that the paucity of GM plaques observed in acute and RRMS[133] actually reflects rapid and extensive cortical remyelination early in the disease course, but that this remyelinating capacity becomes exhausted with repeated episodes of demyelination[240].

There is evidence that GM lesions show a reduced number of inflammatory cells in comparison to WM plaques[130, 135, 222], although this has not been demonstrated in the spinal cord specifically. The induction of acute inflammation stimulates remyelination in animal models of chronic demyelination[299]. Animal studies also suggest that both macrophages and lymphocytes facilitate remyelination[300, 301]. Weerth et al have suggested that the complement factor C5 promotes remyelination following inflammatory-mediated injury, demonstrating that C5-deficient

mice with chronic EAE show a reduced ability to remyelinate in comparison with control animals[302]. Interestingly, Brink et al report that GM MS lesions in the cortex show markedly reduced complement deposition in comparison to WM lesions[137]. It is therefore interesting to speculate that the GM environment may be less conducive to remyelination than the WM in MS.

In contrast to the highly-specific IHC staining there is a degree of background staining associated with the LFB Cresyl Violet, resulting in less contrast between the myelinated and demyelinated tissue. While GM demyelination was more readily appreciated using myelin protein IHC, the great majority of plaques were also detected by LFB-staining. This is not the case in the cerebral cortex where a significant proportion of GM plaques are not detectable using conventional histochemical stains, even when inspected alongside the corresponding IHC-stained sections[127]. This may reflect, in part, differences in myelin density between the GM of the spinal cord and that of the cerebral cortex. Furthermore, identification of the GM portion of the mixed GM/WM lesions – which constitute a large proportion of GM lesions in the cord - is aided by following the plaque border from the WM portion of the plaque into the GM. The fact that LFB, which stains the phospholipid component of the myelin sheath, reveals a similar pattern of plaque morphology confirms that the staining pattern obtained with the IHC is not unique to this particular PLP antibody.

3.5 Conclusion

We demonstrate extensive GM demyelination in the spinal cord in MS, with a proportion of plaques showing a distinct morphology that has not been described previously. A greater understanding of these GM plaques may provide important clues regarding MS pathogenesis and mechanisms of disability in the disease. Further work is required to establish whether the pattern of residual plaque morphology that we observe reflects differences in the extent of demyelination between WM and GM in the cord or a relative failure of remyelination in the GM.

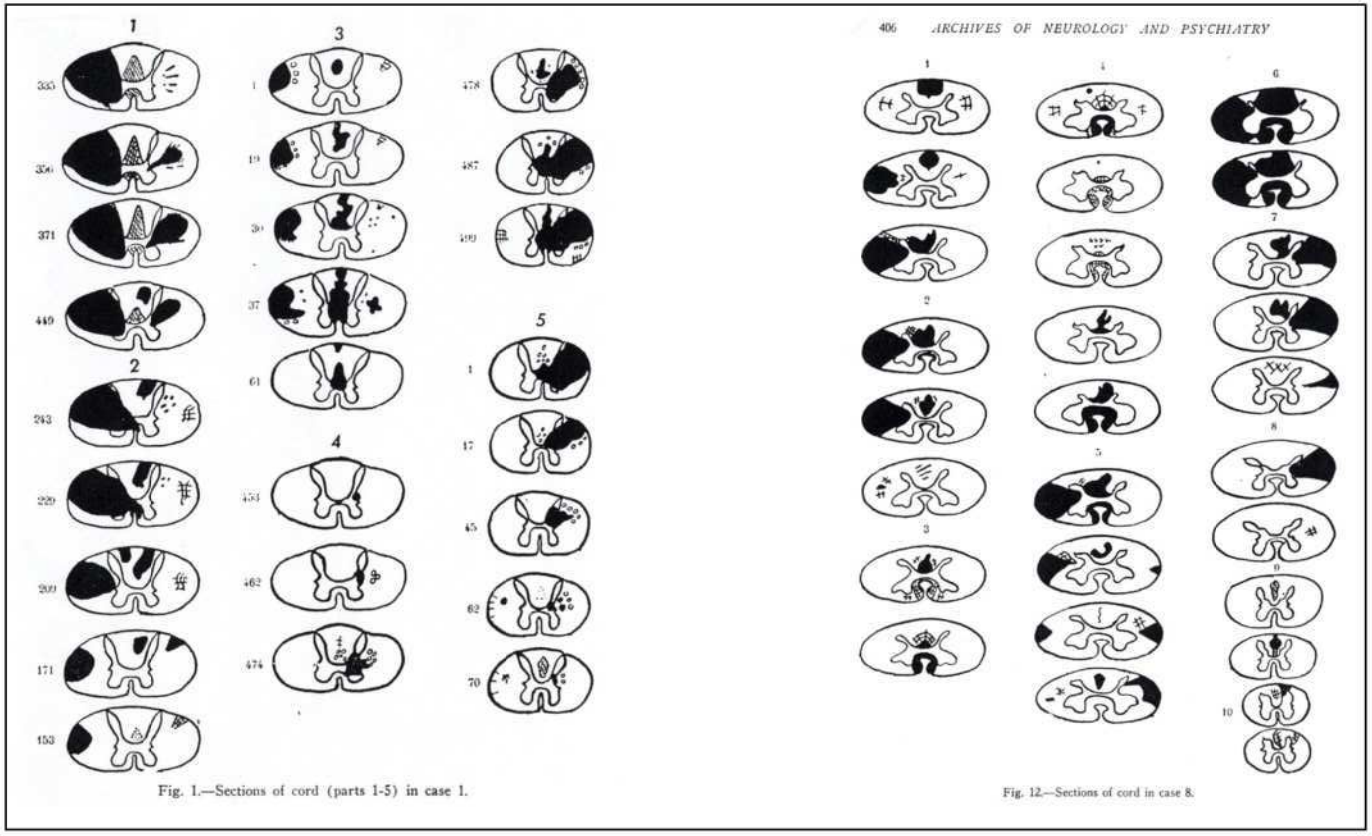

Figure 3.1 - *Illustrations from Fog's paper "Topographic distribution of plaques in the spinal cord in multiple sclerosis", published in the Archives of Neurology and Psychiatry in 1950. Fog used serial sections, taken over extensive lengths of spinal cord, to study the topographic distribution of plaques in 8 MS cases. Plaques often impinged on the grey matter of the cord. For example, wedge-shaped lesions of the lateral white matter columns frequently extended into the dorsal horns, while the grey matter surrounding the central canal was a typical site for the fusion of lesions. Fog reported that many plaques arose on the course of small veins and venules.*

Figure 3.2

*Paraffin sections from MS (**A-E, H-K**) and control spinal cords (**F-G**), immunohistochemically stained with anti-Proteolipid Protein antibodies (**A-G, H, J**) and Luxol Fast Blue (**I, K**). **A** – Extensive demyelination in the lumbar cord. Areas of complete myelin loss (green box, also shown at high magnification in **B**) and markedly reduced myelin density (red box, **D**) are observed in the grey matter. Similarly, the white matter contains areas of complete myelin loss (blue box, **C**) and markedly reduced myelin density (orange box, **E**).*

***F, G** - Areas of grey matter (**F**) and white matter (**G**) in a control case demonstrating normal myelin content.*

***H, I** - Other areas of white matter show less striking reductions in myelin density that do not fulfil our criteria for an MS plaque. **J, K -** Higher magnification images from panels H and I (boxes) demonstrating these changes more readily.*

*Scale bars (**B-G, J, K**) represent 50μm.*

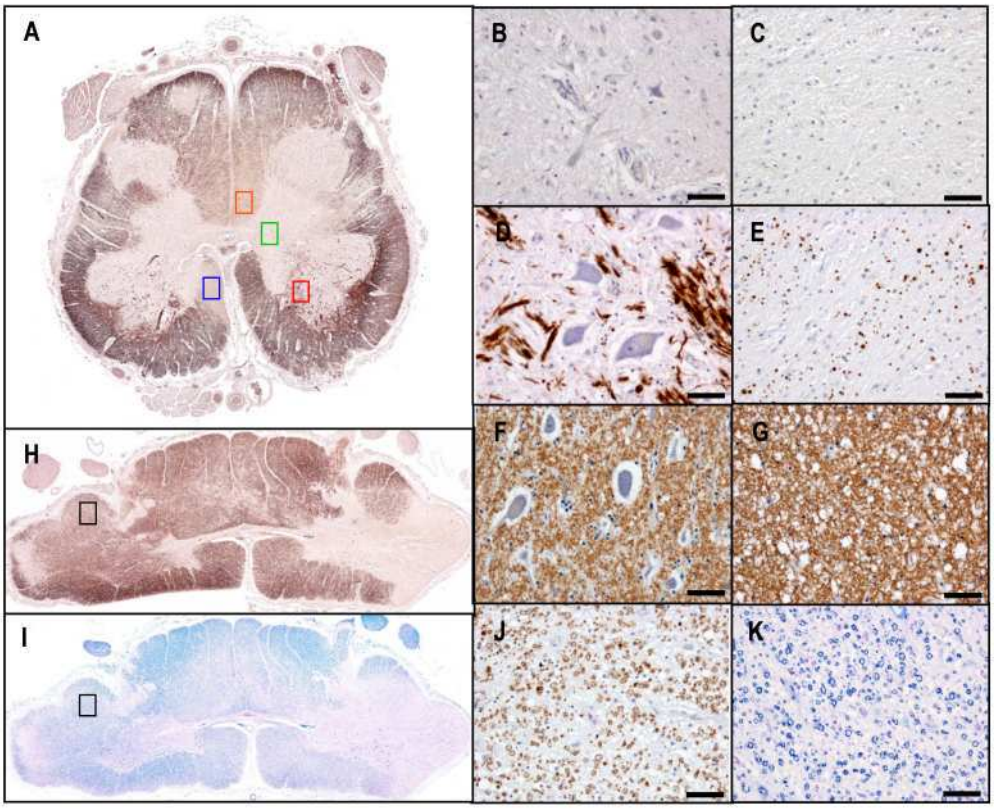
A
B
C
D
E
F
G
H
I
J
K

Figure 3.3

Paraffin sections from MS spinal cords, immunohistochemically stained with anti-Proteolipid Protein antibody. ***A, C*** *- Sections were scored for lesions, defined as sharply demarcated areas characterised by either complete myelin loss or markedly reduced myelin density. Areas of demyelinated grey matter and white matter were measured separately; according to this system panel* ***A*** *contains two grey matter lesions and one white matter lesion, while panel* ***C*** *contains one grey matter lesion and four white matter lesions.* ***B, D*** *– The lesions are shaded (white and grey), and the grey matter / white matter boundary outlined (black lines).*

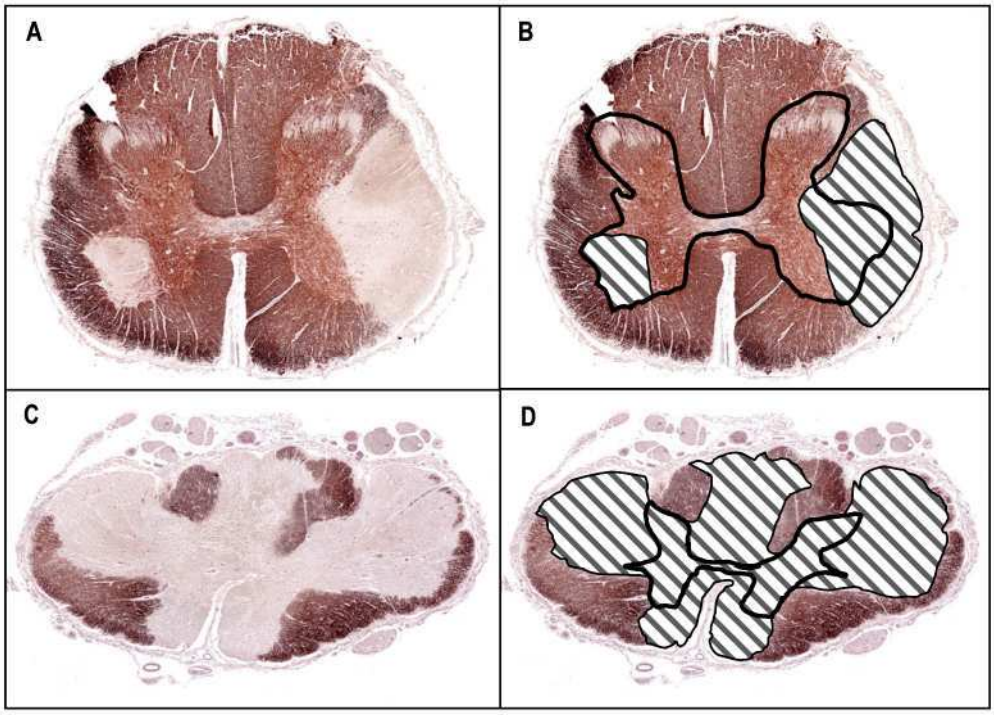
A
B
C
D

Figure 3.4

*Paraffin sections from control (**A-G**) and MS (**H-K**) spinal cords stained with anti-Proteolipid Protein (PLP) antibodies (**A-H, J**) and Luxol Fast Blue (LFB)(**I, K**).*

***A.** Staining in the non-diseased cord demonstrating a paucity of myelin in the grey matter commissure (solid box) and the Substantia Gelatinosa (dashed box), shown at a higher magnification in panels **B** and **C** respectively. **D**. In the thoracic cord there is also a paucity of myelin in the lateral horn of the grey matter. **E -** Higher magnification image from panel D (box). **F, G** - Grey matter commissure in a different control demonstrating a reduction in myelin density in comparison with panels A and B.*

***H-K.** Sections from MS spinal cords stained with PLP antibodies (**H**) alongside an adjacent section stained with LFB (**I**). **J-K** - Higher magnification images from boxes in panels H and I. A number of pure GM plaques are characterised by a complete loss of myelin within the GM commissure, which is more clearly delineated using PLP-staining.*

*Scale bars (**B, C, E, G, J, K**) represent 500μm.*

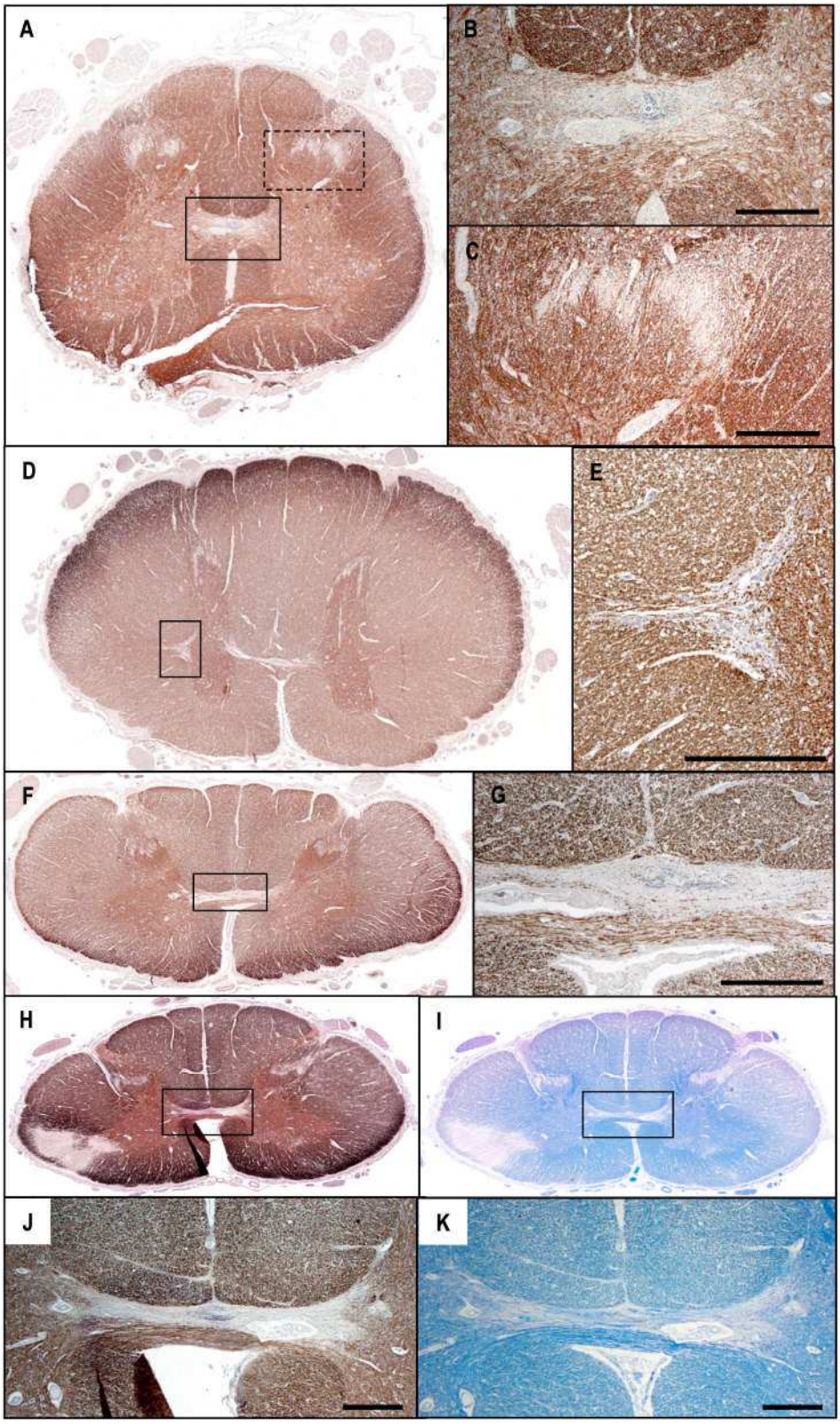
A
B
C
D
E
F
G
H
I
J
K

Figure 3.5

Bar chart of proportion of grey matter (GM) and white matter (WM) that is demyelinated at different levels of the spinal cord. UC=upper cervical; LC=lower cervical; UT=upper thoracic; LT=lower thoracic; Lum=lumbar. Values represent mean ± standard error.

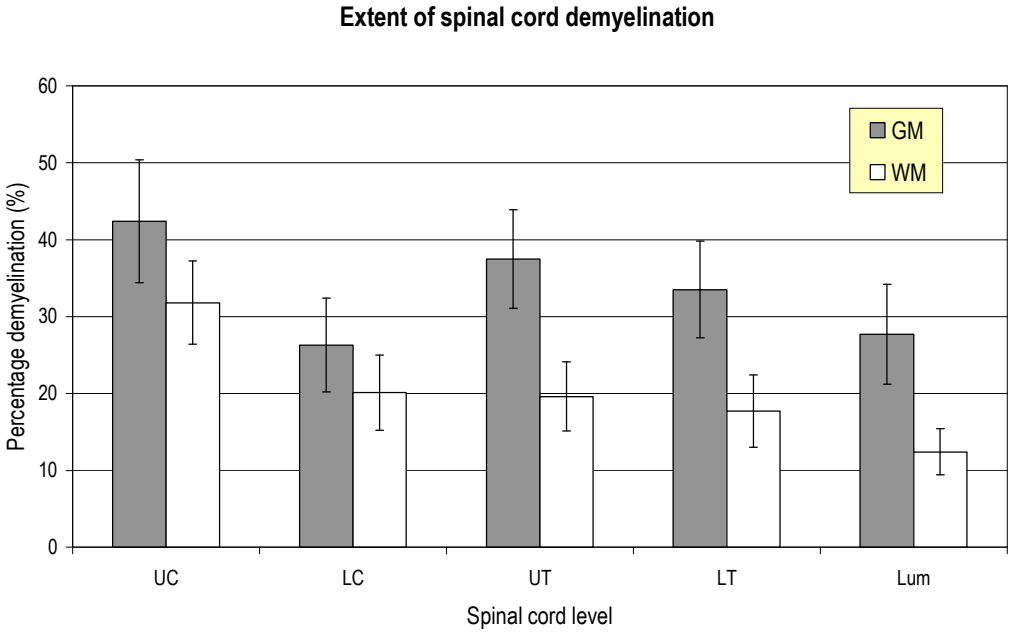

Figure 3.6

Bar chart of proportion of grey matter (GM) and white matter (WM) that is completely demyelinated at different levels of the spinal cord. UC=upper cervical; LC=lower cervical; UT=upper thoracic; LT=lower thoracic; Lum=lumbar. Values represent mean ± standard error.

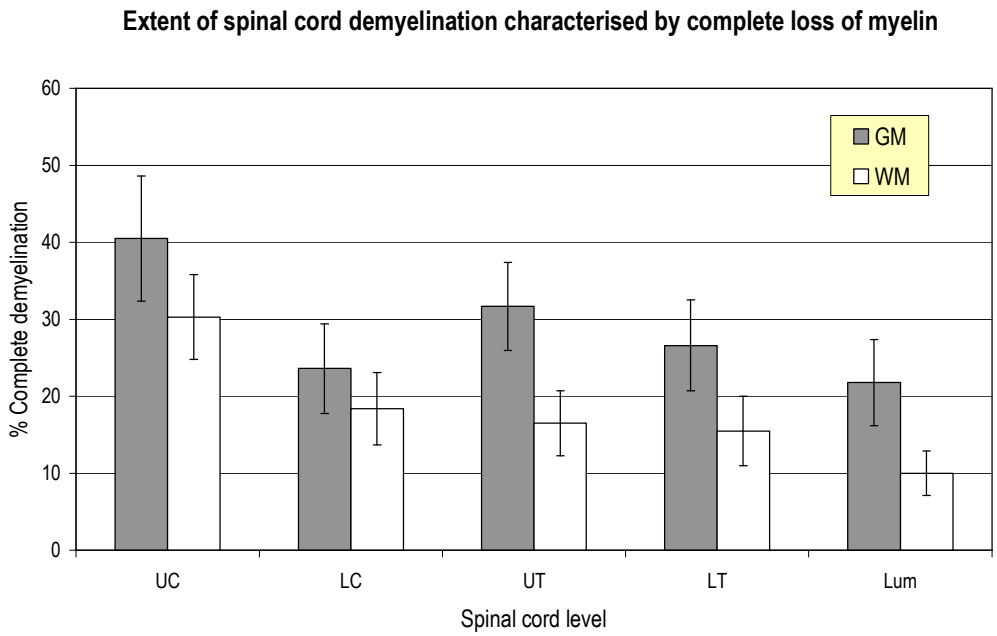

Figure 3.7

*Paraffin sections from MS spinal cords, immunohistochemically stained with anti-Proteolipid Protein antibody. Many MS plaques show a similar morphology to those described previously using conventional staining techniques for myelin. The principal predilection sites for white matter (WM) plaques are the central portion of the posterior columns (**A**) and wedge-shaped plaques in the lateral columns which frequently extend laterally to the pial surface of the cord and medially to the grey matter (GM), displaying a complete disregard for the GM/WM boundary (dashed line) (**B**). **C** - Involvement of the anterior WM tracts is relatively infrequent with the exception of "paramedian" lesions, symmetrical areas of demyelination on either side of the anterior median fissure. **C** - Lesions frequently "fuse" within the GM and show a striking symmetry about the midline.*

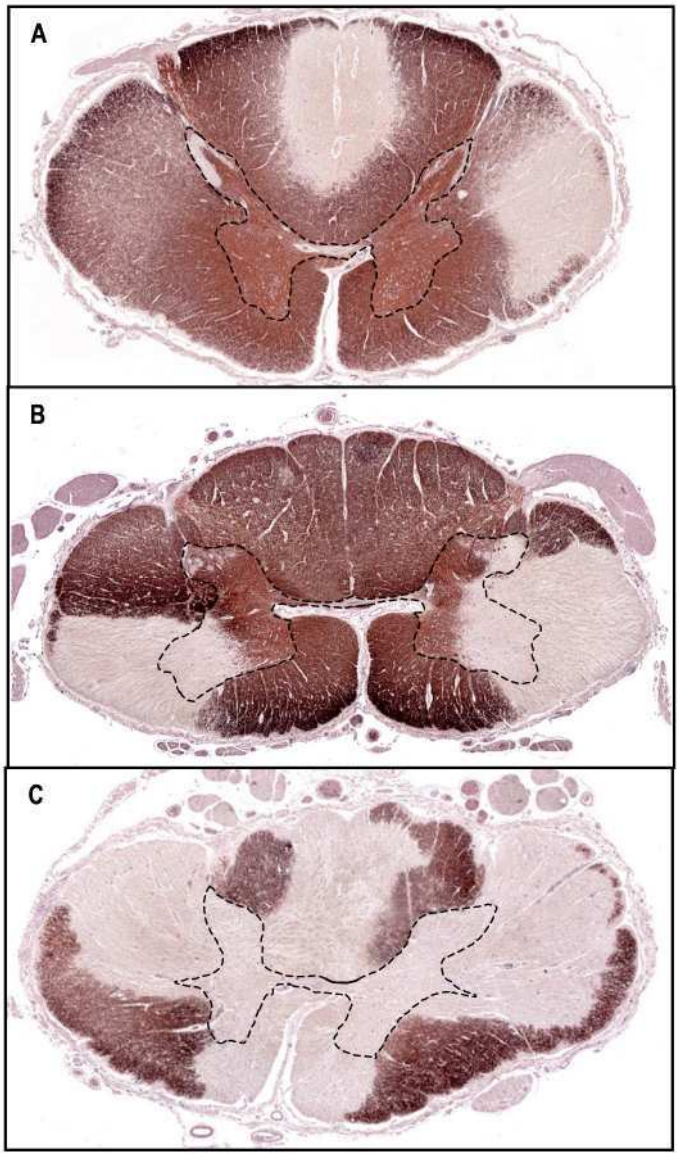
A
B
C

Figure 3.8

*Paraffin sections from MS spinal cords stained with anti-Proteolipid Protein (PLP) antibodies (**A, B, E-G, I, J**) and Luxol Fast Blue (LFB)(**C, D, H, K**). A proportion of mixed GM/WM (**A, C**) and pure GM lesions (**E, G, H**) appear to "expand" within the GM whilst maintaining a strict respect for the GM/WM boundary. **A, C** - Lesion morphology demonstrated using both PLP- and LFB-staining. **B, D -** Higher magnification images from panels A and C (boxes) demonstrate complete demyelination of the GM commissure while the myelin in the adjacent WM appears entirely normal using both LFB- and PLP-staining. **E** - Lesion involves the entire right anterior horn, respecting the GM/WM boundary, and extends to the contra-lateral GM horn via the GM commissure. **F -** High magnification image from panel **E** (box) demonstrating sparing of the adjacent WM. **G, H -** The GM lesion on the left respects the GM/WM boundary. **I -** In some cases, completely demyelinated areas of GM were observed adjacent to areas of WM with subtle reductions in myelin staining density. **J, K -** PLP- and LFB-stained sections corresponding to the area of reduced myelin staining intensity from panel I (box) at high magnification. Scale bars (**B, D, F, J, K**) represent 150µm.*

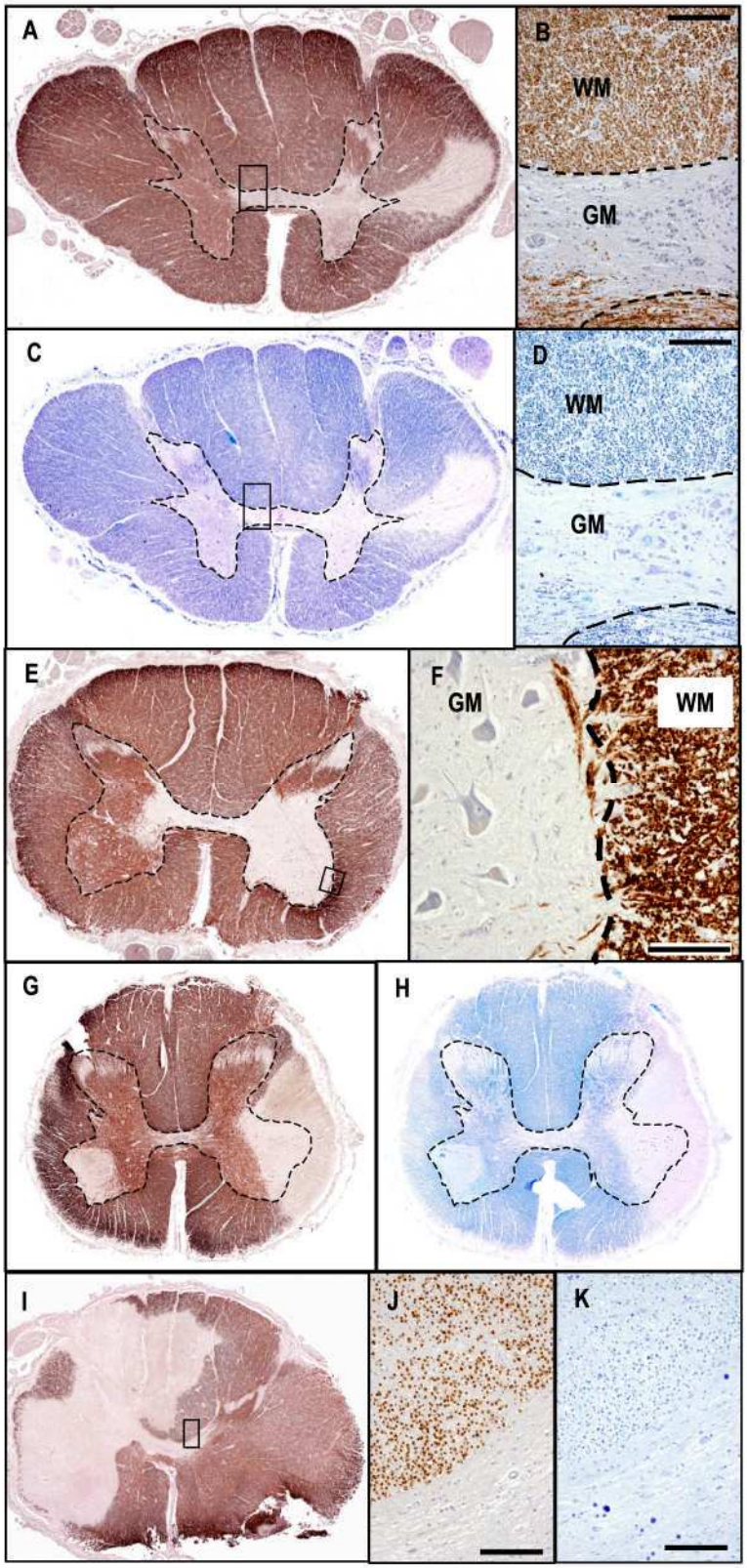
A
B
WM
GM
C
D
WM
GM
E
F
GM
WM
G
H
I
J
K

Figure 3.9

*Paraffin sections from MS (**A - F, H, I, K, L**) and control (**G, J**) spinal cords stained with anti-Proteolipid Protein antibodies (**A - C**) and GFAP (**D – F**, corresponding to sections A - C respectively, and **G - L**). GFAP staining in the myelinated white matter (WM) tracts – both in controls (**G**) and MS cases (**H**, corresponding to panel D, black vertical arrow) - is characterised by an abundance of GFAP staining due to a dense network of astrocytic processes, the vast majority of which run longitudinally, buttressing the fibre tracts. **I** (corresponding to panel D, black horizontal arrow) - there is a loss of the isotropic distribution of glial filaments within the WM tracts in the demyelinated state , with a reduction in the density of longitudinally orientated filaments and a substantial increase in the proportion of astrocytic processes running radially in the plane of section (i.e. anisotropic gliosis).*

*The density of GFAP staining in both grey matter (GM) and WM lesions is extremely variable; for example some GM lesions demonstrate an increase in GFAP staining (panel **F**, black arrow) while others show reduced GFAP staining (panel **E**, arrow). This apparent reduction in GFAP staining may represent "dilution" by some other process such as oedema or inflammatory cell infiltration within the MS plaque. Note – the pale staining in the posterior aspect of the spinal cord panel F is artefactual.*

*In comparison to the WM, glial filaments within the myelinated GM of controls (**J**) and MS cases (**K**, corresponding to panel D, white arrow) are aligned haphazardly. There is evidence of astrocytic activation within some GM plaques. For example in panel **L** (high magnification image of GM plaque in panel F, white arrow) the astrocytes have larger cell bodies and more conspicuous nuclei in comparison with myelinated grey matter (K). Scale bars (G-L) represent 50µm.*

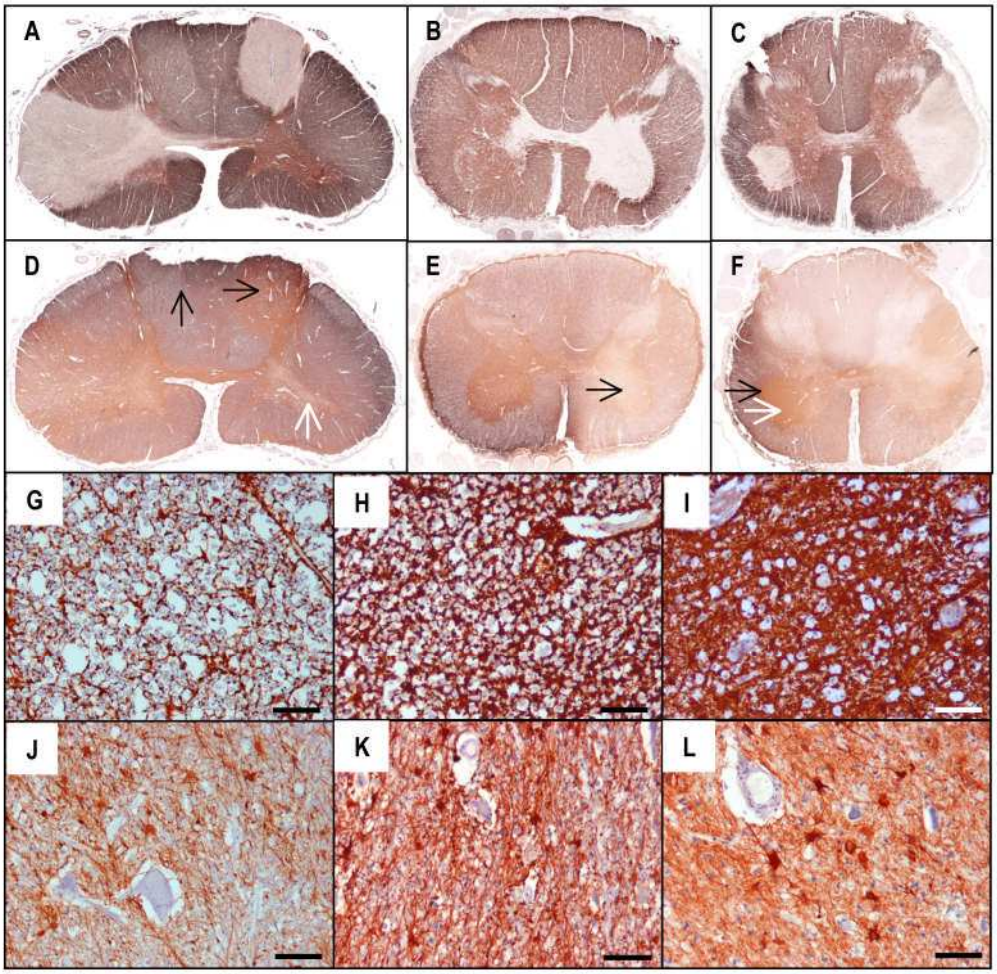
A
B
C
D
E
F
G
H
I
J
K
L

Figure 3.10

*Paraffin sections from MS spinal cords stained with anti-Proteolipid Protein (PLP) antibodies (**A, C, E, G, I, K**) alongside adjacent sections stained with Luxol Fast Blue (LFB) (**B, D, F, H, J, L** respectively). Lesion morphology is more readily appreciated using immunohistochemistry, with the PLP-stained sections demonstrating greater contrast between the myelinated and demyelinated grey matter (GM). **C - F** - Higher magnification images from solid **(C, D)** and dashed **(E, F)** boxes in panels A and B. **G, H** - Pure GM plaque, also shown at high magnification (**I, J**). **K, L** - Demyelination of the GM commissure is more clearly delineated using PLP-staining. Scale bars (**C-F, I, J**) represent 500µm.*

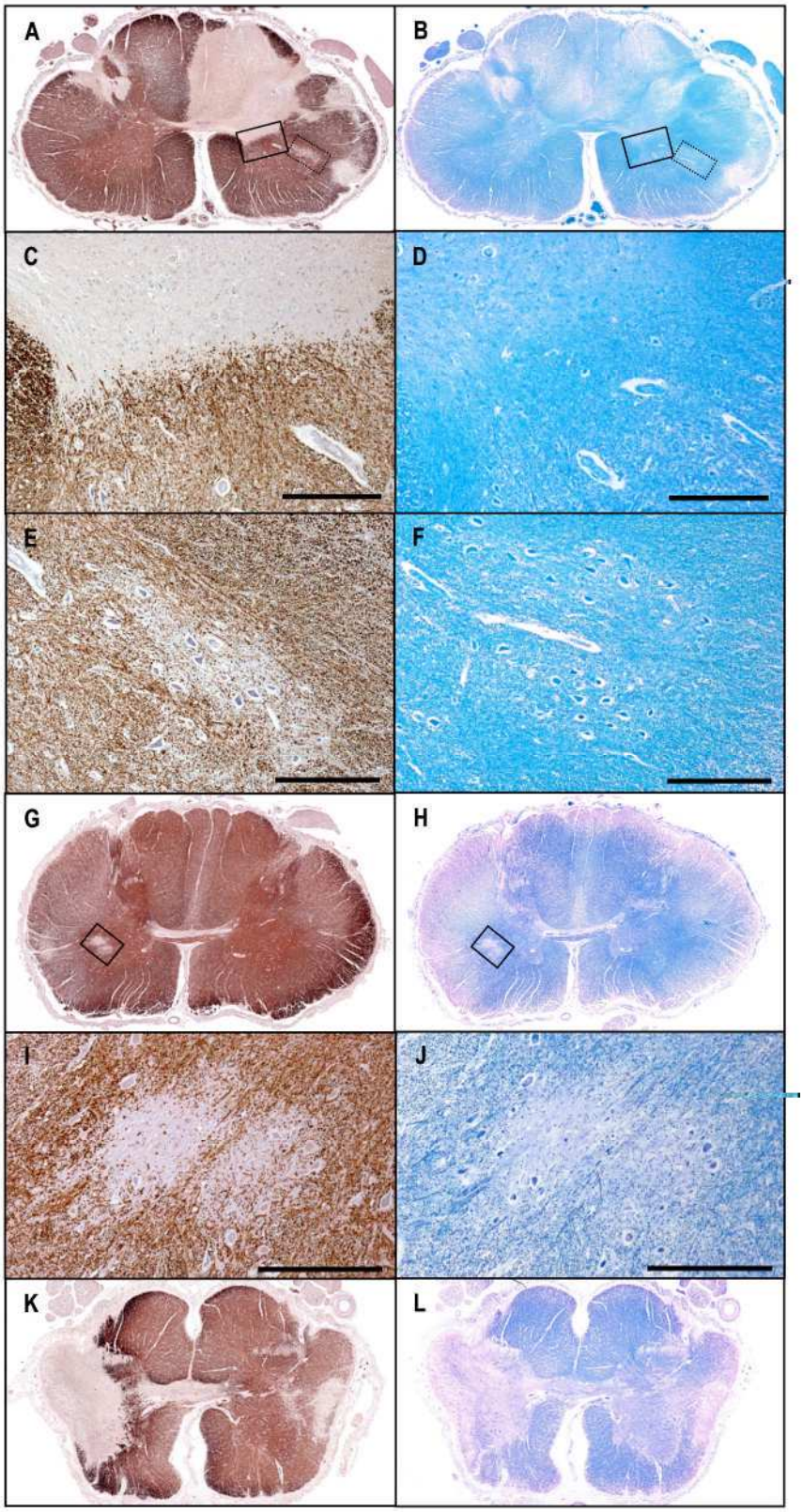
A
B
C
D
E
F
G
H
I
J
K
L

Chapter 4: Spinal Cord atrophy in Multiple Sclerosis - relative contributions of white matter and grey matter tissue loss

4.1 Introduction

Spinal cord atrophy in MS has been shown to correlate with clinical disability in both cross-sectional and longitudinal imaging studies[110, 212]. However, the relative contribution of WM and GM tissue loss to spinal cord atrophy has not been adequately examined. Characterising the extent of GM atrophy in this clinically eloquent site is required in order to better understand mechanisms of permanent disability in MS.

4.1.1 Evidence of GM atrophy in the brain in MS

A number of MRI-based techniques have been used to quantify GM volume loss in MS including a variety of segmentation-based and automated registration-based methods[303]. Different methods vary in terms of accuracy, reproducibility and efficiency with operator-independent, automated techniques being highly reproducible and therefore particularly suitable for longitudinal studies[184, 195, 304-308].

A number of cross-sectional MRI studies have examined the relative contributions of WM and GM volume loss to brain atrophy in MS, with some apparently inconsistent results. These are likely to reflect a combination of methodological factors and differences between the patient cohorts. A small number of reports suggest brain atrophy is attributable to WM - but not GM - volume loss[118, 309]. Other studies indicate reductions in both WM and GM volumes[139, 184, 192, 194, 310] while some groups report that brain atrophy is predominantly[311] - or exclusively[195, 312] - due to GM volume loss. Consistent with this work, three longitudinal MRI studies have reported progressive GM atrophy in the MS brain in the absence of WM volume loss[138-140].

4.1.2 Atrophy in specific GM structures

Reductions in normalised cortical volumes have been reported in both RR and PPMS in comparison to controls[181, 185, 191]. Sailer et al reported that cortical thinning predominantly involves fronto-temporal regions, a finding supported by Prinster et al[313]. More disabled patients and those with longer disease durations also showed thinning of the motor cortex[314]. Somewhat consistent with these studies, Carone et al reported cortical atrophy predominantly

involving frontal and parietal areas[311]. Cortical atrophy has also been reported in longitudinal studies[193, 196]. For example, Chen et al demonstrated cortical thinning in patients with progressive MS over a 1 year period with the parietal and precentral cortex showing the fastest rates of atrophy[193]. Only one post-mortem study has examined cortical atrophy in MS; using material from 21 MS cases and 16 controls, Wegner et al demonstrated a 10% reduction in neocortical thickness in the MS cases, with thinning being most prominent in the motor cortex[131].

Atrophy has also been demonstrated in the thalamus, caudate and other deep GM structures, both in cross-sectional[157, 158, 304, 313, 315] and longitudinal imaging studies[196, 316]. In addition to imaging the thalamus *in vivo*, Cifelli et al quantified thalamic pathology using post-mortem material from 10 MS patients and 10 controls, reporting a mean 21% reduction in volume in the medial dorsal nucleus in the MS cases[157].

4.1.3 Mechanisms of GM atrophy in MS

The substrate of GM atrophy in MS is poorly understood. Loss of neuronal tissue – both neuronal shrinkage and neuronal loss - is likely to contribute, as suggested by both post-mortem[157, 317] and MRS studies[153, 154, 157, 158]. Demyelination, gliosis and axonal / dendritic loss may also contribute to volume loss[130, 318].

One potential mechanism of atrophy is a direct effect of local GM demyelinating lesions. Myelin loss alone is unlikely to explain the extent of atrophy given the small amounts of myelin in GM[314, 319]; myelin has been estimated to constitute only 3-5% of the GM volume, in comparison with 24% of the WM volume[320], although this figure is likely to vary considerably between different CNS structures. Cortical plaques appear to be associated with neuronal, axonal and dendritic loss[130-132]. However there is little evidence that GM plaques directly cause atrophy; Wegner et al found no correlation between neocortical thickness and extent of cortical demyelination[131].

Alternatively, GM atrophy may occur secondary to the effects of distant WM lesions, through either retrograde or anterograde degeneration. It has been suggested that prominent atrophy of the motor cortex may reflect axonal injury – with secondary retrograde neuronal degeneration – in the corticospinal tracts[131, 193, 314]. The diffusion of neurotoxic factors (e.g. cytokines,

chemokines, reactive oxygen and nitrogen species, excitatory amino acids or proteases), either from nearby WM lesions or via the CSF, may also mediate neuronal pathology[80].

Correlations between WM lesion loads and the extent of GM atrophy in MS vary greatly between studies. Some cross-sectional studies suggest there is no relationship between lesion load measures and GM volume loss[183, 193, 315], while several others show moderate correlations[118, 139, 191, 194, 195, 310, 312-314, 321]. For example, in a large study of 425 early RRMS patients, Charil et al found significant correlations between WM lesion load measures and mean cortical thickness, particularly in the cingulate, insula and associative cortical regions[321]. Several studies suggest that lesion load measures correlate more closely to GM atrophy than to WM atrophy[118, 194, 310, 312]. A number of longitudinal studies have reported correlations between changes in GM volumes and changes in lesion loads[138, 191 , 196, 316] while others have failed to do so[139, 140, 192]. Overall, correlations are at best modest, suggesting that GM atrophy in MS occurs at least partially independently of WM lesions. Potential mechanisms of neuronal pathology in MS are further discussed in **Chapter 5**.

4.1.4 Clinical relevance of GM atrophy

A number of groups have observed correlations between GM volumes and disability measures[191-196, 321] while others have not[118, 139, 312, 313, 315, 322]. In some cases Expanded Disability Status Scale appears to be more closely related to GM atrophy than to WM atrophy[194, 195].

GM atrophy may contribute to cognitive dysfunction and mood disturbance. Amato et al demonstrated lower cortical volumes in cognitively impaired MS patients than in cognitively preserved patients, despite no differences in lesion load measures or brain volume between the two groups[181, 185]. Within the cognitively impaired patients, the cortical volume correlated with scores of verbal memory, verbal fluency and attention. Morgen et al demonstrated correlations between cognitive function and cortical atrophy, with cognitively impaired patients showing more extensive volume loss in frontal, temporal and parietal regions[183]. Sanfilipo et al also suggested that brain volume measures related to neuropsychological performance with GM atrophy being the best predictor of verbal memory, euphoria, and disinhibition[184], while Feinstein et al reported that MS patients with major depression had reduced GM volume in comparison to those without[180].

4.1.5 Spinal cord atrophy in MS

Spinal cord atrophy in MS has been reported in post-mortem studies[203, 210] and in cross-sectional[205, 211-214] and longitudinal imaging studies[110, 215-218]. Atrophy occurs early in the disease course[203, 218, 323] and progressive cord atrophy has been detected over as little as 6 months[110]. A strong correlation between cervical cord volume and disability has been reported in cross sectional studies[108, 109, 205, 211-214, 216, 284]. A number of longitudinal studies have found a correlation between changes in cord area and disability scores[110, 114, 115], although others have not[215-218].

It is unclear whether spinal cord atrophy in MS reflects tissue loss in the WM or GM compartments. Due to the small cross-sectional area of the spinal cord GM, the resolution of current MRI scanners is not sufficiently high to investigate spinal cord GM pathology *in vivo*. Histopathological studies are therefore required. The aim of this post-mortem study is to assess the relative contributions of WM and GM tissue loss to spinal cord atrophy in MS. In view of the extensive GM demyelination in the cord we hypothesise that there will be substantial GM atrophy.

4.2 Materials and methods

4.2.1 Clinical material

Human autopsy material was obtained from 55 pathologically confirmed cases of MS and 33 controls. This material was derived from the neuropathology department, Oxford Radcliffe NHS Trust and comprised all of the MS and control cases available. The MS patients (29 male, 26 female) were aged 25-83 years (mean 57.5 years) with disease durations of 2-43 years (mean 17.1 years). The controls (15 male, 18 female), aged 31-81 years (mean 57.9 years), had no evidence of spinal cord disease. This autopsy material has been used in previous studies[79, 101, 203].

4.2.2 Preparation of the sections

For each of the MS and control cases formalin-fixed paraffin-embedded transverse sections were taken from 5 levels of the spinal cord (upper cervical, lower cervical, upper thoracic, lower thoracic and lumbar levels). 10µm thick sections were stained for neuronal elements with Palgrem silver stain and 15µm sections were stained for myelin with LFB Cresyl Violet using a protocol described by Lowe and Cox[273].

4.2.3 Measurements of GM and WM areas

384 Palmgren silver sections were digitally photographed at low power (Olympus DP10 camera mounted on a Leica WILD MZ8 dissecting microscope). These sections were used to improve the blinding of the observer (CPG) to the disease state, as the myelin-stained sections highlight demyelination. Cases were coded to blind the observer to the clinical information. The cross-sectional GM areas were traced manually on the digital images using image analysis software ("AnalySIS Pro" running SIS software) (**figure 4.1**). The Palmgren silver sections, examined via microscopy (10x, Leitz Dialux 20EB microscope), were used as a reference to help identify the GM boundaries. The cross-sectional area of the spinal cord sections, measured previously[203], was used to calculate the WM cross-sectional area (i.e. total spinal cord area – GM area). A shrinkage factor of 0.71, calculated in our laboratory in a previous study[324], was applied to the measured areas to correct for changes in tissue size as a result of fixation and embedding processes. In this way comparisons can be made between our spinal cord areas, published MRI studies and previous work using this post-mortem material[79, 203].

It was not possible to accurately identify the GM boundaries on a few sections, either because there was a tear in the section or there was gross disruption of the normal tissue architecture secondary to an MS plaque. Measurements were made from 356 of the 384 Palmgren silver sections. It was possible to make measurements from an additional 12 sections using the myelin-stained material. In 16 cases it was only possible to measure the GM area on one half of the section; in these cases this area was doubled to give an estimate of the GM area. It was not possible to make measurements on the remaining 16 sections because the GM boundaries could not be accurately identified.

4.2.4 Validation and reproducibility of methods

To evaluate intra-observer reproducibility the GM areas of 45 randomly selected Palmgren silver sections were measured on two separate occasions, 2 months apart (coefficient of variation=1.36%)[325, 326]. To validate the use of the myelin stained sections for some of the measurements, the GM areas of 15 Palmgren silver sections and the corresponding 15 Luxol Fast Blue sections were measured (coefficient of variation=2.94%). 15 Luxol Fast Blue sections were measured on two separate occasions (coefficient of variation=1.42%). Finally the GM areas on the right hand sides of 15 sections were compared with the GM areas on the left hand sides of the sections (coefficient of variation=4.00%), validating the use of "half-sections" to make a small number of measurements as detailed above.

4.2.5 Statistical analysis

Multiple regression analyses were used to examine the influence of age, sex, cord location, disease state and disease duration on cross-sectional GM and WM area. The regression coefficient was calculated for each of these variables. We do not have detailed clinical information regarding disability and are therefore unable to examine the correlation between clinical disability (e.g. Expanded Disability Status Scale) and tissue atrophy.

4.3 Results

4.3.1 WM area measurements

The cross-sectional WM area of the spinal cord was significantly reduced in the MS cases compared to controls, controlling for age, sex and cord location (coefficient of regression = -5.80, p = 0.001, that is, controlling for other variables, the WM area is reduced in the MS cases by an average of 5.80mm^2). Specifically, the WM area was reduced at the upper cervical (coefficient of regression = -12.17, p = 0.039), lower cervical (coefficient of regression = -10.47, p = 0.035) and upper thoracic (coefficient of regression = -7.50, p = 0.021) levels in comparison to controls, but not at the lower thoracic (coefficient of regression = 0.55, p = 0.836) or lumbar (coefficient of regression = -1.55, p = 0.599) levels. These results are presented in **figure 4.2A**. As expected from previous work[203], the WM area in the MS cases is strongly influenced by the disease duration (coefficient of regression = -0.71, p = 0.001).

4.3.2 GM area measurements

In contrast to the WM area measurements, the cross-sectional GM area was not significantly different between MS cases and controls (coefficient of regression = -0.15, p = 0.705). Similarly, the GM area was not reduced at the upper cervical (coefficient of regression = -0.26, p = 0.754), lower cervical (coefficient of regression = -0.27, p = 0.734), upper thoracic (coefficient of regression = -0.04, p = 0.946), lower thoracic (coefficient of regression = 0.26, p = 0.592) or lumbar (coefficient of regression = -0.51, p = 0.740) levels in the MS cases (**figure 4.2B**). The GM area in the MS cases was not significantly influenced by the disease duration (coefficient of regression = 0.03, p = 0.13).

4.4 Discussion

There is evidence that the degree of spinal cord atrophy in MS correlates with clinical disability[108-110, 114, 115, 205, 211-214, 216, 284]. Neuro-pathological and imaging studies suggests that tissue loss in the brain is not restricted to the WM but also affects GM structures[157, 158, 191, 310, 314]. However, the relative degree of WM and GM atrophy has not been adequately assessed in the spinal cord.

Our series represents the largest post-mortem study of spinal cord atrophy in MS. We use material from 55 MS cases and 33 controls, measuring the cross-sectional GM and WM areas at five different cord levels. The results demonstrate that spinal cord atrophy in MS is due to WM, rather than GM, volume loss.

4.4.1 WM atrophy is restricted to the upper cord

Spinal cord WM atrophy in MS is likely to be driven by axonal loss, although other processes such as myelin and oligodendrocyte loss may contribute[318]. The role of gliotic scarring in atrophy has not been established; it is conceivable that gliosis either contributes to, or counteracts atrophy. Post-mortem studies indicate that substantial axonal loss occurs in the spinal cord in MS, both within WM plaques and myelinated WM[76-79, 210]. For example Lovas et al estimated that 65% of the axons in the cervical cord are lost in SPMS, with small calibre fibres being predominantly affected[78].

Our finding of WM atrophy restricted to the upper regions of the spinal cord is consistent with previous work using this post-mortem material[79, 203]. Evangelou et al reported that atrophy is

seen in the upper, but not the lower regions of the spinal cord[203], while DeLuca et al observed reductions in the cross-sectional areas of the lateral and posterior WM columns in the upper but not the lower cord[79]. In an attempt to explain this pattern of atrophy we shall consider the distribution of WM plaques within the cord and their influence on tissue loss, both locally and in the non-lesioned WM.

The cervical cord has a predilection for WM plaques, while fewer lesions are seen in the lumbar and sacral levels[24]. Using the same autopsy material as the current study we have demonstrated a relative paucity of WM demyelination in the lumbar cord (12.4% of the WM was demyelinated, in comparison with 31.8% in the upper cervical level; see **figure 3.6, Chapter 3**). However, Evangelou et al reported that tissue loss within MS lesions does not have a significant influence on local cord atrophy[203]. Indeed, lesions at the thoracic level caused significant cord expansion[203]. Bjartmar et al estimated that spinal cord plaques in severely disabled patients showed between a 45% and 84% reduction in total axonal number[210]. Taken together, these two studies suggest that the axonal and myelin loss within WM lesions is countered by some other process, such as BBB breakdown, oedema, inflammatory cell infiltration, gliosis or expansion of the extracellular space[58]. MRI studies also suggest that tissue loss in MS may be confounded by inflammatory WM lesions. Tiberio et al assessed the cerebral WM volume in MS patients over a two year period; a reduction in WM volume was observed in patients exhibiting a reduction in Gadolinium-enhancing lesion volume over the course of the study, while patients with an increase in Gadolinium-enhancing lesion volume showed an increase in WM volume[139].

While WM lesions appear to make a minimal contribution to *local* atrophy[203], the distribution of WM lesions within the cord may still influence the pattern of atrophy. Bjartmar et al analysed axonal pathology using autopsy material from a patient with a 9 month history of MS who died from a lesion at the cervicomedullary junction, but who had no other cord lesions[76]. They observed a 22% loss of axons in the descending “normal appearing” WM tracts at the C7 level of the spinal cord, consistent with axonal loss secondary to Wallerian degeneration. In contrast the estimated axonal number in the ascending tracts at the same level was normal, suggesting that substantial retrograde axonal degeneration does not occur in the spinal cord in MS. Similarly DeLuca et al reported that both (i) the cross-sectional area of the posterior WM columns and (ii) the total axonal number in this tract were only reduced in the upper cord;

preservation of ascending WM tracts in the lower cord may reflect the relative paucity of WM lesions in this region and explain, in part, the preservation of WM volume in the lower cord[79].

It is perhaps surprising that we do not observe atrophy in the lower cord subsequent to axonal loss in the descending tracts. DeLuca et al report that the volume of the lateral WM columns is well preserved in the lumbar cord in MS, despite a significant reduction in axonal number[79]. Ganter et al found no correlation between the size of the lateral columns and axonal density in this tract[77]. It therefore appears that, as in WM plaques, axonal loss in the "normal appearing" WM is not necessarily accompanied by atrophy. There is evidence from post-mortem studies in MS that the myelin sheath surrounding degenerated axons may persist for some time, helping to maintain the WM volume[76]. Indeed it may take months or even years to clear CNS myelin debris following Wallerian degeneration[327]. Additional factors including inflammatory cell infiltration and gliosis may also contribute to the maintenance of WM volume in the lower cord in MS.

While we report substantial WM atrophy in the spinal cord, we note that several imaging studies have failed to detect WM atrophy in the brain in MS[195, 312]. There are a number of potential explanations for this apparent inconsistency. Firstly, the average disease duration in our study is considerably longer than one would expect in an MRI study. Secondly, there is likely to be fewer active inflammatory lesions (i.e. which may cause local swelling, confounding tissue loss) in longstanding cases. Finally, the degree of atrophy is likely to vary between different sites in the CNS[108]. This may relate to regional variations in (i) the number of plaques, (ii) the inflammatory content of plaques, or (iii) anatomical factors[328].

4.4.2 Spinal cord GM volume is preserved in MS

The well defined and simple anatomy of the spinal cord GM makes it ideally suited for quantitative post-mortem studies[202]. In comparison, measurements of cortical thickness are difficult to obtain due to its highly folded structure and considerable regional heterogeneity[321, 329], while the boundaries of the thalamic nuclei may be ill-defined on autopsy material[330]. In addition, the morphology of the cord is well preserved in formalin fixed, paraffin embedded material and - in contrast with the cerebral cortex and the subcortical nuclei – sections are easy to orientate anatomically[202]. There are additional technical difficulties associated with measuring GM volumes in the brain by MRI. The complex anatomy and thinness of the cerebral cortex (estimated at 2.5 to 4.4 mm on MRI[193]) makes it particularly susceptible to

partial volume effects, either with the CSF or subcortical WM. It is also possible that cortical demyelination, which is grossly underestimated by conventional MRI[128], may cause subtle changes in tissue signal intensity which affect GM / CSF segmentation, reducing the apparent GM volume[195, 303, 331]. There are also challenges in examining deep GM structures on MRI. The anatomical boundaries of the thalamus are frequently poorly defined on MRI[313]. Furthermore the nuclei of the thalamus are interspersed with a substantial amount of WM; the thalamic atrophy reported in imaging studies may therefore partly reflect WM tissue loss[157, 158, 316].

To our knowledge only one other study has reported the relative degrees of GM and WM atrophy in the spinal cord in MS. Bjartmar et al studied spinal cord material from 5 severely disabled MS patients and 6 controls, demonstrating a reduced spinal cord cross-sectional area in the MS cases[210]. The GM:WM ratio was similar in the cases and controls, suggesting that atrophy affects both tissue compartments. In contrast, our study – which contains substantially larger numbers of cases - suggests that GM volume is well preserved in MS.

MRI and post-mortem studies of the brain demonstrate significant reductions in cortical thickness[131, 314] and thalamic volume[157, 158, 316] in MS patients. Several reports suggest that this volume loss occurs early in the disease course[138, 139, 181, 191, 192, 310, 322]. Two previous autopsy studies have examined GM atrophy in the MS brain, demonstrating a 10% reduction in cortical thickness and a 21% reduction in the volume of the medial dorsal nucleus of the thalamus[131, 157]. Therefore there appears to be substantial regional heterogeneity in the degree of GM atrophy.

Loss of neuronal tissue is likely to contribute to the substrate of GM atrophy in the brain, as suggested by post-mortem studies[131, 157, 317] and MRS studies demonstrating reductions in NAA in the cerebral cortex and thalamus[153-159, 320, 332, 333]. However the mechanisms of this neuronal pathology are poorly understood. One possibility is a direct effect of local GM demyelinating lesions. Extensive GM lesions, as described in the cerebral cortex[127, 130], could contribute to GM atrophy via loss of myelin, transection of neurites or apoptotic neuronal death[130]. We have demonstrated substantially greater GM demyelination in the spinal cord in comparison with the cerebral cortex and the thalamus (see **Chapter 2**). Whether these plaques are associated with neuronal and axonal loss requires further investigation. Another important consideration is the degree of gliosis, which could potentially counter tissue loss within MS plaques. In contrast with the lesions in the cerebral cortex and thalamus[132], a number of spinal cord GM plaques appear

to be associated with a significant gliotic reaction (**figure 3.10, Chapter 3 and figure 6.4Q, Chapter 6**). Similarly inflammatory cell infiltration and oedema may act to preserve the GM volume, and it is feasible that these processes are more pronounced in the spinal cord GM.

Alternatively, GM atrophy in the brain may occur as a consequence of distant WM lesions. Transected axons in such lesions may result in neuronal pathology through retrograde or anterograde transynaptic degeneration[317]. It has been suggested that the extensive connections of the thalamus with other brain structures make it particularly sensitive to the effects of pathology in distant sites[157]. Differences in the connectivity of the spinal cord GM and the GM of the cerebral cortex and thalamus may leave the spinal cord GM less susceptible to the effects of distant WM lesions. Further work is required to determine whether there is a reduction in the number or size of neurons in the spinal cord, despite the preservation of GM volume. Interestingly, Wenger et al reported a reduction in the thickness of myelinated cortex in MS cases, despite finding no apparent decrease in neuronal or glial cell density - further highlighting that GM atrophy is not synonymous with neuronal loss[131]. Similarly Bjugn et al observed atrophy of the ventral horns in the lumbar spine following transection of the thoracic cord in adult mice, despite no reduction in the number or size of neurons[334]. Conversely, our observation of preserved GM volume in MS does not necessarily imply an absence of neuronal pathology in the spinal cord GM.

4.4.3 Influence of disease duration

In the MS cases, WM area was strongly influenced by disease duration, while GM area was not. Using the same post-mortem material, Evangelou et al observed that disease duration was an important determinant of cord atrophy, with the rate of atrophy being particularly high in early disease (3.5% per year in patients that died within 10 years of disease onset, in comparison with 0.75% per year overall)[203]. However it is likely that MS patients who die soon after diagnosis will tend to have more aggressive disease. Similarly DeLuca et al, observed correlations between disease duration and the cross-sectional areas of the corticospinal tracts and the posterior columns, although no correlation existed between disease duration and the estimated axonal number in either tract[79]. Imaging studies also demonstrate correlations between cervical cord area and disease duration[108, 216].

Evangelou et al noted that age and gender did not influence whole cord atrophy in MS cases[203], while DeLuca et al reported that gender did not correlate with axonal density or cross-

sectional area in either the corticospinal tract or the posterior columns[79]. Similarly Ganter et al found no gender difference related to corticospinal tract cross-sectional area, although axonal density was reduced in males in comparison with females[77].

4.4.4 Limitations of our study

There are a number of limitations to our study. In some of the MS cases disruption of the tissue architecture was observed on the Palmgren silver sections, potentially interfering with blinding. The use of a small number of myelin stained sections may also interfere with blinding. Despite our efforts to measure the GM area on each of the sections, this was not possible in every case, particularly when the GM boundaries were indistinct due to local inflammatory plaques. This may bias the sample to include a greater proportion of "normal appearing" material. However, given the large number of sections included in our study, we are confident that these factors have not had a significant influence on our results.

There is considerable variation in spinal cord size, even between healthy subjects[335]. Imaging studies frequently normalise brain or spinal cord volumes to intracranial volume, reducing the effects of inter-individual variation and thereby increasing the power of the study[318]. Unfortunately we are unable to normalise spinal cord areas to variables such as subject height, or control for such variables in the statistical analysis. Furthermore we have been unable to use tissue sections from precisely the same segmental levels in all the MS and control cases, introducing further variability to our results and reducing our ability to detect small reductions in the MS cases[200]. However it is questionable whether such subtle degrees of GM atrophy would be of any functional significance.

Considerable dimensional changes occur in tissue post-mortem as a result of dehydration, fixation, embedding and sectioning[336, 337]. Paraffin is the embedding material that induces the largest degree of shrinkage, resulting in a volume reduction of approximately 10%[336]. Other factors likely to influence the degree of shrinkage include the age of the subject, the nature and duration of the terminal illness, the post-mortem delay and the length of fixation[338]. While our cases are well matched for age we are unable to control for other variables such as post-mortem interval and fixation time. Further work is required to establish if tissue shrinkage differs between the "healthy" and diseased states - for example, due to the high water content associated with MS plaques - and whether there is differential shrinkage of the GM and WM compartments[202, 337, 339].

Our results suggest that previously observed correlations between spinal cord atrophy and disability reflect WM, rather than GM, volume loss. However due to a lack of detailed clinical information, we are unable to test this formally. Similarly we are unable to compare patterns of atrophy between different MS subtypes. Cross-sectional immaging studies have failed to detect spinal cord atrophy in RRMS patients in comparison with controls[110, 213, 340, 341], despite longitudinal reductions in spinal cord volumes being observed in this disease subtype[110, 340]. Brex et al examined spinal cord atrophy in patients with a clinically isolated syndrome suggestive of MS, observing reductions in baseline cord area in those with an abnormal brain MRI in comparison to controls[323]. However no reductions in cord area were observed over the following year, either in these patients or in those who developed clinical MS. One interpretation of these findings is that cord area may actually increase in the very early stages of the disease process, for example secondary to inflammation.

4.5 Conclusion

In this study - the largest post-mortem examination of spinal cord atrophy in MS - we demonstrate that spinal cord atrophy in MS is due purely to WM volume loss, suggesting that correlations between spinal cord atrophy and disability reflect WM, rather than GM atrophy. Our observation of preserved GM volume is an important one, suggesting important differences between the GM of the spinal cord and the GM structures of the brain. A greater understanding of the mechanisms of GM atrophy is required to explain these differences.

Figures

Figure 4.1

Transverse section of the spinal cord at the lumbar level (Palmgren silver stain). Grey matter (white line) and total cord (black line) cross-sectional areas outlined in B.

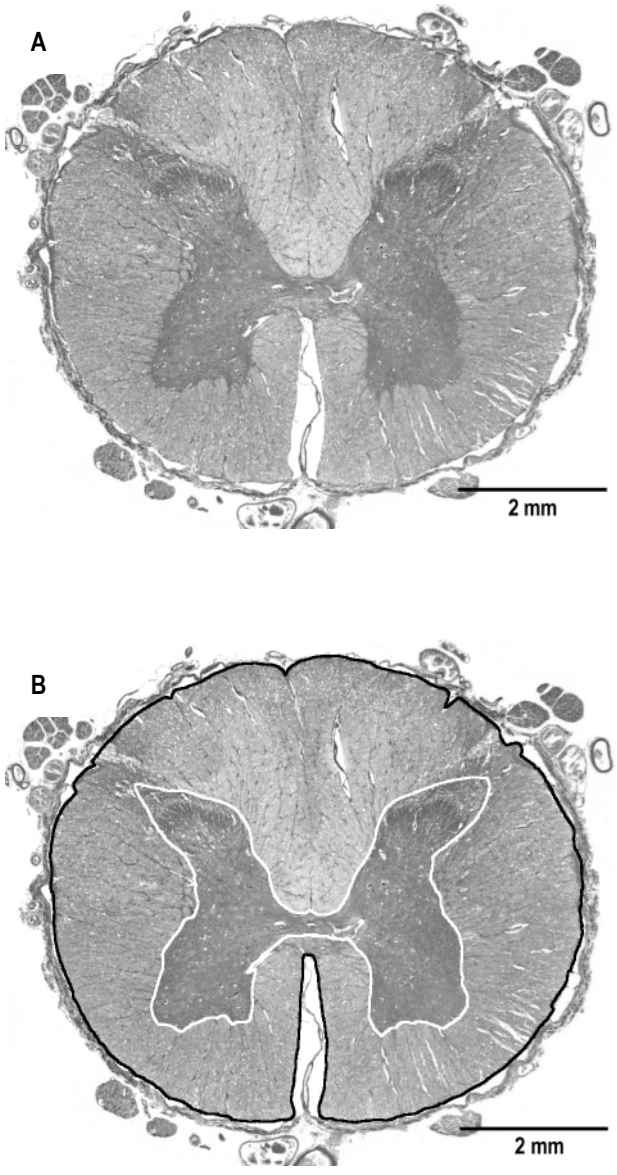

Figure 4.2

*Bar chart of cross-sectional area of white matter (A) and grey matter (B) at different levels of the spinal cord. UC = upper cervical; LC = lower cervical; UT = upper thoracic; LT = lower thoracic; LUM = lumbar. Values represent mean ± standard error. * p < 0.05*

A

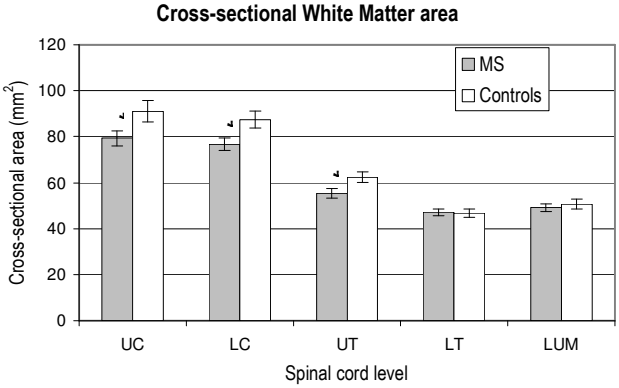

B

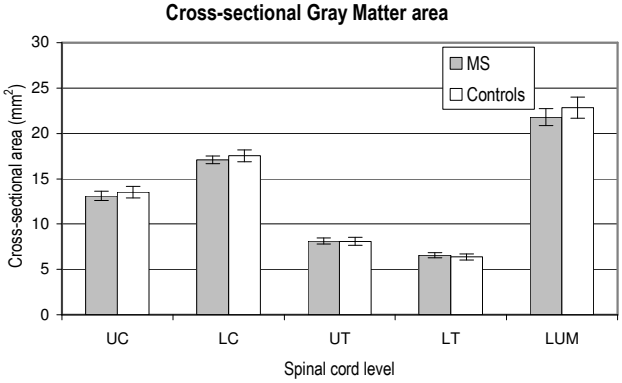

Chapter 5: Neuronal Pathology in Multiple Sclerosis

5.1 Introduction

Neuronal pathology may represent an important substrate of permanent disability in MS, along with demyelination and axonal loss. MR Spectroscopy studies provide indirect evidence for neuronal pathology in the brain, while post-mortem studies demonstrate reductions in neuronal number and size in the cerebral cortex and thalamus[131, 132, 153-159, 317, 320, 332, 333]. It has been proposed that these changes may occur either as a consequence of GM demyelination or secondary to axonal injury in the WM, via retrograde or transynaptic degeneration. However the relative importance of these processes is unclear. While a number of early post-mortem studies report various pathological changes within neurons in MS[220, 342, 343] few quantitative studies have characterised these changes in detail, and these have contained relatively small numbers of cases[131, 132, 157, 317]. To our knowledge no study has quantified neuronal pathology in the spinal cord in MS.

5.1.1 Evidence of neuronal pathology secondary to GM demyelination

Neuronal injury in MS may occur as a direct consequence of local GM plaques. Examining 22 cortical lesions from 7 MS brains, Peterson et al demonstrated transected axons and dendrites within cortical plaques, along with TUNEL-positive neurons, a marker of apoptotic death[130]. Such changes were less prominent within myelinated cortex, suggesting a direct effect of the cortical plaques in mediating neuronal injury. Vercellino et al studied neuronal pathology using autopsy material from 6 MS cases; in the 2 cases with particularly extensive cortical demyelination, a 20% reduction in neuronal density was observed within cortical plaques in comparison with areas of myelinated cortex[132]. The authors also reported neuronal expression of caspase-3 – a major effector protease in apoptosis – within the cortical lesions, providing further evidence of apoptotic neuronal death[132]. Comparisons in neuronal densities were not made between MS and control cases.

Further evidence of neuronal loss within cortical plaques comes from Wegner et al who performed neuronal counts in the deep cortical layers of the frontal lobe in 9 MS cases and 9 controls[131]. Examination of the GM portion of type I cortical lesions (i.e. mixed GM/WM lesions) revealed reductions in the density of neurons (10% reduction, associated with a 9% reduction

in neuronal size), glial cells (36% reduction) and synapses (suggested by reductions in the synaptic proteins synaptophysin and GAP-43) in comparison with myelinated MS neocortex. Myelinated neocortex did not show significant changes in neuronal density or neuronal size in comparison with controls, although neurons were more circular in the MS cases, raising the possibility of more subtle changes outside of the cortical plaques. Kutzelnigg et al demonstrated neuronal pathology within the cerebellar cortex in MS; examining autopsy material form 17 MS cases and 8 controls, they observed modest reductions in Purkinje cell density in demyelinated areas in comparison with the myelinated cerebellar cortex of MS patients and controls[204, 242].

Neuronal pathology has also been reported in deep GM structures. Cifelli et al demonstrated substantial neuronal loss in the medial dorsal nucleus of the thalamus in a post-mortem study of 10 MS patients (1 RRMS, 6 SPMS, 3 PPMS) and 10 controls[157]. The volume of the nucleus was reduced by 21% in the MS group, while neuronal density was reduced by 22%, giving an estimated 35% reduction in total neuronal numbers in patients relative to controls. Neuronal pathology in the thalamus has also been examined by Evangelou et al who - in a study of 8 MS cases and 8 controls - demonstrated neuronal atrophy in the lateral geniculate nucleus (LGN) in MS cases[317]. Neither study examined the influence of GM plaques on these neuronal changes. However, in view of the relatively modest degree of GM demyelination that we observe in the thalamus, it seems likely that additional mechanisms contribute to the considerable neuronal pathology observed in this structure[157, 317].

Neuronal pathology has not been extensively examined in the spinal cord in MS, although abnormalities have been described in the cells of Clarke's column and in motoneurons[220, 342, 343]. While a small number of descriptive studies have reported a variety of pathologic changes in relation to anterior horn cells lying within demyelinated plaques[342, 343], the spinal cord has not been the subject of more rigorous, quantitative studies. However there is evidence for motoneuron pathology in EAE. Mice with MOG-induced EAE develop demyelination and inflammation in the lumbosacral cord associated with perikaryal atrophy of local motoneurons, dendritic pathology, but no reduction in motoneuron density[344]. Using a rat model of EAE, Giardino et al demonstrated that spinal motoneurons undergo phenotypical changes indicative of cellular stress including reductions in choline acetyl-transferase (ChAT) expression and increases in calcitonin gene-related peptide (a trophic peptide for motoneurons) and $p75^{LNGFR}$

(a neurotrophin receptor that binds Nerve Growth Factor, Brain Derived Neurotrophic Factor and neurotrophin 3-4)[345].

5.1.2 Neuronal loss may occur within GM plaques via a number of mechanisms

The myelin-oligodendrocyte complex provides the neuron with important neurotrophic factors[346]. The sub-population of satellite (perineuronal) oligodendrocytes which lie opposed to the perikarya of neurons are likely to be particularly important in this respect, as well as having additional roles in maintaining neuronal homeostasis[125, 126, 346-348]. Loss of this trophic support following oligodendrocyte death may therefore lead to neuronal pathology within the GM plaque[349]. Alternatively, a number of inflammatory factors are potential mediators of neuronal injury:

T cell mediated neuronal injury

T cell mediated neuronal destruction has been implicated in a number of conditions including Rasmussen's encephalitis[350] and several paraneoplastic neurological syndromes[351]. In the "healthy" state CNS neurons express a minimal amount of MHC class I but expression may be increased if the neuron is functionally compromised[352, 353]. For example, when electrically paralysed hippocampal neurons are exposed to the pro-inflammatory cytokine IFN-γ in vitro, MHC class I is dramatically upregulated rendering the neuron susceptible to attack by $CD8^+$ T cells[353, 354]. Similar conditions (i.e. blockade of electrical activity and high levels of IFN-γ) are likely to be seen in the acute MS plaque. MHC restricted cytotoxicity may occur either via the Fas / Fas ligand pathway, or the release of toxic granules containing perforins or granzymes. In Rasmussen's encephalitis $CD8^+$ T cells may induce apoptosis in MHC class I^+ neurons by releasing the serine protease granzyme B[350].

$CD4^+$ and $CD8^+$ T cells may also mediate cytotoxicity in cultured human neurons in a non-MHC restricted fashion, again via the Fas / Fas Ligand pathway[355]. Studying "living" cortical slices from mice, Nitsch et al observed that T cells mediate contact-dependent, MHC-independent neuronal death, which could be prevented by blocking both perforin-mediated cytotoxicity and glutamate receptors[356]. Smith et al reported a novel mechanism of neuronal loss in Lewis rats with MBP-induced EAE[357], whereby T cells were seen to attach to the cell membrane of spinal motoneurons, becoming internalised and undergoing apoptosis; this sequestration of lymphocytes resulted in neuronal degeneration, with a 30% reduction in neuronal density. This

interaction between T lymphocytes and neurons is poorly understood and has not been described previously in the context of EAE or MS.

Antibody mediated neuronal injury

Antibodies to gangliosides[92], neurofilaments[93] and other neuronal antigens have been described in MS[91, 94]. For example Lily et al reported that a proportion of MS patients – mainly with SP disease – express serum IgM antibodies that bind neurons in vitro[94]. Whether such antibodies have any pathogenic significance is unclear; antibody mediated neuronal pathology is not a well recognised phenomenon, although it has been implicated in mediating neuronal pathology in Tropical Spastic Paraparesis, a myelopathy associated with Human T Lymphotrophic Virus type 1[358]. This antibody - targeted against the neuronal antigen heterogenous nuclear ribonuclear protein-A1 - appears to be biologically active, inhibiting the firing of cultured rat neurons[358].

Soluble factors

Neurons may also be susceptible to bystander injury secondary to a number of toxic products secreted by activated microglia and macrophages:

- Pro-inflammatory cytokines such as TNFα can kill human neurons in vitro[359, 360], as can the chemokine CXCL10[361, 362], which is expressed by macrophages in MS plaques [363]. There is also evidence that the death ligand tumour necrosis factor-related apoptosis-inducing ligand (TRAIL) - secreted by or expressed on activated T cells - has a role in neuronal death in EAE[364].

- Reactive nitrogen and oxygen species may induce programmed neuronal death[365]. Free radicals also oxidise the myelin breakdown product cholesterol to 7-ketocholesterol. 7-ketocholesterol is elevated in the CSF of MS patients and within acute MS plaques[366] and may mediate neuronal injury directly[366-369]. Interestingly GM hypointensities are commonly detected on T2-weighted MRI scans in MS, both in the cortex and subcortical structures[160, 370, 371]. These changes are likely to reflect pathologic iron deposition, although it is unclear whether this is simply a disease epiphenomenon or if it contributes to neurotoxicity by promoting free radical production[160].

- Glutamate-induced neuronal damage has been implicated in neuronal injury in a variety of neurodegenerative conditions including spinal motoneuron loss in Motoneuron Disease[372]. Neurons, activated inflammatory cells / microglia and injured astrocytes may all release glutamate, and glutamate-mediated excitotoxicity is a potential mechanism of oligodendrocyte and neuronal loss in MS. Groom et al reported motoneuron loss in rats with EAE in association with changes consistent with glutamate-mediated excitotoxic injury[373].

- Finally, activated macrophages secrete proteases such as tissue plasminogen activator and the matrix metalloprotease MMP-9, both of which are expressed in MS plaques[30, 374-377]. Exposure to tissue plasminogen activator renders neurons more susceptible to excitotoxic glutamate induced death[378], while MMP-9 induces anoikis, whereby the cell is detached from the extra-cellular matrix and undergoes apoptosis[379]

These soluble factors may originate from local GM plaques or nearby WM plaques. Alternatively they may be generated in distant inflammatory plaques or areas of meningeal inflammation and diffuse within the CSF, mediating neuronal pathology in the so-called "normal appearing" GM. Alcazar et al demonstrated apoptotic death in cultured neurons exposed to CSF from patients with aggressive PPMS, while CSF from patients with stable PPMS or non-inflammatory neurological diseases did not induce neuronal apoptosis[380]. Furthermore Cid et al reported apoptosis of cultured neurons following treatment with CSF from RRMS patients; the degree of neuronal loss correlated with both lesion load measures and residual disability after relapse[381].

5.1.3 Neuronal pathology secondary to axonal injury in distant WM lesions

Additional factors, independent of local GM demyelinated plaques, may influence neuronal pathology in MS. It is hypothesised that neuronal injury in myelinated GM may occur secondary to axonal transection in distant WM plaques[157, 317].

Retrograde degeneration

Following axonal transection the distal portion of the axon undergoes Wallerian degeneration. In certain circumstances this will be accompanied by retrograde degeneration or shrinkage of the cell body itself. Whether retrograde degeneration occurs following axotomy is influenced by several factors including neuronal type, age at time of injury and the proximity of the injury to

the neuronal body[382]. Axotomy-induced retrograde degeneration is most prominent in the immature CNS but has been demonstrated in a number of neuronal systems in adult animals[383-385].

Animal studies demonstrate that axotomy may lead to considerable retrograde degeneration in the spinal cord. For example thoracic cord transection in adult cats results in a 40% loss of neurons within Clarke's nucleus at the lumbar cord level, with surviving neurons showing a 50% reduction in mean soma size[384]. However, there is little evidence for significant retrograde axonal degeneration in MS, particularly in the spinal cord [76, 79]. Bjartmar et al analysed axonal pathology using autopsy material from a patient with a 9 month history of MS who died from a lesion at the cervicomedullary junction[76]. Despite substantial axonal loss in the descending WM tracts of the spinal cord, consistent with Wallerian degeneration, the estimated axonal number in the ascending tracts was normal. Similarly DeLuca et al reported preservation of ascending WM tracts in the lower cord despite multiple plaques at higher cord levels suggesting there is little retrograde degeneration of these fibres[79].

Retrograde degeneration has been demonstrated in an animal model of MS. Rats with MOG-induced EAE develop optic neuritis accompanied by axonal transection, resulting in retrograde degeneration and reductions in retinal ganglion cell density comparable to those seen after surgical transection of the optic nerve[386, 387]. While retrograde degeneration is the predominant mechanism of neuronal loss in this model, other processes appear to be important[387]. Early in the disease course 73% of retinal ganglion cells are lost in comparison with only 55% of optic nerve axons, suggesting a proportion of neurons die secondary to axonal demyelination per se[387]. The electrical activity of the axonal membrane influences the expression of multiple genes including those governing the synthesis of neurotrophins and their receptors[388, 389]. For example depolarisation of retinal ganglion cells up-regulates the neurotrophin receptor TrkB, increasing responsiveness to Brain Derived Neurotrophic Factor and improving cell survival[390, 391]. Conversely, electrophysiological dysfunction – secondary to demyelination - may result in neurons becoming insensitive to endogenous trophic factors. Loss of electrical activity may also render the neuron susceptible to MHC class I-mediated cytotoxicity as mentioned previously. Alternatively, chronically demyelinated axons may degenerate as a result of "virtual hypoxia" as described in **Chapter 1.2.6**.

Transneuronal Degeneration

Neuronal survival in the adult CNS is maintained, in part, by trophic signals from both efferent targets and afferent inputs. Loss of trophic signals from efferent targets is likely to be an important trigger for retrograde neuronal degeneration following axotomy[392]. Similarly neurons may degenerate or atrophy following interruption of their afferent connections (so–called anterograde transneuronal degeneration) or after the death of the neurons upon which they project (retrograde transneuronal degeneration)[382]. As is the case with retrograde degeneration, susceptibility to transneuronal degeneration varies between different species and different neuronal populations and occurs more commonly in the immature nervous system[382]. Sequential transneuronal degeneration is also recognised[382]. For example, following enucleation of the eye, anterograde transneuronal changes may occur not only in the LGN (primary anterograde transneuronal degeneration) but also in the visual cortex (secondary anterograde transneuronal degeneration). Likewise lesions of the limbic cortex may result in retrograde degeneration in anterior thalamic nuclei followed by (primary) retrograde transneuronal degeneration in the medial mammillary nucleus and (secondary) retrograde transneuronal changes in the ventral tegmental nuceus of the midbrain.

Animal studies demonstrate anterograde and retrograde transneuronal degeneration in a number of neuronal systems within the CNS[382, 393]. Anterograde degeneration is most clearly observed in the LGN of the thalamus following degeneration of its retinal afferents[88, 89]. Such changes have also been described in adult man secondary to ocular pathology[394, 395]. For example Golby reported a 59 year old male who lost 50% of neurons in the right LGN following enucleation of the left eye 40 years previously[394]. Kupfer et al examined 7 patients who died between 1 month and 73 years after either the loss of an eye or the development of a macular lesion; in cases that died within 2 years there was no evidence of cell loss in the LGN while substantial neuronal loss was observed after longer survival periods[394, 395]. Both studies suggest that the smaller parvocellular neurons of the LGN are more sensitive to deafferentation and show a greater reduction in size than the larger magnocellular neurons[394, 396]. There is less evidence for pronounced transneuronal retrograde degeneration in adult man, although Beatty et al reported atrophy of the right LGN associated with axonal degeneration in the right optic radiation and optic tract 40 years after surgical resection of the right occipital lobe[395].

Quantitative MRI abnormalities have been reported in the posterior visual pathway following isolated attacks of unilateral optic neuritis, possibly reflecting anterograde transynatic

changes[397, 398]. Ciccarelli et al observed a reduction in connectivity – assessed by diffusion tractography – in the optic radiations[397] while Audoin et al detected a selective reduction in MTR in the visual cortex[398]. In a post-mortem study of 8 MS patients and 8 controls, Evangelou et al examined the cross-sectional area of neurons in the LGN; the parvocellular neurons were significantly smaller in the MS group, while there was no difference in magnocellular neuron size[317]. The parvocellular neurons receive input from small calibre axons - known to be particularly susceptible to axonal injury in MS[77-79] - while magnocellular neurons receive input from larger axons. The axonal density in the optic tracts correlated with the extent of parvocellular neuron atrophy, suggesting neuronal shrinkage may be secondary to anterograde degeneration of axons that have received size related damage in the anterior visual pathway. Alternatively there may be a size-related vulnerability to neuronal injury that is independent of the calibre of the afferent or efferent connections or the presence of demyelinated plaques in the visual pathways.

If anterograde transynaptic degeneration occurs in the spinal cord in MS we might expect to observe similar mechanisms of neuronal death in animal studies and in other disease states. There is conflicting evidence as to whether the transection of descending WM tracts induces anterograde degeneration of ventral horn neurons in mature animals. Young et al observed shrinkage of anterior horn cells in cats following cord transection[399]. Similarly Eidelberg et al - studying adult rats - observed a 25% reduction in the number of lumbar motoneurons following either thoracic cord transection or bilateral ablation of the motor cortex, with neuron loss being detectable as early as day one[400]. However other groups have found no reduction in the number or size of anterior horn cells following cord transection in rodents, even at 1 year following injury[334, 401].

There is a striking paucity of literature assessing the effect of corticospinal tract transection on anterior horn cells in adult man. The few studies that have been performed fail to demonstrate significant transynaptic changes[402, 403]. Kaelan et al found no reduction in motoneuron number in 4 adults with long-standing transection of the spinal cord in comparison with 4 controls[402]. Similarly there is little evidence of transneuronal degeneration as a consequence of stroke in the adult literature. Terao et al studied 4 patients with severe hemiplegia who died 1 to 8 years following a stroke; despite extensive axonal loss in the corticospinal tracts, the stoke cases showed no reductions in anterior horn cell number or size in comparison with age-matched controls[404].

5.1.4 MRS studies suggest there is substantial neuronal pathology in MS

MRS provides quantitative indices of several tissue metabolites including NAA, an amino acid localised almost exclusively to neurons and neuronal processes in the adult brain[405]. NAA is therefore used as an index for axonal / neuronal injury or loss in vivo, and has provided substantial indirect evidence for neuronal pathology in MS. Significant NAA reductions have been reported in cortical and subcortical GM structures in both relapsing and progressive disease forms, even early in the disease course[153-159, 320, 332, 333]. A meta-analytic review suggests these changes may be important clinically, providing some evidence for greater NAA reductions in association with increased disease severity[333].

However, there are a number of limitations to MRS studies. Firstly, one can only speculate on the substrate of NAA reductions, which may reflect neuronal loss, atrophy of individual neurons, axonal/dendritic loss, neuronal/axonal metabolic dysfunction or a combination of these factors. Secondly, *reversible* reductions in NAA have been reported both in MS plaques and in "normal appearing" WM, indicating that changes in NAA are not entirely specific for neuronal/axonal loss[406, 407] . Inhibition of the mitochondrial respiratory chain results in reductions of NAA synthesis, suggesting mitochondrial dysfunction may produce potentially reversible NAA changes[408]. Alternatively restoration of the NAA concentration may reflect resolution of oedema or pseudo-normalisation as a consequence of atrophy[74, 407]. Thirdly, the specificity of the NAA signal has been questioned by work demonstrating oligodendrocyte expression of NAA in vitro[409].

Numerous technical limitations further hamper the utility of MRS for examining neuronal pathology. Due to the thin, highly folded nature of the cortex and the relatively large volume of spectroscopic voxels, there will be significant partial volume contamination of "cortical" voxels from both the CSF and the adjacent WM. Therefore NAA reductions in "cortical" voxels will in part reflect brain atrophy (i.e. atrophy will increase the proportion of CSF in the voxels) and axonal injury in the subcortical WM. To avoid spectral contamination by intense lipid signals from subcutaneous adipose tissue and bone marrow, voxels must be placed away from the skull, making most cortical GM difficult to access[410]. Such methodological issues may contribute to apparent inconsistencies in the literature; for example, three studies have failed to detect cortical NAA reductions, particularly in RR disease[155, 159, 332]. While the deep GM structures are less susceptible to many of these technical problems the thalamic nuclei are

interspersed with large amounts of WM, and the caudate and putamen are small and difficult to delineate on MRI[320].

5.1.5 Aims

The spinal cord is a predilection site for both WM and GM demyelination and a site of substantial axonal loss in MS[76-79, 101, 210]. However no study has quantified neuronal pathology in this clinically eloquent region. In this post-mortem study we investigate neuronal pathology in the spinal cord in MS, comparing the number and size of motoneurons and interneurons between MS cases and controls. We assess the extent of neuronal pathology, both within GM plaques and in the myelinated GM.

5.2 Methods

5.2.1 Clinical Material

Human autopsy material was obtained from 37 pathologically confirmed cases of MS and 22 controls. This material was derived from the neuropathology department, Oxford Radcliffe NHS Trust. The cases were selected at random from a collection of 55 MS cases and 33 controls studied previously[79, 203]. For each of the MS and control cases formalin-fixed paraffin-embedded transverse sections were taken from the upper cervical, upper thoracic and lumbar levels of the spinal cord. Sections were cut at a microtome setting of 15 µm and stained for Nissl substance and myelin with LFB Cresyl Violet. Corresponding PLP-stained sections were available for a number of MS cases (n = 30).

5.2.2 Assessment of neuronal number and size

The sections were positioned on the microscope stage with the GM commissure orientated parallel to the *x*-axis and the anterior median fissure parallel to the *y*-axis. Neuronal counts were restricted to the anterior horn of the GM, defined - for the purposes of this study - as the area ventral to the anterior border of the GM commissure (**figure 5.1**). The entire anterior horn was systematically viewed using a video camera (KY-F55B 3-CCD JVC Color Video Camera) linked to microscope (40x, Leitz Dialux 20EB microscope). Neurons were photographed and counted if the nucleolus was visible in the plane of the section. A small number of sections were excluded from the analysis because either the neurons were too darkly stained to identify the nucleoli (n = 8 sections) or there was a tear in the section (n = 7 sections). A further 3

sections from the UT cord were omitted because they were from the T1 spinal level, which has a markedly different morphology in comparison with the other thoracic levels.

The Nissl stain readily differentiates between neurons and non-neuronal cell populations when viewed at high magnification. Neuron are larger cells with a well defined nucleolus and a cell body rich in endoplasmic reticulum while neuroglia are smaller with denser nuclei, less conspicuous nucleoli and a greater nucleus: cytoplasm ratio. Where possible, we excluded neurons from the intermediolateral column and Clarke's nucleus from the neuronal counts. In general these neuronal populations are readily identified; the large neurons of Clarke's nucleus are arranged in a well defined column within the thoracic cord, lying dorsolateral to the central canal while the intermediolateral column is composed of large preganglionic autonomic neurons, forming a well defined cluster in the lateral horn, most conspicuous from ~T1 – L2.

The neuronal bodies and nucleoli were outlined manually using image analysis software ("AnalySIS Pro" running SIS software). Neuronal processes were traced to include proximal processes, but not the axon or the dendrites per se. The cross-sectional area of the neuron was determined as was the maximum and minimum neuronal diameter (for neuron classification), and the nucleolar diameter (for application of the Abercrombie correction), with all measurements being made in the plane in which the nucleolus appeared largest. To evaluate intra-observer reproducibility neuronal size measurements were made on two separate occasions – 2 months apart - using a randomly selected tissue section with 34 neurons (coefficient of variation=6.7%; inter-observer coefficient of variation=6.5%)[325, 326].

Neurons were classified as motoneurons or interneurons according to size criteria; those with a maximum diameter of at least 30μm and a minimum diameter of at least 13.5μm were classified as motoneurons; all other neurons were classified as interneurons. Light levels were adjusted for optimal viewing of the nucleolus allowing for section thickness and staining intensity and avoiding optical bleaching of the tissue. Counts were performed on both anterior horns of each section. Raw counts were converted using the Abercrombie formula. Section thickness was measured at a workstation with a video camera (JVC TK-1380) attached to a microscope (Olympus BX50 using x100 oil-immersion lens) with a motorised stage (Prior, Fulbourm, UK) that controlled movements in the z-axis. This system was connected to a PC running CAST software (Computer Assisted Stereological Toolbox, Olympus).

On any given section, measurements (i.e. neuronal counts, size measurements and extent of demyelination) were made for each anterior horn (i.e. right and left) separately.

5.2.3 A note on profile based counting techniques and the Abercrombie correction

When autopsy material is sectioned, structures are often cut and therefore appear on multiple sections. If 5µm thick transverse sections are cut from the spinal cord, a large object such as a motoneuron will appear on several adjacent sections (e.g. a 100µm tall motoneurnon will appear on 20 consecutive sections) while a smaller object, such as an interneuron, will appear on a smaller number of sections. Simple profile counts on single sections therefore over-estimate the number of objects in a structure, with the size of the error depending on both the section thickness and the height of the object being counted. The error is greatest when large objects are counted in thin sections, but even a nucleolus will have an appreciable height in relation to the thickness of the section[411].

A variety of methods, including the Abercrombie method[412], attempt to correct the overestimates generated by "raw" counts of cellular profiles. The Abercrombie formula states:

$$N = \frac{n \cdot t}{t + H}$$

n: number of objects counted in the sampled portion
N: estimate of true number of objects
t: section thickness
H: mean height of the object (i.e. nucleolus), which we estimate by measuring the diameter in the xy plane

5.3.4 Assessment of demyelination

The extent of demyelination within the anterior horn (expressed as the proportion of the total area that was demyelinated) was assessed using the PLP-stained sections, which were available for 30 of the MS cases. In the remaining 7 cases demyelination was assessed using the LFB-stained sections. We have previously demonstrated that – in the spinal cord at least – close inspection of LFB-stained sections at high magnification can reliably detect GM demyelination.

The influence of myelin loss on neuronal pathology was assessed in the MS cases by comparing anterior horns that were completely myelinated (n = 81 hemisections, from 29 MS cases) with those that were completely demyelinated (n = 33 hemisections, from 13 MS cases).

5.3.5 Statistics

Nonparametric statistical tests (unpaired Wilcoxon rank sum test) were used to compare neuronal numbers between MS cases and controls, and between the myelinated and demyelinated regions within the MS group. Unpaired t tests were used to make comparisons in neuronal sizes. Multiple regression analyses were used to examine the influence of age, sex, disease state and, in MS cases, disease duration and the extent of demyelination on neuronal size and number ("Stata" version 9, StataCorp, Texas USA).

5.3 Results

5.3.1 Neuronal counts

Interneuron and motoneuron number is reduced in MS cases

Total neuron count was reduced in the MS cases in comparison with controls at the upper cervical ($p = 0.0024$) and upper thoracic ($p = 0.0145$), but not the lumbar ($p = 0.7158$) level. Similarly, in comparison to control cases, both interneuron and motoneuron number were reduced in MS cases at the upper cervical (interneuron $p = 0.0549$; motoneuron $p = 0.0073$) and upper thoracic (interneuron $p = 0.0507$; motoneuron $p = 0.0144$) but not the lumbar (interneuron $p = 0.6081$; motoneuron $p = 0.7931$) level (**figure 5.2**). In keeping with these results multiple regression analysis suggests that - controlling for age and gender - disease state had a significant influence on total neuronal number at the upper thoracic level ($p = 0.010$, with MS cases showing a 30.3% reduction in neuronal number). There was a trend towards significance at the upper cervical level ($p = 0.069$; 23.8% reduction in MS cases), but not the lumbar level ($p = 0.632$).

Neuronal loss is greater in plaques than in myelinated grey matter

Total neuronal count was reduced in the GM plaques in comparison with controls at the upper cervical ($p = 0.0018$) and upper thoracic ($p = 0.0043$), but not the lumbar ($p = 0.9652$) level. Similarly interneuron count was reduced in the GM plaques in comparison with controls at the upper cervical ($p = 0.0262$) and upper thoracic ($p = 0.0099$), but not the lumbar ($p = 0.7600$) level. Motoneuron count was reduced in the GM plaques at the upper cervical ($p = 0.0021$), but not the upper thoracic ($p = 0.1326$) or lumbar ($p = 0.3594$) levels.

Total neuronal count was not reduced in the myelinated GM of MS cases in comparison with controls at any of the cord levels (upper cervical, p = 0.2530; upper thoracic, p = 0.0797; lumbar, p = 0.7799). Similarly interneuron count was not reduced in the myelinated GM of MS cases in comparison with controls at any of the cord levels (upper cervical, p = 0.9317; upper thoracic, p = 0.2079; lumbar, p = 0.8459). Motoneuron count was reduced in the myelinated GM of MS cases in comparison with controls at the upper thoracic (p = 0.0190) but not the upper cervical (p = 0.1039) or lumbar (p = 0.7706) levels.

Within the MS cases, the total neuronal count was reduced within the GM plaques in comparison to the myelinated GM at the upper cervical level (p = 0.0504) but not at the upper thoracic (p = 0.2130) or lumbar (p = 0.9666) levels. There was a trend towards a reduction in interneuron count within the GM plaques at the upper cervical (p = 0.0808) and upper thoracic (p = 0.0915) but not the lumbar (p = 0.8672) levels. Motoneuron count was reduced within GM plaques at the upper cervical (p = 0.0276) but not the upper thoracic (p = 0.4093) or lumbar (p = 0.2097) levels.

5.3.2 Measurements of neuronal size

Interneuron cross-sectional area is reduced in MS cases in comparison with controls

The mean interneurons cross-sectional area was smaller in MS cases in comparison to controls at all three cord levels (upper cervical, 147.4μm^2 in MS cases versus 185.1μm^2 in controls, p = 0.0000; upper thoracic, 147.2μm^2 versus 162.9μm^2, p = 0.0002; lumbar, 186.8μm^2 versus 193.9μm^2, p = 0.0337) (**figure 5.3A**).

There was no significant difference in motoneuron size between MS cases and controls in the upper cervical (p = 0.7416; 655.1μm^2 in MS cases versus 645.9μm^2 in controls) and upper thoracic (p = 0.6426; 583.7μm^2 in MS cases versus 570.9μm^2 in controls) levels. However the mean motoneuron size was greater in MS cases than controls at the lumbar level (p = 0.0059; 1001.0μm^2 versus 908.4μm^2) (**figure 5.3B**).

Multiple regression analysis also indicated that disease state had a significant influence on neuronal size, with interneurons being smaller in the MS cases at the upper cervical and upper thoracic levels (UC, p = 0.000; UT, p = 0.000; Lum, p = 0.404) and motoneurons being larger in the MS cases at the lumbar level (UC, p = 0.461; UT, p = 0.706; Lum, p = 0.016).

Interneuron cross-sectional area is reduced in both myelinated and demyelinated grey matter

Mean interneuron size was reduced in the GM plaques in comparison with controls at the upper cervical (122.8μm^2 in GM plaques versus 185.1μm^2 in controls, p = 0.0000), upper thoracic (139.2μm^2 versus 162.9μm^2, p = 0.0004) and lumbar (173.6μm^2 versus 193.9μm^2, p = 0.0041) levels. Motoneuron size was not significantly different between the GM plaques and the controls at any of the cord levels (upper cervical, 633.7μm^2 in GM plaques versus 645.9μm^2 in controls, p = 0.7555; upper thoracic, 531.9μm^2 versus 570.9μm^2, p = 0.3199; lumbar, 993.4μm^2 versus 908.4μm^2, p = 0.2958).

Interneurons within the myelinated GM of MS cases were significantly smaller than in controls at the upper cervical (158.0μm^2 in the myelinated GM of MS cases versus 185.1μm^2 in controls, p = 0.0000) and upper thoracic (149.8μm^2 versus 162.9μm^2, p = 0.0033), but not the lumbar level (193.2μm^2 versus 193.9μm^2, p = 0.8694). Motoneuron size was not significantly different between myelinated GM in MS cases and controls in the upper cord (upper cervical, 665.0μm^2 in the myelinated GM of MS cases versus 645.9μm^2 in controls, p = 0.5847; upper thoracic, 598.6μm^2 versus 570.9μm^2, p = 0.3817), but was increased in the MS cases at the lumbar level (1023.4μm^2 versus 908.4μm^2, p = 0.0025).

Within the MS cases, interneuron size was reduced within the GM plaques in comparison to the myelinated GM at the upper cervical (122.8μm^2 in GM plaques versus 158.0μm^2 in myelinated GM, p = 0.0000) and lumbar (173.6μm^2 versus 193.2μm^2, p = 0.0148) levels. There was no significant difference at the upper thoracic level (139.2μm^2 versus 149.8μm^2, p = 0.1268). There was no significant difference in motoneuron size between GM plaques and myelinated GM in the MS cases (upper cervical, p = 0.4415; upper thoracic, p = 0.1144; lumbar, p = 0.7358).

5.4 Discussion

While previous studies have quantified neuronal pathology in relatively small numbers of MS cases (n < 10)[131, 132, 157, 317], we have examined autopsy material from 37 MS cases and 22 controls, making measurements from 8989 neurons. We have performed neuronal counts on Nissl-stained sections, adjusting the “raw” counts using the Abercrombie correction. We demonstrate substantial neuronal pathology in the spinal cord in MS, with changes being

observed within both demyelinated plaques and in myelinated tissue. Our results suggest that neuronal loss occurs predominantly within GM plaques.

5.4.1 Evaluation of study methodology

Previous studies have measured the number or density of neurons in the cerebral cortex and thalamus in MS. Performing neuronal counts in the cerebral cortex is challenging on account of its highly folded structure and considerable regional heterogeneity[329] while the boundaries of the thalamic nuclei may be ill-defined on autopsy material[330]. In both structures it is difficult to obtain sections that are consistently cut in the same plane. In contrast the well defined, simple anatomy of the spinal cord render it more suitable for quantitative studies[202]. The spinal cord is particularly well suited to examine the influence of demyelination on local neuronal loss due to the high frequency of GM plaques. However a number of issues need to be considered when performing neuronal counts:

i. Post-Mortem changes in tissue

Considerable dimensional changes occur during the processing of tissue post-mortem, as described in **Chapter 4.4.4**[336, 337, 339]. Due to a lack of detailed information we are unable to control for variables such as post-mortem interval and fixation time. Tissue shrinkage may also differ between the "healthy" and diseased states[202, 337]. Therefore shrinkage may be greater in MS plaques in comparison with myelinated tissue due to a higher water content or a difference in the integrity of the tissue.

ii. Identification of neurons

We use the nissl stain Cresyl violet to identify neurons within the anterior horns of the spinal cord. A recent study has employed a similar technique to perform neuronal counts in the cerebral cortex[131]. IHC stains, for example Neu-N, are available for the identification of neurons. NeuN is a monoclonal antibody against a nuclear antigen and is a highly sensitive and specific neuronal marker[413, 414]. However NeuN staining is often extremely variable when used on formalin-fixed tissue, particularly when fixation times are long (personal communication Christiana Wegner, Oxford, and Lars Bö, Amsterdam). Nissl stains such as Cresyl violet are more robust when used on archival material and readily differentiate between neurons and non-neuronal cell populations. There are additional merits to using conventional staining techniques when performing measurements of neuronal number and size. NeuN is predominantly a nuclear stain; staining of the perikaryal cytoplasm is not observed in all

neuronal populations, limiting its use in the assessment of neuronal size[414]. There are also disadvantages to applying IHC techniques when using relatively thick tissue sections, as used in this study; incomplete penetrance of the stain is a particular problem for IHC procedures[339]. Furthermore, because NeuN identifies nuclei – rather than nucleoli – even thicker sections would have to be used in order to accurately apply the Abercrombie correction. We do acknowledge however that the LFB stain interferes with blinding of the heavily demyelinated sections.

For the purposes of performing neuronal counts, several groups have defined the anterior horn as the area ventral to the central canal[404, 415-418]. However the intermediolateral column frequently lies within this area, as does the anterior portion of Clarke's nucleus[419]. We were keen to minimise contamination of our counts by these neuronal populations. In addition we wished to exclude neurons from the GM commissure as these are smaller than ventral horn interneurons and more difficult to distinguish from glia[274]. Therefore we restricted our neuronal counts to the area ventral to the anterior border of the GM commissure, although we note that a small number of motoneurons lie posterior to this area and will not be counted[419].

iii. Distinction between motoneurons and interneurons

While neurons and non-neuronal cell populations are readily differentiated using the nissl stain, distinguishing between motoneurons and interneurons may be less straightforward. Retrograde labelling techniques, which are frequently used to identify motoneurons in animal studies, cannot be employed post-mortem. The two cell types cannot be differentiated according to their location within the anterior horn; motoneurons do not always appear in well demarcated, discrete columns on transverse section and, even when they do, these columns also contain a significant number of interneurons[274]. We are not aware of a marker that is 100% specific to either neuronal subtype that can be reliably applied to formalin fixed material. The cholinergic markers choline acetyltransferase (ChAT) and acetylcholinesterase (AChE) have been used to stain motoneurons[420, 421]. However AChE lacks specificity while ChAT is extremely sensitive to fixatives and is poorly visualised in formalin-fixed material[421, 422]. IHC staining for non-phosphorylated neurofilaments (e.g. using the antibody SMI-32) is a relatively reliable marker of motoneurons with a similar efficacy to nissl staining although staining is less conspicuous with prolonged formalin-fixed material[421]. The Calcium Binding Proteins calbindin, parvalbumin, calmodulin and calretinin offer some promise as potential markers for particular subpopulations of interneuron but are not sufficiently sensitive or specific[423-426]. All four proteins are also

expressed by a proportion of motoneurons[424, 427]. Motoneuron expression is upregulated following axonal injury, which is likely to further limit their use as interneuron markers in a disease such as MS[428].

Several groups have distinguished motoneurons and interneurons using size criteria[404, 415-417, 429]. Tomlinson et al defined cells as motoneurons if they were greater than 30μm in diameter and fulfilled particular morphological criteria, namely a multipolar shape with 3-5 sides, a centrally placed nucleus and a well defined nucleolus, 3-6 μm in diameter[430]. In reality a multipolar neuron may appear circular, oval, unipolar or bipolar in cross-section. In view of this - and in an effort minimise bias and improve efficiency - we were keen to adopt a less subjective system of classification. We frequently observe thin bipolar interneurons that are greater than 30μm in diameter. We therefore defined motoneurons as cells with a maximum diameter of at least 30μm and a minimum diameter of at least 13.5μm with all other neurons being classified as interneurons. There are limitations to this system of classification. Firstly, there is some overlap in size between motoneurons and interneurons, even in the non-diseased state[274]. Secondly, if there is perikaryal atrophy of motoneurons in the diseased state a proportion of pathologically shrunken neurons may be misclassified as interneurons.

iv. Neuronal Counts

The disector method is regarded by several groups as the most accurate method of estimating cell density despite a distinct lack of evidence that it is superior in practice[431]. Whereas profile-based counting techniques use single sections as counting probes, the physical disector uses pairs of parallel sections, a “reference” section and a “lookup” section. Objects (e.g. nucleoli) that appear in the reference section but not in the look-up section are counted; the number of these objects divided by the volume of space bounded by the outer surfaces of the two sections represents the density of objects. The two sections need not necessarily be adjacent, but should be close enough so that no objects are lost between them. In addition it must be possible to determine which profiles belong to the same object. Despite its theoretical advantages, the disector method can be difficult to apply in practice. Serial sections are required; therefore a number of valuable slide collections are unsuitable for such methods[339, 432]. Furthermore, cutting serial sections is time consuming and requires technical expertise. The process of co-registering the section pairs is also labour intensive, particularly if performed without expensive specialist equipment and will be associated with a degree of error[339, 433].

There is much debate as to the relative advantages and disadvantages of profile-based counts in comparison with stereological-based methods such as the disector[339, 411, 432-438]. We have performed counts of neuronal profiles using single sections, correcting these "raw" counts for object size and section thickness using the Abercrombie formula. When applied appropriately profile-based counts can provide extremely accurate estimates of neuronal number[439]. To avoid bias the object height (H) should not exceed one third of the section thickness (t)[411, 440]. We have therefore counted nucleoli (i.e. we have only counted neurons if the nucleolus can be seen in the plane of the section) - rather than nuclei or neuronal cell bodies – because they have a well defined shape and are small relative to the section thickness. In performing such counts we assume that every neuron has one, and only one, identifiable nucleolus. It may not be possible to recognise very small fragments of nucleoli that are sectioned by the microtome; modifications of the Abercrombie correction address this problem of "lost caps" but the resulting error is likely to be minimal and so was not applied in this study[441].

In practice investigators often estimate H by measuring profile diameters in the *xy* plane, rather than measuring it directly in the *z*-axis. In doing this we assume that the nucleloi are spherical, or at least isotropically orientated (i.e. orientation in all possible axes is equally likely) so that mean H and mean object length in the section plane are equal[411]. These are reasonable assumptions although the mean nucleolar diameter - as measured - will be slightly less than the true nucleolar diameter because a proportion of measurements will be made from nucleolar fragments lying at the section surfaces[411]. However this error is unlikely to significantly bias our results considering the small size of the nucleoli relative to the section thickness.

We make further assumptions when measuring the size (i.e. cross-sectional area) of the neurons, specifically that the nucleolus is approximately in the centre of the neuron and its position doesn't change in the diseased state. It is well recognised that axonal injury may lead to chromatolysis, a retrograde reaction in the neuronal cell body characterised by swelling of the neuronal cell body, peripheral displacement and deformation of the nucleus, and loss of nissl substance from the central part of the cell. Eccentric placement of the nucleolus would result in an apparent reduction in neuronal cross-sectional area as we have measured this parameter in the plane of the nucleolus. However the light microscopy changes of chromatolysis - best studied in nissl-stained sections - were not observed in this study and we find no evidence suggesting that the nucleolus becomes eccentrically placed in the pathological state.

When applied appropriately, profile-based counts can be extremely accurate, producing results within 2% of the counts obtained by complete 3-dimensional reconstruction from serial sections, the "gold standard" technique for counting cells[439]. In contrast, the disector can be inaccurate when compared against 3-dimensional reconstruction[442-445]. Furthermore, particular morphological characteristics of the spinal cord were considered in planning the sampling procedure; motoneurons are not distributed evenly throughout the ventral horn but form aggregates, arranged in longitudinal columns, referred to as 'motor nuclei' due to their appearance in transverse section. There is evidence that the physical disector is particularly inaccurate when applied to neurons distributed in such a non-uniform fashion. Popken et al performed neuronal counts in the dorsal root ganglion of adult rats, an area showing a markedly heterogenous distribution of neurons[443]. When the recommended sampling protocol for the physical disector was employed (i.e. sampling 100-200 objects)[446-449], estimates derived from repeated measurements differed by over 50%. Comparisons between the physical disector, profile-based counts and 3-dimensional reconstruction demonstrated that counts of nucleoli profiles were more reliable than those derived from the physical disector[443].

We have reported absolute counts, rather than neuronal densities, counting all neurons in the anterior horn, regardless of the anterior horn volume. Cell density measurements can be difficult to interpret if changes in the reference space may occur in the disease state[338]. For example, neuronal density may be influenced by a variety of factors including oedema, inflammatory cell infiltration and gliosis, in addition to neuronal loss per se[58]. Density measurements may also be inaccurate if the neurons are arranged in clusters, as they are in the spinal cord.

v. Sources of statistical variability

We perform neuronal counts at three spinal cord levels; upper cervical, upper thoracic and lumbar. There is a considerable inter-individual variation in neuron number, even in the non-diseased state[450, 451]. There is marked intra-individual variation in motoneuron number between adjacent spinal cord segments, for example between L2 and L3[450]. However, the exact segmental level is not known in all of our cases, making it difficult to control for this variability. Even greater variability is observed when counts are performed on a single section [430]. All of these factors are likely to add substantial statistical noise to our results. Consequently subtle differences in neuronal size or number between MS cases and controls may go unnoticed, despite our relatively large sample size.

5.4.2 There is substantial neuronal loss in the spinal cord in MS, particularly within GM plaques

We observe substantial reductions in both motoneuron and interneuron number in the MS cases in comparison with controls. Our results suggest that neuronal loss occurs predominantly within GM plaques; neuronal counts in demyelinated tissue are reduced in comparison with both control tissue and with the myelinated GM of MS cases. These changes only reach statistical significance in the upper regions of the cord. The apparent preservation of neuronal number in the lumbar cord may reflect a number of factors. Firstly, within the lumbar region, relatively few sections demonstrate demyelination of the *entire* anterior horn (i.e. when comparing neuronal counts between GM plaques and myelinated GM we consider only anterior horns that are either *completely* demyelinated or *completely* myelinated). This is likely to reflect (i) the relative sparing of the lumbar region in our cohort (we have previously reported that 42% of the GM is demyelinated in the upper cervical level in comparison with 38% at the upper thoracic and 28% at the lumbar level, although these differences do not reach statistical significance, **figure 3.5**) and (ii) the GM cross-sectional area is considerably larger in the lumbar cord, so the anterior horn is less frequently *completely* demyelinated at this level. Secondly, there is a high degree of inter-individual and inter-level variability in neuronal number in the lumbar cord[450], so modest reductions in neuronal numbers may go undetected. Finally, motoneurons are larger in the lumbar cord than at other levels (**figure 5.3**); if neuronal susceptibility to injury *is* size-related, we may expect motoneurons in the lumber cord to be relatively resistant to neuronal loss.

The mechanism of neuronal loss within GM plaques is poorly understood. Demyelination per se may lead to neuronal injury, depriving the neuron of trophic support[349]. Alternatively, a number of components of the inflammatory milieu are potential mediators of neuronal injury. For example, lymphocyte-mediated neurotoxicity has been reported in a number of settings, via a number of mechanisms[350, 352-356]. Neurons may also be susceptible to bystander injury secondary to cytokines[359, 360, 364], chemokines[361, 362], reactive nitrogen and oxygen species[365], glutamate and proteases[374, 378, 379].

Post-mortem studies suggest that cortical GM plaques show little inflammatory cell content[135, 137]. Whether inflammatory cells are present during the earlier stages of plaque genesis is less clear; animal models of cortical demyelination suggest that transient inflammation may occur[240]. The inflammatory content of spinal cord GM plaques has not been examined in detail,

but at least a proportion of such lesions show an abundance of macrophages. Alternatively soluble factors may diffuse from nearby WM plaques. This may be particularly relevant in the spinal cord, where the majority of GM lesions are mixed GM/WM plaques.

Axonal loss in MS almost exclusively affects small calibre axons[77-79]. We do not observe such a striking size-related susceptibility to neuronal injury, with similar proportions of interneurons and motoneurons being lost. Given the magnitude of the anterior horn cell loss that we observe it is perhaps surprising that we do not observe the classical signs of lower motoneuron pathology in the clinical setting more frequently. However, it is estimated that 50% of motoneurons are lost in Motoneuron Disease before muscle wasting and fasiculations are evident clinically[452]. Focal muscular atrophy is a relatively uncommon but well recognised feature of MS, estimated to occur in 6-7% of patients; In a study of 523 men in the armed forces, Kurtzke observed focal muscle atrophy in 38 cases, while Fisher et al observed atrophy in 9 out of 150 patients[453, 454]. The cause of this atrophy is unclear; several mechanisms have been proposed including involvement of motoneurons or ventral exit zones by MS plaques, neuropathy secondary to subtle abnormalities in peripheral myelin[455] and peripheral nerve compression[453]. There is some electrophysiological evidence that focal muscle atrophy is most consistent with injury at the motoneuron or ventral exit zone level[456, 457], although other studies disagree[453]. Two post-mortem studies have directly implicated demyelinating plaques involving motoneurons in muscle atrophy in MS, noting a variety of pathologic changes in the anterior horns (i.e. at the level corresponding to the focal muscle atrophy), including neuronal shrinkage, central chromatolysis and subjective reductions in neuronal numbers[342, 343].

There appears to be minimal neuronal loss within myelinated regions of the spinal cord, although we do detect a reduction in motoneuron number in the myelinated GM at the upper thoracic level. Consistent with our work, Wegner et al found no evidence of neuronal loss within the myelinated cortex of MS cases[131]. Even in the non-diseased state there is considerable inter-individual variation in neuronal number[450, 451]. Therefore despite our relatively large sample size, our study may lack the statistical power to detect subtle neuronal loss within the myelinated GM.

Substantial neuronal loss has been reported in the thalamus in MS[157, 317]. Cifelli et al reported a 35% reduction in neuronal number in the medial dorsal nucleus in MS patients relative to controls[157]. While the role of local GM plaques in mediating these changes has not been

assessed in detail, it seems unlikely that the modest degree of thalamic demyelination (~ 7 % according to our estimations, **Chapter 2.3.3**) could account for such marked changes. It has been suggested that neuronal loss in the thalamus occurs secondary to the transection of axons in distant WM lesions[157]. However we note that despite extensive axonal loss in the corticospinal tracts in MS[79, 101] we find little evidence for neuronal loss in the myelinated GM of the spinal cord, suggesting that transneuronal degeneration is not a prominent mechanism of neuronal death in this region. It is hypothesised that susceptibility to transneuronal degeneration is dependent on the extent of collateral connectivity, with neurons possessing relatively few sources of synaptic contact, such as those in the LGN, being particularly vulnerable to injury following de-afferentation or de-efferentation[334, 458, 459]. In contrast many spinal cord neurons are involved in complex neuronal networks, receiving multiple inputs and synapsing on multiple targets. They may therefore derive trophic support from numerous sources including propriospinal neurons within the cord, peripheral nerves and motoneurons, in addition to descending tracts from the brain[334, 402]. Such an abundance of synaptic connections may be sufficient to maintain neuronal survival, even following removal of descending afferents, potentially explaining the apparent resistance of spinal neurons to transneuronal degeneration[334, 401-404, 459].

Taken together, these studies suggest there is marked regional heterogeneity both in the extent of neuronal pathology in MS and in the mechanisms driving these changes. It appears that neuronal loss is greater in the thalamus (35% reduction[157]) and the spinal cord (e.g. 24% reduction in the upper cervical cord, 30% reduction in the upper thoracic cord) than in the cerebral cortex (10% reduction within lesions, no loss within myelinated areas[131]), although there are obvious limitations in comparing studies using different MS cohorts, different counting techniques etc.. Such variability may reflect regional differences in (i) the extent of GM demyelination and (ii) susceptibility to retrograde and transneuronal degeneration, which varies considerably between neuronal populations[382]. Therefore, neuronal loss in the spinal cord and the cerebral cortex occurs predominantly – if not exclusively - within local GM plaques while it is likely that transneuronal degeneration is more prominent in the thalamus. It is also interesting to note that despite substantial neuronal loss and myelin loss, the volume of the spinal cord GM is well preserved in the MS cases. Conversely atrophy of the cerebral cortex occurs despite no change in neuronal density[131], highlighting the complex interaction between tissue loss and atrophy in MS. Presumably loss of neurons – and myelin – within the spinal cord is countered

by some other process such as oedema, gliosis or expansion of the extracellular matrix, thus maintaining GM volume.

5.4.3 MS-related changes in neuronal size

In addition to reductions in neuronal numbers in the MS cases, we find significant differences in neuronal sizes between MS cases and controls. The average interneuron cross-sectional area is significantly reduced in the MS cases, suggesting there is shrinkage of these cells in MS. While these changes appear to be most marked within demyelinated areas (e.g. interneurons within GM plaques in the upper cervical cord show a 34% reduction in size in comparison with controls), reductions in interneuron size are also observed within myelinated areas of the MS cases. Again the mechanisms behind these changes are unclear. Evangelou et al suggested that anterograde transneuronal changes - in particular atrophy of the parvocellular neurons - occurs in the LGN of the thalamus secondary to axonal loss within plaques in the anterior visual pathway[317]. Similarly interneuron shrinkage in the myelinated GM of the spinal cord may reflect transneuronal damage following axonal injury in the WM tracts (the majority of descending corticospinal and rubrospinal tract fibres synapse on interneurons rather than motoneurons[429]).

There is some evidence that motoneuron size is increased in the MS cases in comparison with controls. The difference only reaches statistical significance in the lumbar region. The significance of this finding is unclear; changes in motoneuron size are particularly difficult to interpret in the context of neuronal loss. An apparent increase in motoneuron size could result from (i) pathological swelling of motoneurons (ii) a preferential loss of smaller motoneurons (i.e. a size-related susceptibility to motoneuron loss) resulting in an increase in the average size of remaining motoneurons, or even (iii) perikaryal shrinkage so that small motoneurons are incorrectly classified as interneurons.

We have not examined for changes in neuronal shape or dendritic architecture. Spinal motoneurons have extremely large dendritic trees, constituting 97% of the surface area and 75% of the volume of the neuron[460]. They frequently extend beyond the GM into the WM, and may therefore be susceptible to injury secondary to WM and well as GM pathology[460]. Damage to spinal motoneuron dendrites has been reported in EAE[344, 461], but further work is required to assess the extent of dendritic pathology in MS.

5.4.4 Clinical significance

Axonal degeneration is commonly considered to be the major cause of permanent, progressive neurological disability in MS patients[53]. Using the same spinal cord autopsy material, we have reported a 41% reduction in axonal number in the corticospinal tract at the upper cervical level, with a 26% reduction in the lumbar cord [79]. In contrast we report a ~ 25% reduction in neuronal number at the upper cervical level. It is therefore possible that this neuronal loss is a significant contributor to permanent disability in MS, along with demyelination and axonal loss. The substantial reduction in interneuron size may also be relevant clinically. Sastre-Garriga et al observed correlations between disability scores and GM NAA concentrations in the brain[156], while other groups have found no relationship[159, 320, 332]. Due to a lack of detailed clinical information we are unable to investigate the functional significance of neuronal pathology.

There are numerous subpopulations of interneurons with varying functions including the processing of sensory information, modulating motoneuron activity and co-ordinating motor activity between different spinal levels[459]. Interneuron pathology (i.e. reductions in the number and size of interneurons) may therefore contribute to a number of MS-related symptoms including motor and sensory disturbance. For example, it has been proposed that loss of dorsal horn inhibitory GABAergic interneurons following peripheral nerve injury contributes to neuropathic pain, resulting in a reduction in inhibition of nociceptors that terminate in the dorsal horn[462]. Similarly, interneuron loss may contribute to spasticity, a commonly experienced symptom in MS[459].

5.5 Conclusions and future work

In summary, neuronal loss in the spinal cord appears to occur predominantly within GM plaques, with both motoneurons and interneurons being affected. While we find little evidence of neuronal loss within the myelinated GM, we do observe changes in neuronal size, indicating that pathology is not exclusive to GM plaques. Further work is required to elucidate the mechanisms of this neuronal injury. Additional studies are also required to establish whether particular subpopulations of interneurons are more susceptible to neuronal injury than others.

Figures

Figure 5.1

*Paraffin sections from the upper thoracic level of the spinal cord stained with anti-Proteolipid Protein antibody (**A**), used to assess the extent of grey matter demyelination, and Luxol Fast Blue Cresyl Violet (**B - H**), used to perform the neuronal counts. Our assessment was restricted to the anterior horns of the GM, defined as the area ventral to the GM commissure (**B - D**). **E, F** - Measurements of neuronal number and cross-sectional area (panel **F**, shaded) were made for all neurons in which the nucleolus was visible within the plane of section. **G, H** - Neurons were classified as motoneurons or interneurons according to size criteria; Neurons with a maximum diameter of at least 30μm and a minimum diameter of at least 13.5μm were classified as motoneurons (**G**); all other neurons were classified as interneurons (**H**). Scale bars (**E - H**) represent 20μm.*

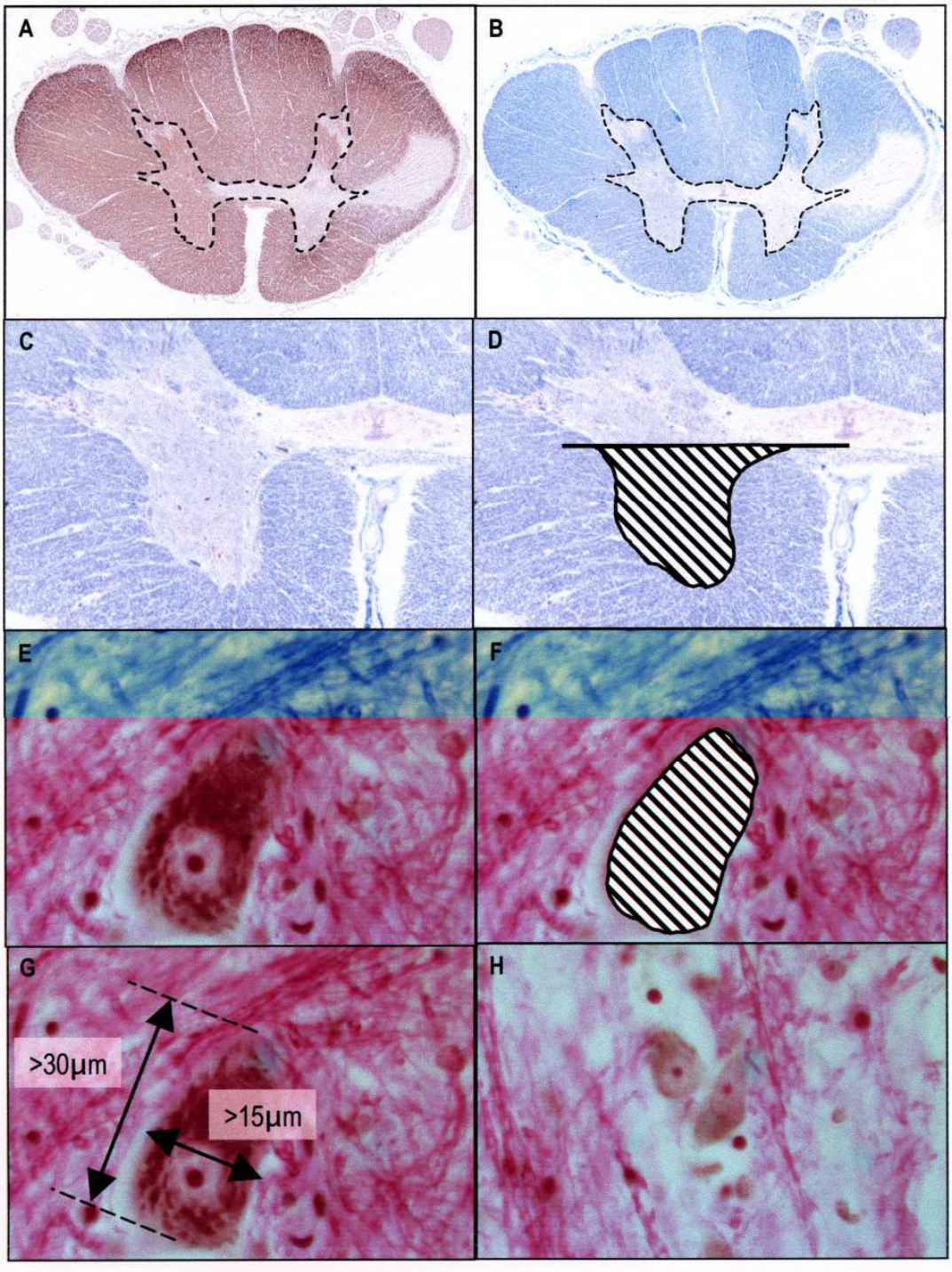
A
B
C
D
E
F
G
>30µm
>15µm
H

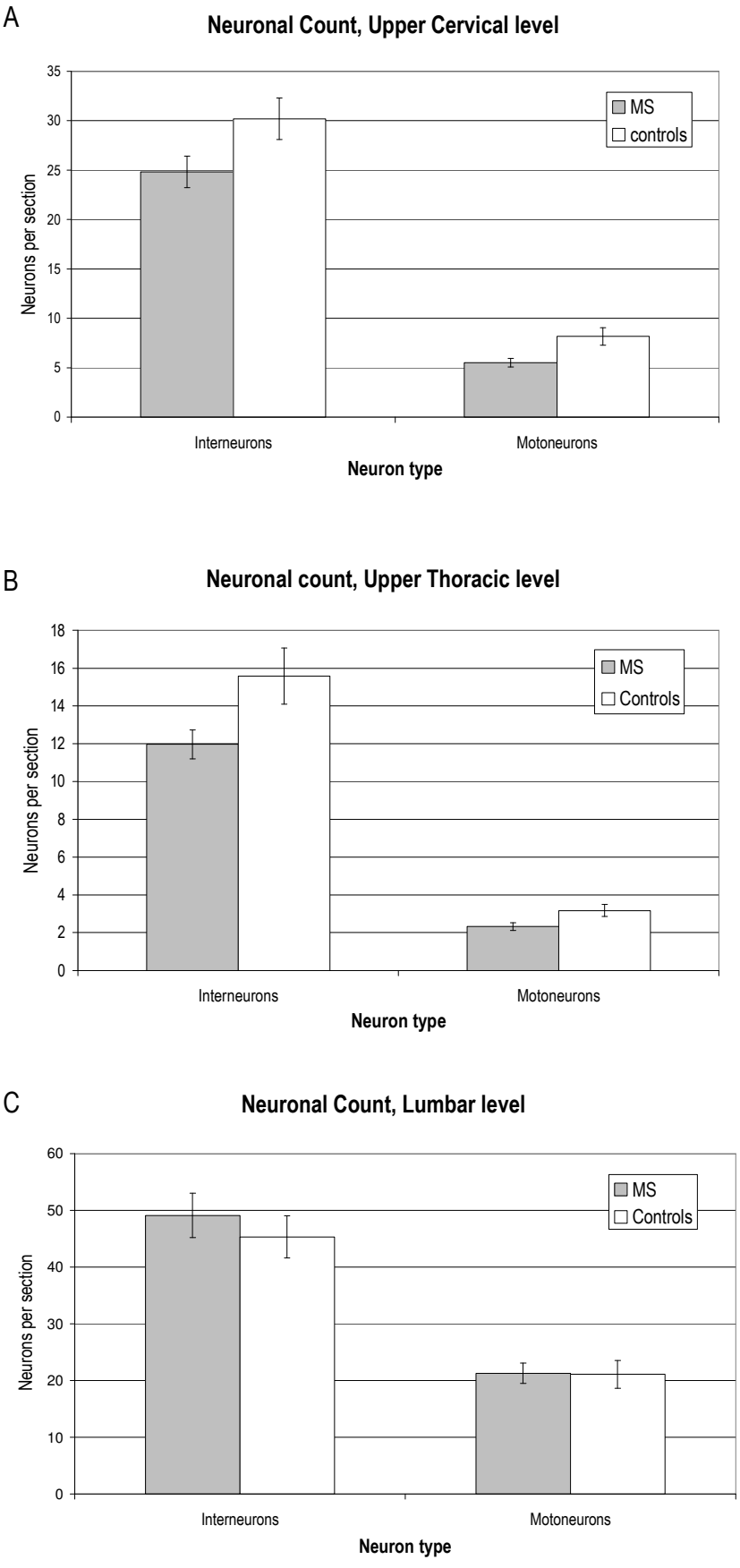

Figure 5.2 - *Bar charts of the number of interneurons and motoneurons at the upper cervical (A), upper thoracic (B) and lumbar (C) levels of the spinal cord. Values represent mean ± standard error.*

Figure 5.3

Bar charts of the cross-sectional areas of interneurons (A) and motoneurons (B) at different levels of the spinal cord. UC=upper cervical; UT=upper thoracic; LUM=lumbar. Values represent mean ± standard error.

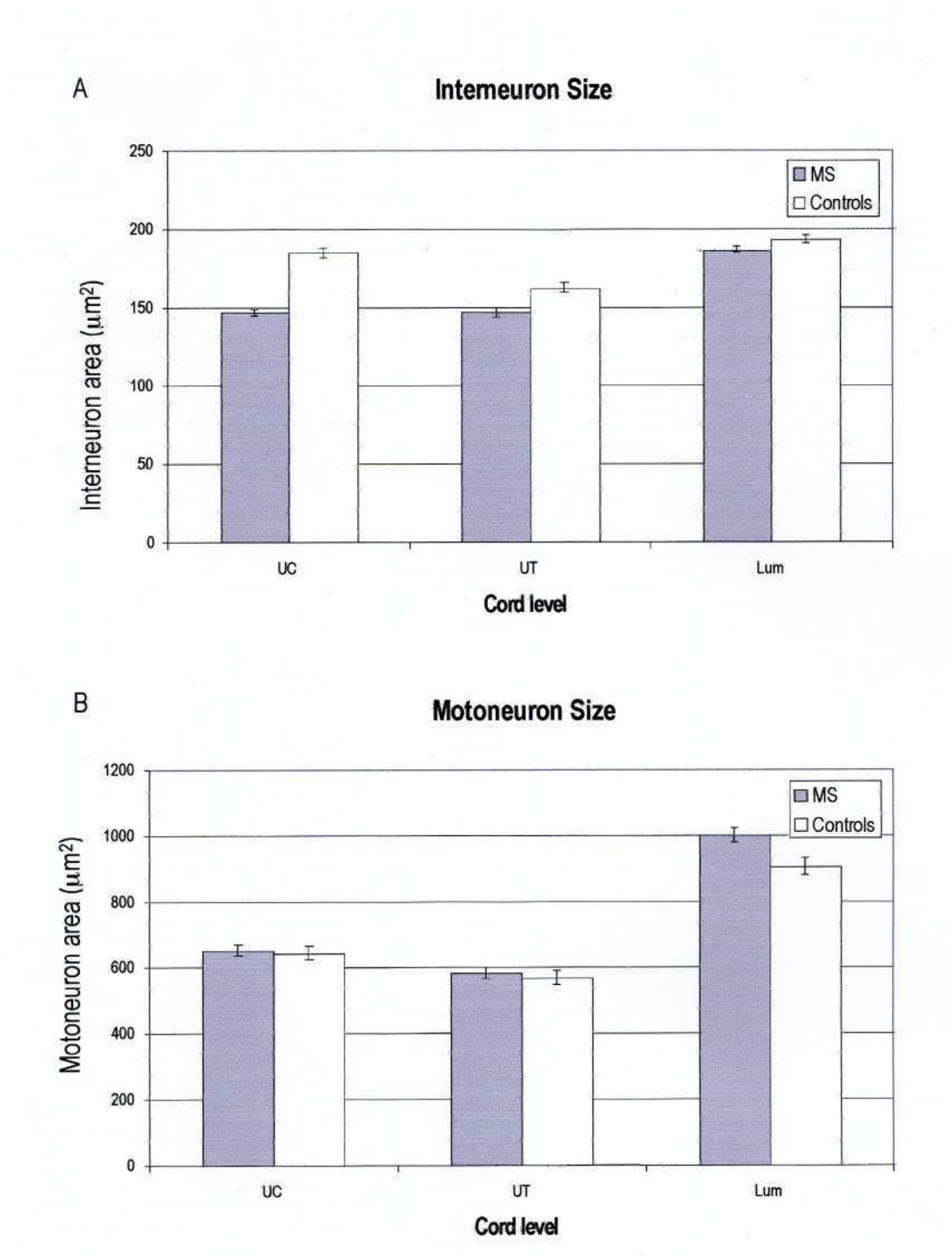

Chapter 6: The sensitivity of 4.7 Tesla MRI for detecting spinal cord grey matter demyelination in Multiple Sclerosis - a post-mortem MRI-histopathological correlative study

6.1 Introduction

Post-mortem studies demonstrate extensive GM demyelination in the brain and spinal cord in MS[132-135]. It is feasible that these lesions result in substantial functional impairment secondary to conduction block, axonal loss and neuronal apoptosis[130, 132]. For example, it has been suggested that cortical plaques could contribute to a range of MS-related symptoms including cognitive dysfunction, seizures, fatigue and depression[134, 178-180]. However the true clinical significance of GM demyelination is uncertain, largely because of the poor sensitivity of MRI for detecting these lesions[128, 222, 463].

MRI-histopathological correlative studies demonstrate that GM demyelination in the brain is grossly underestimated by conventional imaging techniques[128, 129, 222, 463]. For example Newcombe et al imaged autopsy material from 17 MS cases at 0.5 Tesla (T), detecting none of the 39 cortical lesions identified on histology, and only a small proportion of deep GM lesions[463]. Similarly, Kidd et al imaged material at 0.6 T; only 2 of the 14 intracortical lesions and 58 of the 108 juxtacortical lesions were identified on MRI[222]. Moreover, both of these studies used histochemical myelin stains to identify GM lesions on histology; they are therefore likely to have underestimated the extent of GM demyelination, and so overestimated the sensitivity of MRI for detecting such lesions.

Geurts et al assessed the sensitivity of MRI for detecting GM plaques using myelin protein IHC, the "gold standard" staining method for detecting GM demyelination[127, 128, 132]. T2-weighted images of autopsy material were acquired at 1.5T; only 22% of mixed GM/WM cortical lesions, 3% of intracortical lesions and 13% of deep GM lesions were detected on MRI[128]. Employing a 3D FLAIR (fast fluid-attenuated inversion recovery) sequence - a heavily T2-weighted technique used to suppress the CSF signal so the brain / CSF interface can be better visualised - resulted in a very modest increase in sensitivity, revealing 5% of intracortical lesions and 38% of deep GM lesions. When the locations of the histological lesions were

revealed to the MRI readers 74% of the type I (i.e. leucocortical) lesions were identified, in comparison to 66% of intracortical lesions and 63% of deep GM lesions, demonstrating that a substantial number of GM lesions could not even be identified retrospectively[128]. Bö et al have also demonstrated that conventional MRI is particularly poor for detecting subpial lesions[129].

A number of studies have attempted to visual GM demyelination in vivo. For example Geurts et al suggest that cortical lesion detection may be improved by using a double inversion-recovery sequence to suppress the CSF and WM signals simultaneously[464]. Bagnato et al scanned 22 MS patients at 1.5T, co-registering multiple T1-weighted images (12 serial scans, obtained monthly for 1 year) to generate a single mean image with a high signal-to-noise-ratio[465]. Pure cortical lesions were detected in 9 of the 22 MS patients examined. However, only 23% of the cortical lesions were entirely intracortical, suggesting that a great number of subpial lesions were not detected (i.e. neuropathologic studies indicate that the majority of cortical lesions are intracortical[127, 129, 131-134]). MRI-pathology correlative studies are therefore required to assess the true sensitivity and specificity of these techniques.

In comparison to WM plaques - for which MRI is highly sensitive - cortical lesions show a reduced inflammatory cell infiltrate[130, 135, 222], low degrees of complement deposition[137] and an absence of BBB disruption[136]. Such modest inflammation may result in little signal abnormality in the demyelinated cortex, impairing lesion detection. Bö et al studied the extent of $CD3^+$, $CD4^+$, $CD8^+$, and $CD45RO^+$ T cell infiltration in cortical lesions using autopsy material from 10 MS patients[135]. The highest density of T cells was found in WM lesions; fewer were found in the cortical portion of type I lesions, while the lymphocyte density in the intracortical lesions was no greater than in myelinated MS cortex or control cortex. Similarly, Peterson et al reported that cortical lesions contain a 13-fold reduction in lymphocytes and a 6-fold reduction in $CD68^+$ microglia / macrophages in comparison with WM lesions[130]. In addition there were morphological differences between MHC class II-positive cells in WM lesions (the majority of which were phagocytic macrophages) and those in cortical lesions (where MHC class II-positive cells retained the morphology of activated microglia). Brink et al reported that levels of complement activation products (C1q, C3d and C5b-9) were reduced in the GM portion of type I cortical lesions in comparison with active, chronic active and chronic inactive WM lesions[137]. Pure cortical lesions showed even lower degrees of complement deposition. Furthermore, while WM lesions show evidence of BBB disruption (deposition of fibrinogen and IgG, indicating leakage of these proteins from blood vessels into the brain parenchyma) and blood vessel wall

damage (splitting of the basal membrane, demonstrated by staining for type IV collagen), similar changes are not detected in cortical lesions[136].

Bö et al suggest the apparent paucity of inflammation observed in cortical lesions may simply reflect an abundance of chronic inactive lesions in autopsy material[135]. However it is unclear whether cortical demyelination occurs in the absence of inflammation or if inflammation occurs transiently, but subsequently resolves. It is feasible that the relatively low myelin content of the cortex does not incite a prominent inflammatory reaction[466]. Alternatively neurons within the GM may secrete neurotrophins and other substances which promote an "anti-inflammatory" environment[466, 467]. Other differences between GM and WM - perhaps related to the BBB - may also contribute to reduced inflammation in cortical lesions[135, 466].

Merkler et al injected the pro-inflammatory cytokines TNFα and INFγ into the cerebral cortex of MOG-immunised Lewis rats producing extensive subpial demyelination (similar in topography to MS lesions) accompanied by the infiltration of macrophages, perivascular and parenchymal T cells, and complement deposition[240]. However this cortical inflammation was short-lived, resolving within 2 weeks. Interestingly, identical cytokine injections into the WM of the spinal cord or the corpus callosum resulted in dense inflammatory infiltrates that persisted for several weeks, indicating that EAE immunopathology strongly depends on the lesion site[240, 468]. In a separate study Merkler et al examined inflammation during the acute phase of lesion formation in marmosets with MOG-induced EAE, another animal model which shows extensive cortical demyelination[466]. In comparison to their WM counterparts, cortical lesions contained fewer inflammatory cells in the parenchyma. WM and GM lesions contained similar numbers of perivascular inflammatory cells (T- and B-lymphocytes, and MHC-II expressing macrophages/microglia) although the cortical lesions contained a smaller proportion of macrophages expressing the early activation marker MRP14. Interestingly, examination of leukocortical lesions (i.e. mixed GM/WM lesions) revealed that the border between WM and cortex was strictly respected with regard to the density of inflammatory infiltrates within the parenchyma, with fewer inflammatory cells being observed in the GM portion of the lesions.

A number of other factors may contribute to the low sensitivity of conventional MRI for detecting cortical demyelination. Due to its high cellular density and low myelin content, the T2 relaxation time of the cerebral cortex is higher than that of the WM. Therefore while WM lesions show a marked increase in T2 relaxation time with respect to the surrounding "normal appearing" WM,

only small increases occur in cortical lesions, resulting in poor contrast between "normal appearing" GM and cortical lesions[128]. Particular anatomical features may further hinder the detection of cortical lesions. The cortex is a thin, highly folded structure, making it difficult to image[193]. In addition, some GM lesions may be masked by partial volume effects from sulcal CSF[469]. This is likely to be particularly relevant when imaging subpial lesions, which constitute a large proportion of cortical plaques[127].

To our knowledge no imaging study has examined spinal cord GM involvement in MS. We have demonstrated substantial demyelination in the GM of the spinal cord; it is important to be able to visualise these lesions radiologically in order to examine the functional consequences of demyelination in this clinically eloquent site. In this MRI-pathology correlative study we evaluate the sensitivity of high resolution MRI for detecting GM demyelination in the spinal cord in MS.

6.2 Materials and methods

6.2.1 Clinical material

Human autopsy material was obtained from 11 pathologically confirmed cases of MS and 2 controls. This material comprised all of the cases received by the Netherlands Multiple Sclerosis Brain Bank between 1998 and 2001. The MS cases (3 males, 8 females), aged 45 – 83 years (median 70 years) with disease durations of 7 – 52 years (median 23 years), had a post-mortem delay of 5 h 30 min –16 h 45 min (median 8 h 50 min) and a scan delay of 61 – 224 days (median 116 days). The controls (2 females, aged 41 and 83 years), had no clinical or pathological evidence of spinal cord disease. The characteristics of the patients and controls are summarised in **table 6.1**. This autopsy material has been used in a previous study[470].

6.2.2 MR Imaging Protocol

For each of the MS and control cases material was taken from the cervical or the upper thoracic levels of the spinal cord. Proton Density (PD) - weighted images (TR (repeat time) / TE (echo time) : 3000 / 15 ms, 0.1 x 0.1 x 1.0 mm resolution) of this formalin-fixed material - which was immersed in a non-magnetic oil (Fomblin; perfluorinated polyether, Solvay Solexis, Weesp, The Netherlands) - were acquired at 4.7 T (Unity Varian, Palo Alto, CA, USA) using a custom-made solenoidal coil as described by Bot et al[470].

6.2.3 Histological evaluation

Following imaging the specimens were cut at 1cm intervals and embedded in paraffin. Adjacent 5µm sections were taken from predetermined levels of these tissue blocks and stained for MBP, GFAP, and MHC class II.

6.2.4 Immunohistochemistry

Sections were stained for MBP, HLA-DR and GFAP using the EnVision method as described in **Chapter 2.2.3**.

6.2.5 Antibodies

The primary antibodies used were mouse anti-MBP (IgG1, dilution 1:150, MAB387, Chemicon International, Temecula, CA, USA), mouse anti HLA-DR (IgG2b, clone LN3, dilution 1:100, obtained from Dr. J.H.M. Hilgers, VU University Medical Centre, Amsterdam, the Netherlands) and rabbit anti-human GFAP (dilution 1:4000, Z0334, DAKO). For the HLA DR-staining the tissue sections were cooked for 10 minutes in a 10 mM citrate buffer (pH 6.0) for antigen retrieval, cooled and rinsed with PBS prior to incubation with the primary antibody.

6.2.6 Histological Assessment

Digital photographs of the MBP-stained sections (Nikon D1X 105mm camera, Photoshop CS software) were used to manually outline the MS lesions ("Scion Image" image analysis software). Histopathological lesions were defined as sharply demarcated areas characterised by either complete myelin loss or markedly reduced myelin density on the MBP-stained sections (**figure 6.1**). Areas of demyelinated GM and WM were measured separately as described previously (**figure 3.3**). Lesions were identified by two observers (LB and CPG in consensus; LB was blinded to the MRI results, CPG assessed the histology sections 6 months after performing the image analysis and did not re-examine the scans prior to the histological assessment). The cross-sectional areas of the spinal cords and the cross-sectional GM areas were measured in order to calculate the relative proportions of the GM and WM that were demyelinated. The MBP-stained sections, examined via microscopy (10x, Olympus BX40 microscope) were used as a reference to help identify the MS lesions and the GM boundaries.

6.2.7 Assessment of lesion activity

WM lesions were categorised as active, chronic active or chronic inactive on the basis of HLA DR immunoreactivity, using the classification system of Bö et al[31]. Active lesions are

characterised by intense staining for MHC class II-positive cells (activated microglia and macrophages) throughout the lesion. Chronic active lesions show intense staining of MHC class II-positive cells at the lesion edge, with a paucity of staining in the centre. Chronic inactive lesions do not show prominent MHC class II staining. Activated microglia and macrophages are differentiated by morphological criteria; microglia have small perikarya, thin processes and elongated nuclei whereas macrophages have larger, round perikarya and lack processes. Mixed GM/WM lesions were staged according to the activity of the WM component of the lesion. A similar system has been used to classify mixed GM/WM lesions in the cerebral cortex[130].

6.2.8 Image analysis

The tissue sections were matched with the corresponding MR images using anatomical landmarks such as the morphology of the GM and the MS plaques. The readers (CPG and JJGG in consensus) scored the MR images for MS lesions, blinded to the histopathology results. MRI lesions were defined as clearly circumscribed areas of abnormal (hyper-intense) signal intensity on the PD-weighted image. Areas of WM and GM were scored separately using the same system described to score the histopathological sections (**figure 6.1**).

6.2.9 Statistical analysis

In view of the relatively small sample size and the distribution of the data, nonparametric tests were used (SPSS software – version 11.5, SPSS, Chicago). Wilcoxon Signed Ranks Test for paired data was applied to compare the proportion of demyelinated WM to the proportion of demyelinated GM. Spearman's ranked test was used for correlations.

6.3 Results

6.3.1 MBP Staining

The staining pattern of myelin in the control spinal cords was very similar to that observed with the PLP antibody, with a paucity of myelinated fibres in the Substantia Gelatinosa of the dorsal horns and in the GM commissure (**figure 6.2**). Unlike PLP - which is restricted to CNS myelin - MBP is also present in the myelin of the peripheral nervous system. This is evident on comparison of **figure 6.2** and **figure 3.7**, which demonstrate staining of the nerve roots with the anti-MBP, but not the -PLP antibody.

6.3.2 Lesion counts

In the 32 sections studied from the 11 MS cases, 95 demyelinated lesions (51 completely demyelinated areas, 44 areas of markedly reduced myelin density) were detected in the WM and 56 lesions (38 completely demyelinated lesions, 18 areas of markedly reduced myelin density) were detected in the GM. Only one of the GM lesions was restricted entirely to the GM; the remainder were mixed GM/WM lesions.

Overall, a mean 31.1% (median 19.3%) of the WM analysed was demyelinated in comparison with 28.5% (median 10.8%) of the GM. This difference was not statistically significant ($p = 0.721$). There was a significant correlation between the proportion of demyelinated WM and the proportion of demyelinated GM (coefficient = 0.72, $p = 0.013$). The proportion of WM that was demyelinated did not correlate with patient age (coefficient = 0.20, $p = 0.554$) or disease duration (coefficient = 0.20, $p = 0.555$). Similarly the proportion of GM that was demyelinated did not correlate with patient age (coefficient = 0.100, $p = 0.769$) or disease duration (coefficient = 0.009, $p = 0.979$). The proportion of demyelinated WM and GM in each of the MS cases is shown in **table 6.1**.

6.3.3 MHC class II and GFAP expression

3 active lesions (from two different cases) and 5 chronic active lesions (from a third case) were detected. The GM portion of these lesions showed reduced MHC class II-positivity in comparison to the WM portion (**figure 6.4**). The majority of MHC class II-positive cells in the WM portion were macrophages, while those in the GM had the morphology of activated microglia. The remaining lesions were classified as chronic inactive. GFAP expression was highly variable, both within WM and GM plaques (**figure 6.4Q** and **S**).

6.3.4 MRI

The GM and WM of the spinal cord were easily differentiated on the PD-weighted images. In two cases (case numbers 1 and 9, **table 6.1**) the MR images were of poor quality and were excluded from the analysis. MRI analysis of the remaining 9 cases revealed 35 of the 37 completely demyelinated WM lesions that were detected histopathologically (94.6% sensitivity) and 18 of the 24 WM areas with markedly reduced myelin density (75% sensitivity). In the GM, 28 of the 32 completely demyelinated lesions (87.5% sensitivity) and 4 of the 12 areas of markedly reduced myelin density (33.3% sensitivity) were detected on MRI (**figure 6.5**). Therefore, overall the sensitivity of MRI was 87% for detecting all WM lesions, and 75% for all

GM lesions. Furthermore the MR images accurately depicted the outline of the GM lesions. All of the areas of abnormal signal intensity scored on MRI did correspond to an area of demyelination. The average size of the GM lesions that were visible on MRI (mean 1.7mm^2) was greater than those that were not detected (mean size 0.6mm^2).

6.4 Discussion

While post-mortem studies have provided important insights into GM pathology in MS, non-invasive techniques are required to detect GM lesions in-vivo in order to establish (i) how GM lesions evolve over time, (ii) their clinical significance and (iii) response to therapeutic intervention. MRI-pathology correlative studies play an important role in understanding the pathological substrate of MR abnormalities.

6.4.1 Post-mortem MRI is highly sensitive for detecting spinal cord GM involvement in MS

To our knowledge this is the first study to assess the sensitivity of post-mortem MRI for detecting GM lesions in the spinal cord in MS. In contrast to previous work using this autopsy material we use myelin protein IHC to examine the extent of GM demyelination[470]. Our results indicate that post-mortem imaging at 4.7 T is highly sensitive for cord lesions, detecting 87% of WM lesions and 75% of GM lesions. Furthermore MRI was highly specific for GM demyelination, with all areas of abnormal signal hyper-intensity corresponding to plaques.

The spinal cord GM lesions that were not detected on MRI were generally very small and may be beyond the resolution of the scanner. Alternatively they may have been missed due to inaccuracies in the co-registration of the tissue sections to the MR images. Small lesions located in the GM commisure and substantial gelatinosa may be expected to go undetected as these areas appear hyperintense on the PD-weighted images; for example, it is unsurprising that the single pure GM lesion, which was restricted to the GM commissure, was not detected on MRI. In contrast to a previous MRI-pathology correlative study, we have not performed a retrospective, side-by-side comparison of the MR images and tissue sections to look for subtle signal abnormalities corresponding with the histologically-identified lesions initially missed on MRI[128]. Such assessments are subject to bias and it is difficult to evaluate the specificity of the subtle signal changes that are identified. However, we recognise that the readers' skill in analysing post-mortem MR images may improve with experience. Because of a paucity of

autopsy material for use in MRI-pathology studies it is difficult to assess this learning effect although we note that one of the readers (JJGG) has extensive experience in analysing post-mortem MR images[128, 129, 471].

We have previously reported that a number of spinal cord plaques show a distinct morphology whereby a proportion of the plaque border maintains a strict respect for the GM/WM boundary, resulting in areas of demyelinated GM with apparent sparing of the adjacent WM. We observe a similar pattern of demyelination in the current study (**figure 6.1I, J**). However, within our relatively small sample, we do not see any lesions that extend along the GM/WM boundary over large distances. Similarly we only observe a single pure GM lesion, partly reflecting the fact that these are more commonly seen in the lumbar cord where the GM has a larger cross-sectional area. Therefore we are unable to comment on the utility of post-mortem MRI for detecting and defining the morphology of these lesions.

6.4.2 Spinal cord GM plaques may be detected on MRI more readily than brain lesions

In contrast to the current study, a number of previous reports demonstrate that GM demyelination in the brain is grossly underestimated by conventional MRI[128, 222, 463]. The higher sensitivity that we observe is likely to reflect a number of factors:

i. Morphological differences between spinal cord and cortical plaques

The most frequently observed lesions in the cerebral cortex are subpial in location, extending inwards from the surface of the brain, usually to layers 3 or 4 of the cortex[127, 131-134]. Detection of these plaques is potentially hindered by partial volume averaging with the CSF. Furthermore, the density of myelinated fibres is particularly low in these superficial cortical layers, and is likely to result in poor contrast between “normal appearing” GM and subpial lesions on MRI[464]. With the exception of the Substantia Gelatinosa and the GM commissure, the GM of the spinal cord contains more myelin than the superficial cortical layers. This may result in greater contrast between myelinated and demyelinated areas in the spinal cord, aiding lesion detection in this area. Areas of high myelin content may also incite a more intense inflammatory reaction, resulting in even greater signal change and further aiding lesion detection.

The vast majority of spinal cord GM lesions observed in our study were mixed GM/WM lesions. MRI is more sensitive for detecting mixed GM-WM cortical lesions than pure intracortical lesions[128]. Identification of mixed GM/WM lesions is aided by following the plaque border from

the readily identifiable WM portion of the plaque into the GM. Furthermore, the GM portions of mixed GM/WM cortical lesions contain more prominent inflammatory changes than pure intracortical lesions, which may also aid lesion detection[135, 137]. It is interesting to note that, despite these factors, Geurts et al only detected 22% of mixed GM-WM lesions on post-mortem MRI[464]. In contrast we detect 75% of GM lesions in the spinal cord, most likely reflecting the higher field strength employed in our study (4.7T versus 1.5T).

ii. Differences in inflammatory cell content

The low inflammatory cell content of cortical plaques is believed to hinder their detection by MRI[130, 135, 222, 464]. There may be regional differences in the numbers of inflammatory cells in GM plaques, as is the case with WM lesions[328]. It is feasible that, in comparison with cortical lesions, spinal cord GM plaques show a more fulminant inflammatory reaction, which in turn aids their detection on MRI.

Animal studies indicate that there are marked differences between the GM of the brain and spinal cord in terms of their response to injury. Following either traumatic injury or the injection of pro-inflammatory cytokines (TNFα and IL-1β), leucocyte infiltration and BBB breakdown is more pronounced in the spinal cord GM in comparison to the striatum[264, 265]. It has been suggested that these differences reflect, in part, differences in the expression of chemokines in response to injury[472].

As expected in a post-mortem study, we observe relatively few active plaques. Overall, 8 active or chronic active lesions were detected in three MS cases. It is likely that these do not actually represent 8 distinct lesions, but rather that some extensive lesions appear on more than one tissue section. However, our results suggest that the GM portion of these lesions contain fewer MHC class II-positive cells than the WM portion. Whereas the majority of activated cells in the WM lesion were macrophages, those in the GM lesions had the morphology of microglia. Peterson et al made similar observations in relation to mixed GM/WM lesions in the cerebral cortex[130]. Further work is required to assess the degree of lymphocyte infiltration, BBB breakdown and complement deposition in the GM plaques as any of these factors may influence lesion detection by MRI. We have previously attempted to examine lesion activity in a larger number of cases, using the autopsy material derived from the Oxford Radcliffe NHS Trust and used in **Chapter 3**. MHC class II-expression was examined in 28 sections taken from 13 MS cases (23 sections) and 3 controls (5 sections). Despite using an identical staining

protocol to that used in the current study, the staining was unsuccessful in the majority of cases, possibly reflecting the longer fixation times of the Oxford archival material. However a small number of active plaques were observed, including that shown in **figure 6.7** which illustrates that some spinal cord GM plaques can contain large numbers of inflammatory cells, and MHC class-II positive cells within these lesions may have a macrophagic morphology.

iii. Gliosis

There appears to be regional variation in the extent of gliosis within GM plaques. We have used GFAP to examine gliosis in a limitted number of MS cases; further work - using additional astrocyte markers - is required to characterise gliosis in more detail. However our results suggest that a proportion of spinal cord GM plaques are associated with a prominent gliotic reaction (**figure 3.10** and **figure 6.4**). In contrast, Vercellino et al did not observe gliosis within cortical plaques or lesions in the deep GM structures of the brain[132].

iv. Anatomical differences between the brain and spinal cord

Finally, particular anatomical features are also likely to facilitate lesion detection in our study. The morphology of the spinal cord is relatively simple in comparison with the highly folded cerebral cortex. The spinal cord GM is not predisposed to partial volume averaging with the CSF and is less prone to errors in matching the histopathological sections with the corresponding MR images. Accurate matching of the tissue sections to the MR images is further aided by imaging formalin fixed material. All of these factors make the spinal cord well suited for MRI-pathology correlative studies.

6.4.3 Limitations of the study

There are several limitations to our study that require further discussion. Firstly, tissue fixation may affect the distribution of water within tissue, altering a number of MR parameters[222, 473, 474]. However it has been demonstrated through serial imaging of this material that no further changes in relaxation times occur after 45 days of fixation[470]. All of the MR images used in this study were obtained after this time point to minimise possible differences between specimens caused by the effects of formalin fixation.

There are obvious limitations to extrapolating our work to in vivo MRI. Post-mortem imaging permits the acquisition of high resolution images owing to the absence of motion artefact and improved signal-to-noise-ratio through the use of a surface coil and longer scanning times[222].

Currently, poor spatial resolution precludes the use of MR imaging to study spinal cord GM pathology in vivo in adequate detail. Cord image quality is further compromised by artefacts related to surrounding bone, fat and CSF, and by motion artefacts related to respiratory and cardiac movement[475]. Bergers et al compared post-mortem in situ MRI (i.e. imaging of the whole-corpse - before the cord was removed - using a clinical scanner) with in-vitro imaging at high-resolution, demonstrating that in situ MRI underestimated the number and size of spinal cord plaques[475].

6.5 Conclusion

MRI-pathology correlative studies indicate that conventional MRI is insensitive for detecting GM demyelination in the brain in MS. In contrast we demonstrate that post-mortem imaging at 4.7T is highly sensitive for detecting spinal cord GM demyelination. This is likely to reflect a number of factors including the use the improved spatial resolution obtained at 4.7T, anatomical factors and intrinsic differences between GM lesions in the spinal cord with those in the brain. Our work suggests that the spinal cord is a promising site to study the functional consequences of GM lesions, although there are a number of technical challenges related to imaging the GM of the cord in vivo.

Figures

Figure 6.1

Paraffin sections from MS spinal cords, immunohistochemically stained with anti-Myelin Basic Protein antibody. ***A, B*** *- Sections were scored for lesions characterised by either complete myelin loss (blue shading) or markedly reduced myelin density (red shading). The grey matter (GM) / white matter (WM) boundary is outlined (dashed line). This section contains two completely demyelinated plaques (one restricted to the WM, one mixed GM/WM lesion) and one plaque characterised by a marked reduction in myelin density (restricted to the WM).* ***C-E*** *- Areas of GM showing normal myelin density (**C**), markedly reduced myelin density (**D**) and complete myelin loss (**E**) at high magnification.* ***F-H*** *- Areas of white matter showing normal myelin density (**F**), markedly reduced myelin density (**G**) and complete myelin loss (**H**).* ***J*** *- A proportion of lesions maintain a strict respect for the GM/WM boundary. Higher magnification images from panels I (box) demonstrate complete demyelination of the GM with apparent sparing of the adjacent WM. The scale bars in C-H represent 50µm; in J they represent 500µm.*

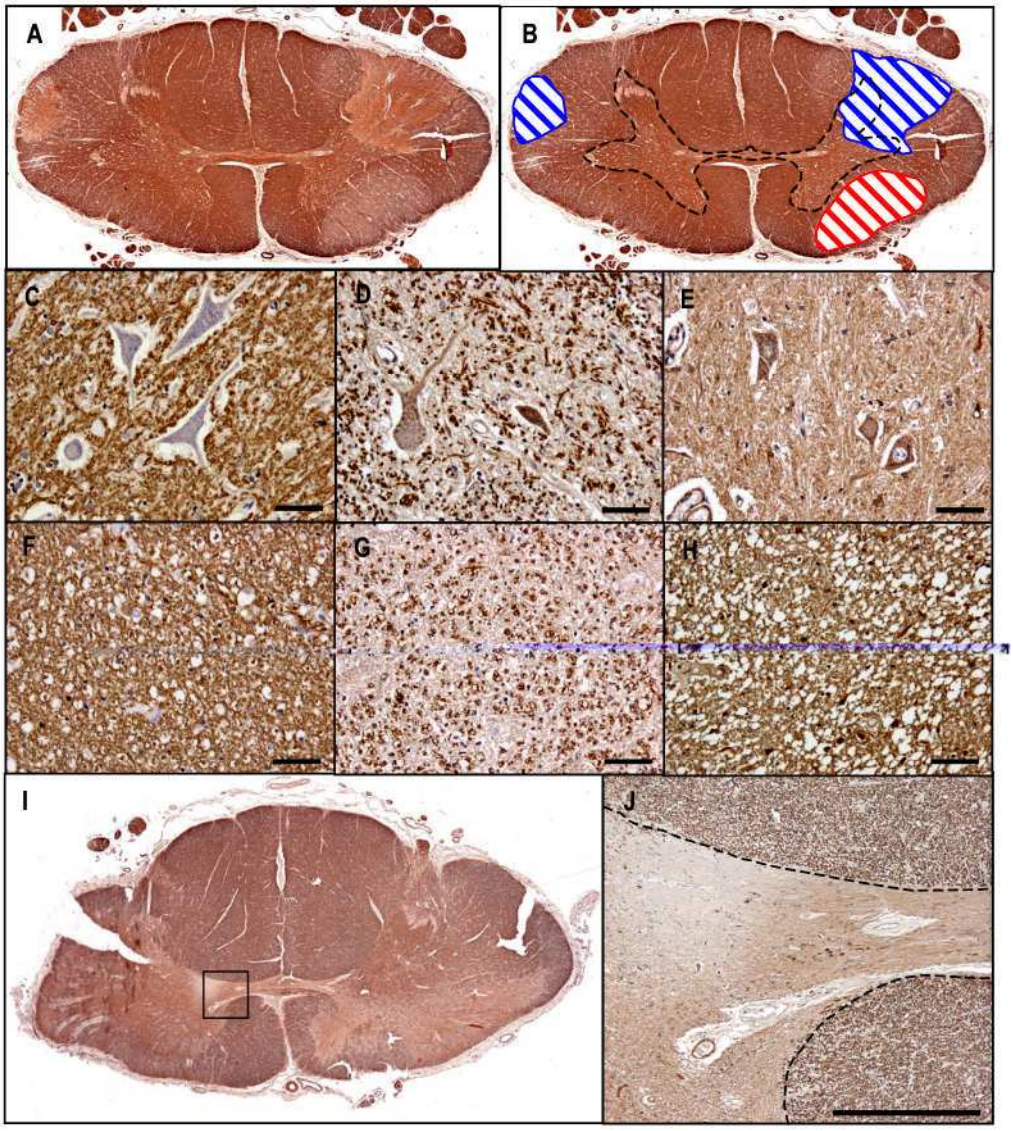
A
B
C
D
E
F
G
H
I
J

Figure 6.2

*Paraffin sections from control spinal cord, immunohistochemically stained with anti-Myelin Basic Protein antibody, demonstrating a paucity of myelin in the Substantia Gelatinosa (dashed box, shown at higher magnification in panel **B**) and the grey matter (GM) commissure (solid box, panel **C**). In contrast to Proteolipid Protein, Myelin Basic Protein is also a component of myelin in the peripheral nervous system and therefore stains the posterior nerve roots. Scale bars (**B, C**) represent 500µm.*

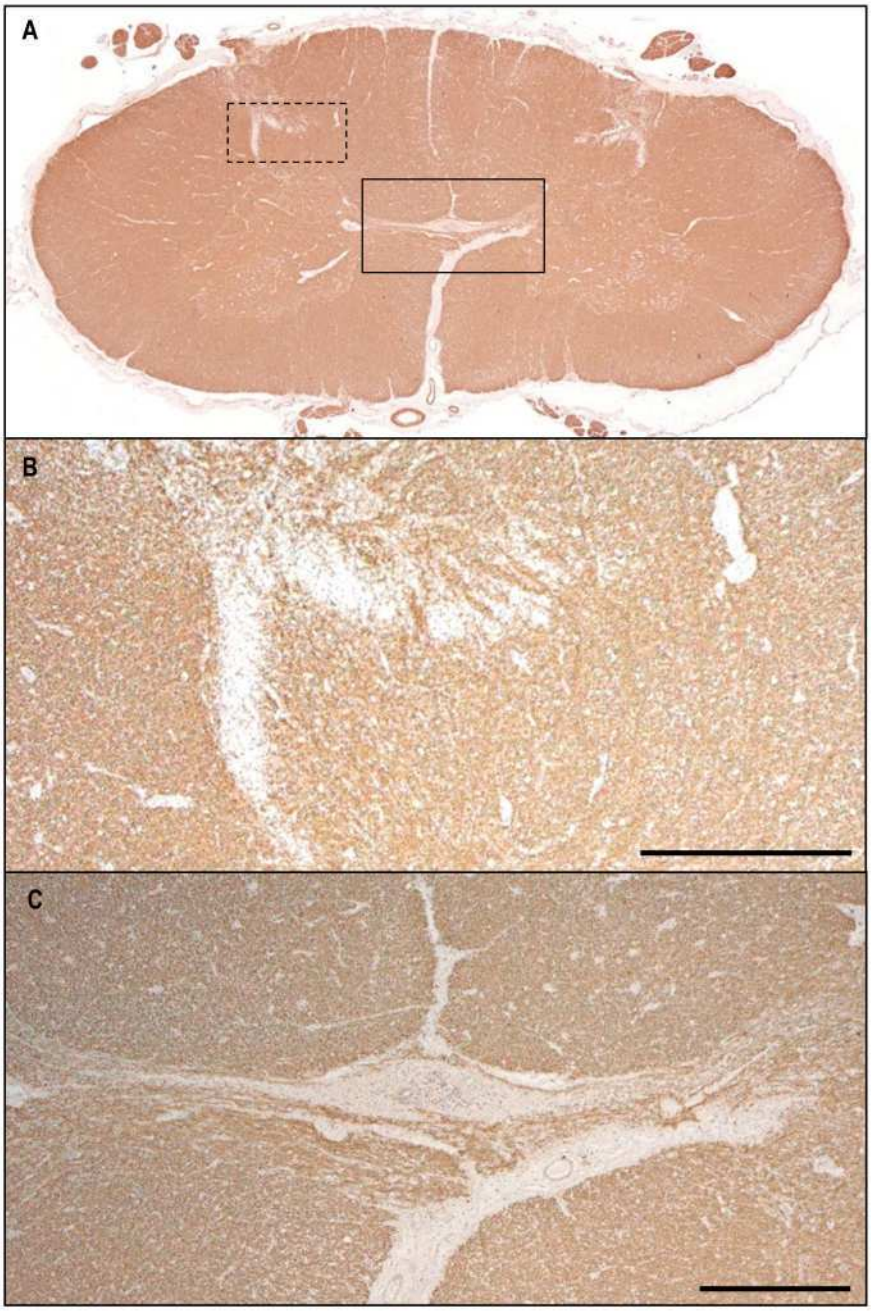
A
B
C

Figure 6.3

*Paraffin sections from MS spinal cords immunohistochemically stained with anti-Myelin Basic Protein (**A, C, E**) antibodies with the corresponding Proton Density-weighted scans of the autopsy material, imaged at 4.7 Tesla (**B, D, F**).*

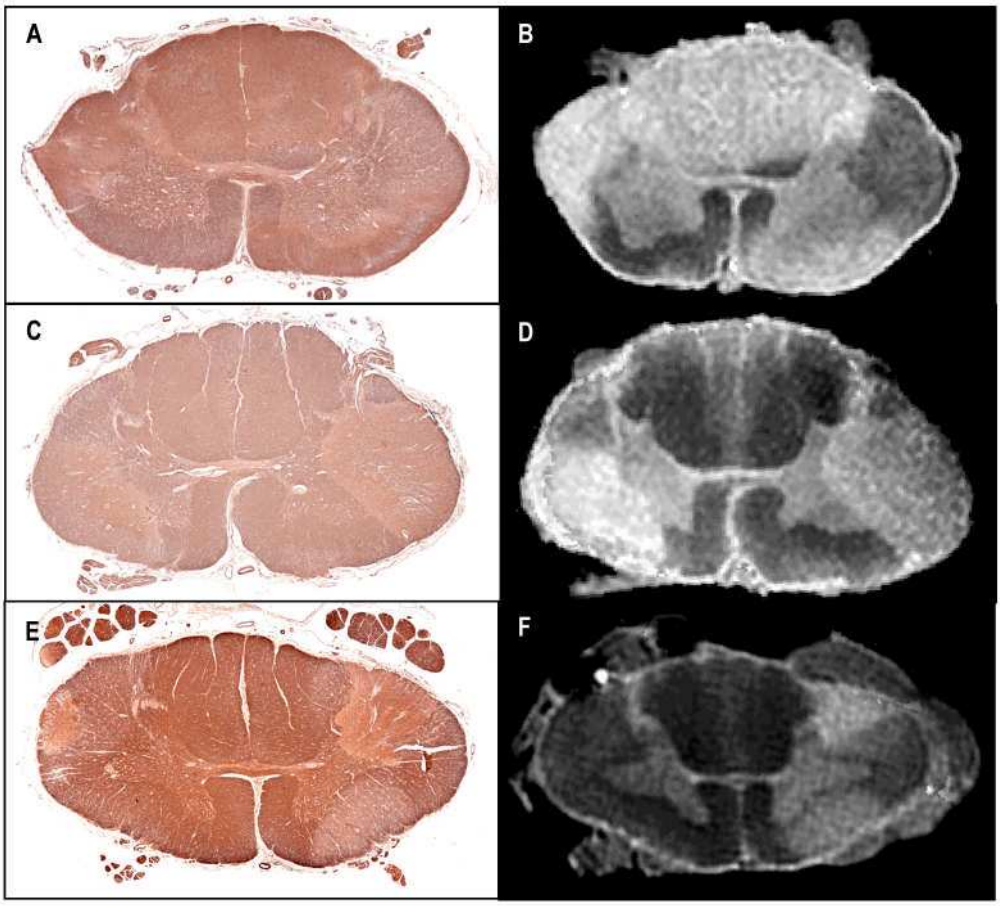
A
B
C
D
E
F

Figure 6.4

*Paraffin sections from control (**A-D**) and MS spinal cords (**E-S**), immunohistochemically stained with anti-Myelin Basic Protein (MBP) (**A, E, M, R**), anti-HLA DR (**B-D, F-L, N-P**), and anti-GFAP antibodies (**Q-S**). **A-D** - Tissue from control cases show low levels of HLA DR-staining (**B**), seen at higher magnification in panels **C** (grey matter (GM)) and **D** (white matter (WM)). **E, I** - Bilateral mixed WM/GM lesions; the lesion on the left is chronic inactive and that on he right is acute active. **F** - Active plaque from panel I (box) at medium magnification demonstrating prominent HLA DR-staining in the WM portion of the lesion and at the plaque border, which lies in the GM. **G** - MHC class II-positive cells, with the morphology of macrophages, are distributed throughout the WM portion of the acute active lesion. **H –** the plaque border – in the GM portion of the lesion - contains MHC class II-positive cells with the morphology of activated microglia. **J.** Staining in the core of the GM portion of the lesion is markedly reduced compared to the WM portion (H), but increased compared to the GM in the chronic inactive lesion (**K**) and control GM (C). **L** - WM in the chronic inactive lesion. **M, N** - Two chronic active lesions and a chronic inactive lesion. **O** - The chronic active lesion in the posterior columns from panel N (box) contains numerous perivascular macrophages seen at higher magnification in panel **P**. **Q** (corresponding to E and I) - A proportion of GM plaques show clear evidence of gliosis. **R, S** - In other cases the gliotic reaction in the GM portion of the plaque is much less pronounced. The scale bars in **F** and **O** represent 500µm; in **C, D, G, H, J-L** and **P** they represent 50µm.*

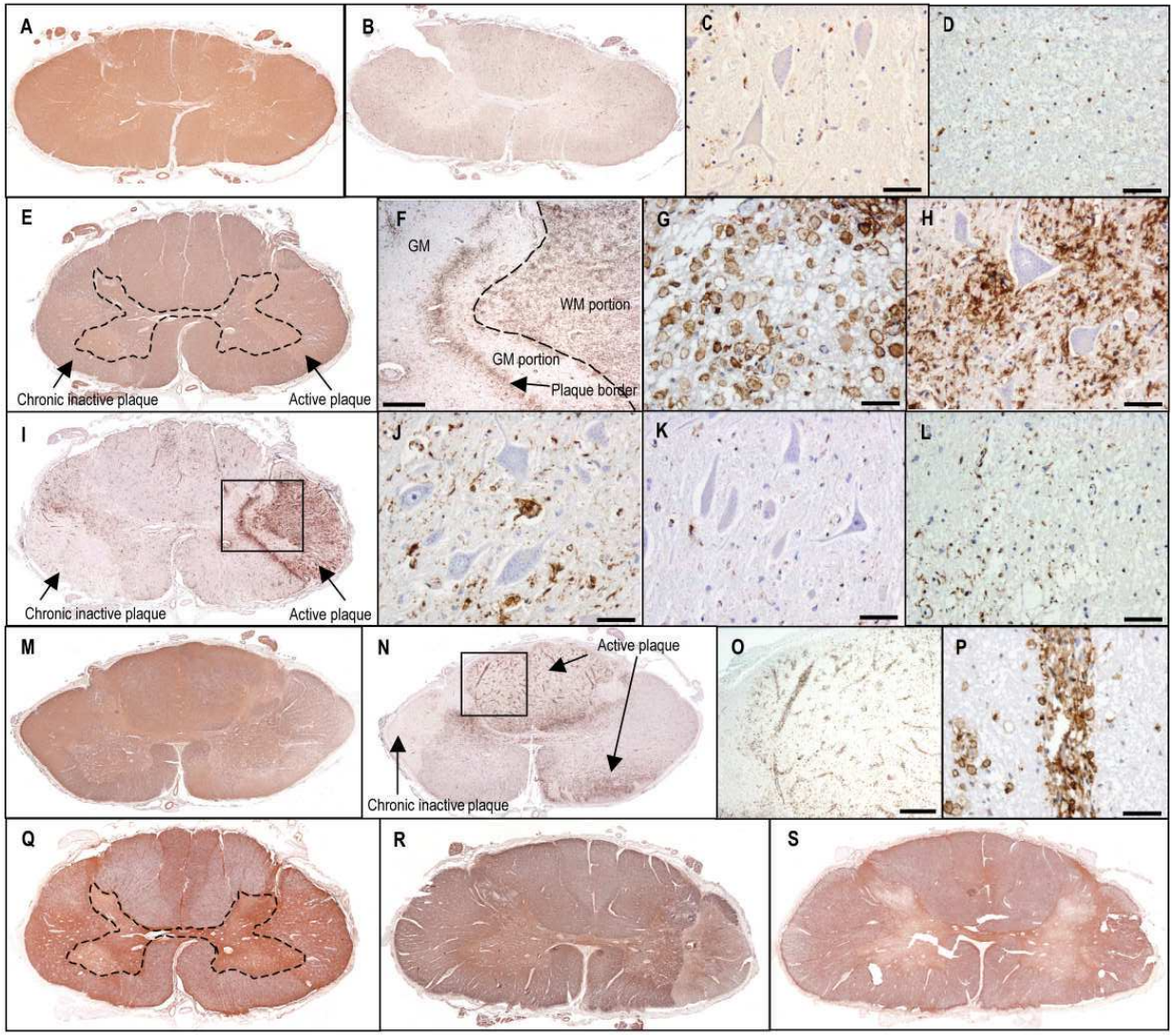
A
B
C
D
E
Chronic inactive plaque
Active plaque
F
GM
WM portion
GM portion
Plaque border
G
H
I
Chronic inactive plaque
Active plaque
J
K
L
M
N
Active plaque
Chronic inactive plaque
O
P
Q
R
S

Figure 6.5

Bar chart illustrating the number of MS plaques detected by histopathological and MRI analysis. "Complete" = completely demyelinated lesions. "Partial" = lesions with markedly reduced myelin density

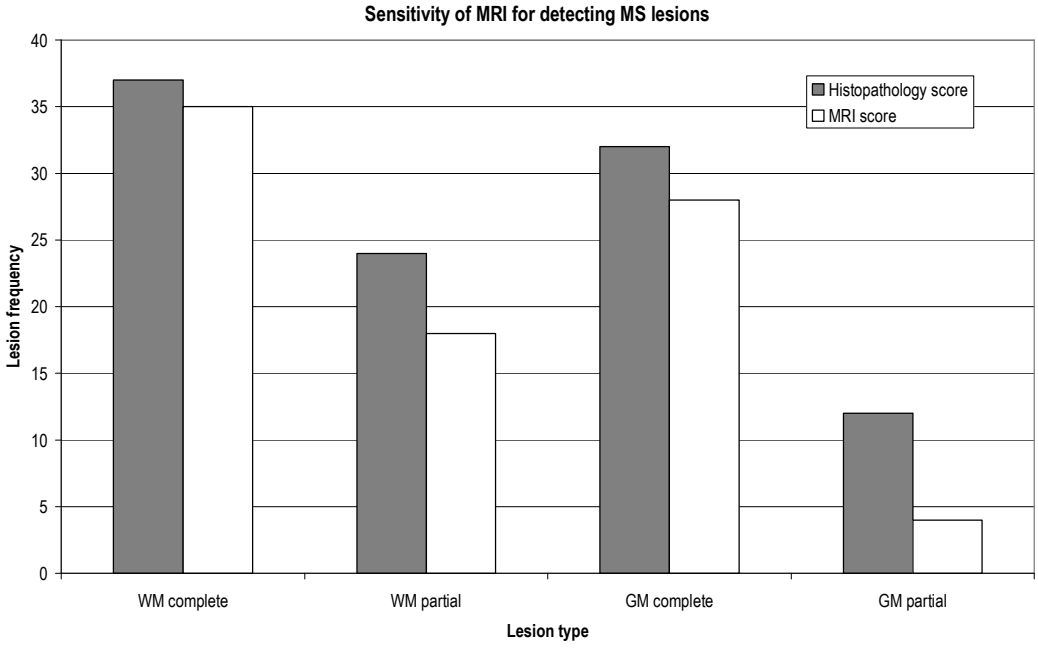

Figure 6.6

*Paraffin sections from an MS spinal cord at the Lumbar level, immunohistochemically stained with anti-Proteolipid Protein (PLP) (**A, B**) and anti-HLA DR antibodies (**C-G**). **A, C** – the mixed grey matter (GM) / white matter (WM) lesion on the left is acute active, and contains numerous PLP-laden macrophages in both the GM (panel **B**, at high magnification, demonstrating macrophage nuclei (horizontal arrow) and intra-cellular PLP (vertical arrow)) and WM portions of the plaque. Large numbers of MHC class II-positive cells, with the morphology of macrophages, are distributed throughout both GM (**D**) and WM (**E**) portions of the acute active lesion. In comparison, much fewer MHC class II-positive cells are observed in the myelinated GM (**F**) and WM (**G**), where they have the morphology of microglia. Scale bars (**B, D-G**) represent 50μm.*

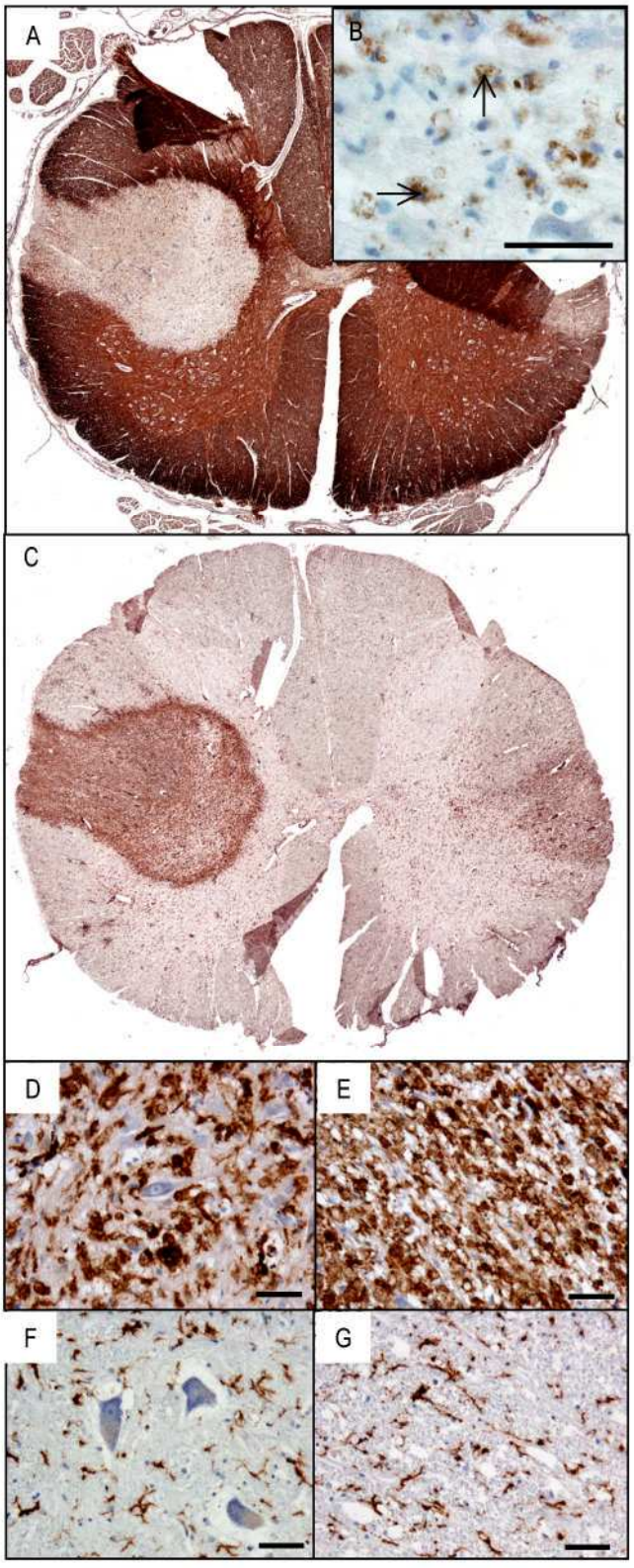
A
B
C
D
E
F
G

NBB number	Age	Sex	Disease course	Disease duration (years)	Cause of death	Post-mortem delay	Scan delay (days)	% Demyelinated Area*	
								WM	GM
98-176	83	M	PP	52	Pneumonia	7 h 5 min	194	28.8	10.8
98-179	60	F	SP	36	Intracerebral haemorrhage	8 h 50 min	214	10.3	36.0
98-185	70	F	PP	19	Pneumonia	8 h 55 min	178	4.7	8.2
99-051	45	F	SP	14	Euthanasia	10 h 55 min	116	44.1	53.0
99-054	58	F	SP	20	Euthanasia	8 h 10 min	224	61.1	21.4
99-062	79	F	PP	44	Cardiac disease	10 h 0 min	107	18.6	7.1
99-066	69	M	SP	46	Ileus	16 h 45 min	66	19.3	4.0
99-073	71	F	ND	23	Pneumonia	8 h 20 min	111	94.1	92.7
99-086	71	F	SP	31	Respiratory failure	10 h 25 min	129	49.7	71.9
99-109	70	M	ND	21	Pneumonia	6 h 25 min	61	11.6	8.9
99-115	57	F	PP	7	Euthanasia	5 h 30 min	66	0	0
00-022	83	F	Control	NA	Myocardial infarct	7 h 45 min	144	NA	NA
00-025	41	F	Control	NA	Bronchial carcinoma	13 h 30 min	144	NA	NA

Table 6.1 *- Clinical characteristics of the autopsy cases and the proportion of GM and WM that was demyelinated. * "% Demyelinated Area" values represent the pooled results from the three spinal cord levels. Abbreviations: NBB (Netherlands Brain Bank), WM (white matter), GM (grey matter), SP (Secondary Progressive), PP (Primary Progressive), ND (not determined), NA (not applicable).*

Chapter 7: Summary of Results

MS is the most common chronic disabling neurological disease affecting young people in the UK. Current therapeutic options offer only modest benefit. A greater understanding of MS pathogenesis and the mechanisms of disability in the disease are required in order to develop novel therapeutic agents. MS has traditionally been considered to be a disease of WM, a view that partly reflects shortcomings in conventional MRI and histological staining techniques - particularly their lack of sensitivity in detecting demyelination in GM structures[127-129]. More recent post-mortem and imaging studies have resulted in an increasing recognition of GM pathology, with there being some evidence that these changes occur in part independently of WM demyelination / inflammation[129, 133, 183, 193, 315]. However this work has focused exclusively on GM structures in the brain.

We believe our series represents the largest post-mortem examination of spinal cord pathology in MS. We have chosen to focus on the cord for several reasons: firstly, in comparison with the cerebral cortex and thalamus, spinal cord GM pathology has received little attention. Secondly the spinal cord is a well-recognised predilection site for demyelination, with lesions in this clinically eloquent area frequently resulting in disabling relapses[205, 206]. Disability in progressive forms of MS is also often attributed to spinal cord pathology. Thirdly, while not easily amenable to study via imaging or tissue biopsy, the simple but well characterised anatomy of the spinal cord lends itself to quantitative neuropathological study using post-mortem material. Finally, in addition to being a predilection site for demyelination, there is marked axonal loss in the spinal cord, making it well suited to examine "neurodegenerative" aspects of MS pathology[76-79, 210].

In this thesis we further our understanding of GM involvement in MS by exploring a variety of aspects of GM pathology in the spinal cord. We have been particularly interested in the factors that govern plaque morphology – both in terms of the topography of individual plaques (including their relationship to blood vessels, the CSF and the GM/WM boundary) and regional differences in the extent of demyelination. Our initial study highlights the extent of demyelination in the spinal cord GM. This study is the first to use myelin protein IHC – the "gold standard" technique for detecting GM demyelination – to compare the extent of both WM and GM demyelination in the spinal cord with that in intracranial structures (namely the cerebral cortex, cerebellum and thalamus). We demonstrate that both GM and WM demyelination is

highest in the spinal cord, although considerable demyelination is also observed in the cerebellar cortex. Previous studies have highlighted an abundance of lesions in subpial structure (both in the cerebral and the cerebellar cortex), suggesting a role for CSF- or meningeal- related factors in mediating this demyelination. It is therefore interesting to note that even greater demyelination occurs in the spinal cord, where the GM is neither bathed in CSF nor intimately related to the meninges. The study also demonstrates that demyelination is more extensive in the GM than in the WM at each of the anatomical sites examined, further challenging the concept that MS is predominantly a disease of WM.

These novel findings prompted us to examine the extent and pattern of GM demyelination in the spinal cord in greater detail. We did this using autopsy material from 37 MS cases, assessing plaque topography at the upper and lower cervical, upper and lower thoracic and lumbar cord levels. We demonstrate that the proportion of GM that is demyelinated is greater than the proportion of WM that is demyelinated at all five levels. While WM demyelination is most prominent at the upper cervical level, there is no significant difference in the extent of GM demyelination between the various cord levels.

We observe striking morphological differences between GM and WM plaques. The factors influencing plaque topography in MS are not fully understood. Previous studies suggest the majority of spinal plaques are perivenular in location, and display a total disregard for anatomical boundaries[21, 24, 204]. However we find that the borders of many spinal cord GM plaques maintain a strict respect for the GM/WM boundary, a pattern of residual plaque morphology that does not appear to occur in a purely “perivenular” distribution. In this respect we have likened these lesions to the type IV lesions of the cerebral cortex and the subpial lesions of the cerebellar cortex, both of which show extensive demyelination within the GM, with sparing of the adjacent WM. We have proposed that these lesions may share a common pathogenic mechanism, possibly reflecting (i) differences in interstitial fluid drainage pathways between GM and WM, (ii) phenotypical differences between GM and WM or (iii) GM/WM differences in the ability to remyelinate.

A number of recent studies highlight the extent of axonal and neuronal pathology in MS, which are likely to represent important substrates for irreversible disability[53]. We demonstrate substantial neuronal loss in the spinal cord in MS, observing reductions in both interneuron and motoneuron numbers. This neuronal loss appears to occur predominantly – if not exclusively -

within GM plaques. We also observe reductions in interneuron size, both within plaques and in the myelinated GM. Despite substantial demyelination in the GM of the spinal cord, and the considerable neuronal loss associated with this demyelination, the spinal cord GM volume does not differ significantly between MS and control cases. Atrophy in MS is loosely considered to be a surrogate marker of tissue loss (that is, axonal loss in the WM and neuronal / axonal loss in the GM) but our studies demonstrate the complex interaction between tissue loss and atrophy. When viewed in the context of previous studies examining neuronal loss and GM atrophy in the brain, this work highlights considerable regional heterogeneity related to (i) the extent of neuronal loss, (ii) the predominant mechanism of neuronal loss, and (iii) the degree of tissue atrophy[131, 157].

Conclusions and further work

A greater understanding of GM pathology may provide important insight into MS pathologenesis and mechanisms of disability in the disease, and identify potential targets for novel therapeutic strategies. We feel that this thesis adds to the current body of literature on GM histopathology in MS, identifying the spinal cord GM as a predilection site for demyelination, and highlighting patterns of plaque morphology that have not been reported previously. In addition, we demonstrate substantial neuronal pathology in the spinal cord. Further work is required to better characterise these processes.

Such extensive demyelination and neuronal pathology is likely to be of clinical importance, both in relapsing and progressive MS, contributing to a number of symptoms including motor, sensory and bladder dysfunction. However, post-mortem studies are unlikely to provide significant insight into the functional consequences of GM pathology. An understanding of the clinical correlate of GM pathology (be it demyelination, neuronal loss or atrophy) will only come with non-invasive *in vivo* techniques. Improved imaging will also provide invaluable information on the early stages of lesion formation and an appreciation of the evolution of pathology. In light of this it is promising that post-mortem MR imaging at 4.7 T is highly sensitive for detecting spinal cord GM demyelination.

References

1. Mumford CJ, Fraser MB, Wood NW, Compston DA. Multiple sclerosis in the Cambridge health district of east Anglia. J Neurol Neurosurg Psychiatry. 1992;55:877-882
2. Compston A. Distribution of multiple sclerosis. In: Compston A, Ebers G, McDonald I et al., eds. McAlpines Multiple Sclerosis. London: Churchill Livingstone, 1998:63-100
3. Alter M, Leibowitz U, Speer J. Risk of multiple sclerosis related to age at immigration to Israel. Arch Neurol. 1966;15:234-237
4. Compston A, Coles A. Multiple sclerosis. Lancet. 2002;359:1221-1231
5. Sadovnick AD, Armstrong H, Rice GP et al. A population-based study of multiple sclerosis in twins: update. Ann Neurol. 1993;33:281-285
6. Dyment DA, Ebers GC, Sadovnick AD. Genetics of multiple sclerosis. Lancet neurology. 2004;3:104-110
7. Lassmann H, Ransohoff RM. The CD4-Th1 model for multiple sclerosis: a critical re-appraisal. Trends Immunol. 2004;25:132-137
8. Benjamins JA. Molecular Structure of the Myelin Membrane. In: Herndon RM, ed. Multiple Sclerosis: Immunology, Pathology, and Pathophysiology. New York: Demos, 2003
9. Cook SD. Evidence for a viral etiology of multiple sclerosis. In: Cook SD, ed. Handbook of multiple sclerosis. New York: Marcel Dekker, 2001:115-138
10. Barnett MH, Prineas JW. Relapsing and remitting multiple sclerosis: pathology of the newly forming lesion. Ann Neurol. 2004;55:458-468
11. Gay FW. Early cellular events in multiple sclerosis. Intimations of an extrinsic myelinolytic antigen. Clin Neurol Neurosurg. 2006;108:234-240
12. Confavreux C, Aimard G, Devic M. Course and prognosis of multiple sclerosis assessed by the computerized data processing of 349 patients. Brain. 1980;103:281-300
13. Weinshenker BG, Bass B, Rice GP et al. The natural history of multiple sclerosis: a geographically based study. I. Clinical course and disability. Brain. 1989;112 (Pt 1):133-146
14. Hawkins SA, McDonnell GV. Benign multiple sclerosis? Clinical course, long term follow up, and assessment of prognostic factors. J Neurol Neurosurg Psychiatry. 1999;67:148-152

15. McDonald WI, Compston A, Edan G et al. Recommended diagnostic criteria for multiple sclerosis: guidelines from the International Panel on the diagnosis of multiple sclerosis. Ann Neurol. 2001;50:121-127
16. Compston A. Treatment and management of multiple sclerosis. In: Compston A, Ebers G, McDonald I et al., eds. McAlpines Multiple Sclerosis. London: Churchill Livingstone, 1998:437-498
17. Samkoff LM, Goodman AD. Disease-modifying therapy for multiple sclerosis in clinical practice. In: Cohen JA, Rudick RA, eds. Multiple Sclerosis Therapeutics. 2 ed. London: Martin Dunitz, 2003:567-588
18. Hartung HP, Gonsette R, Konig N et al. Mitoxantrone in progressive multiple sclerosis: a placebo-controlled, double-blind, randomised, multicentre trial. Lancet. 2002;360:2018-2025
19. Coles AJ, Cox A, Le Page E et al. The window of therapeutic opportunity in multiple sclerosis: evidence from monoclonal antibody therapy. J Neurol. 2006;253:98-108
20. Polman CH, O'Connor PW, Havrdova E et al. A randomized, placebo-controlled trial of natalizumab for relapsing multiple sclerosis. N Engl J Med. 2006;354:899-910
21. Fog T. Topographic distribution of plaques in the spinal cord in multiple sclerosis. Arch Neurol Psychiat. 1950;63:382-414
22. Brownell B, Hughes JT. The distribution of plaques in the cerebrum in multiple sclerosis. J Neurol Neurosurg Psychiatry. 1962;25
23. Lumsden C. The neuropathology of multiple sclerosis. In: Vinken PJ BG, ed. Handbook off clinical neurology. Vol. 9. Amsterdam, 1970:217-309
24. Oppenheimer DR. The cervical cord in multiple sclerosis. Neuropathol Appl Neurobiol. 1978;4:151-162
25. Lassmann H. Pathology of multiple sclerosis. In: Compston A, Ebers G, McDonald I et al., eds. McAlpines Multiple Sclerosis. 3rd ed. London: Churchill Livingstone, 1998:323-358
26. Gay D, Esiri M. Blood-brain barrier damage in acute multiple sclerosis plaques. An immunocytological study. Brain. 1991;114 (Pt 1B):557-572
27. Kwon EE, Prineas JW. Blood-brain barrier abnormalities in longstanding multiple sclerosis lesions. An immunohistochemical study. J Neuropathol Exp Neurol. 1994;53:625-636
28. Cannella B, Raine CS. The adhesion molecule and cytokine profile of multiple sclerosis lesions. Ann Neurol. 1995;37:424-435

29. Schluesener HJ, Meyermann R. Intercrines in brain pathology. Expression of intercrines in a multiple sclerosis and Morbus Creutzfeldt-Jakob lesion. Acta Neuropathol (Berl). 1993;86:393-396
30. Lindberg RL, De Groot CJ, Montagne L et al. The expression profile of matrix metalloproteinases (MMPs) and their inhibitors (TIMPs) in lesions and normal appearing white matter of multiple sclerosis. Brain. 2001;124:1743-1753
31. Bo L, Mork S, Kong PA et al. Detection of MHC class II-antigens on macrophages and microglia, but not on astrocytes and endothelia in active multiple sclerosis lesions. J Neuroimmunol. 1994;51:135-146
32. Bruck W, Schmied M, Suchanek G et al. Oligodendrocytes in the early course of multiple sclerosis. Ann Neurol. 1994;35:65-73
33. Bruck W, Stadelmann C. Pathology of the Normal-Appearing White Matter in Multiple Sclerosis. In: Filippi M, Comi G, Rovaris M, eds. Normal-appearing White and Grey Matter Damage in Multiple Sclerosis. Milan: Springer-Verlag, 2004
34. Allen IV, McKeown SR. A histological, histochemical and biochemical study of the macroscopically normal white matter in multiple sclerosis. J Neurol Sci. 1979;41:81-91
35. Allen IV, Glover G, Anderson R. Abnormalities in the macroscopically normal white matter in cases of mild or spinal multiple sclerosis (MS). Acta Neuropathol Suppl (Berl). 1981;7:176-178
36. van der Valk P, De Groot CJ. Staging of multiple sclerosis (MS) lesions: pathology of the time frame of MS. Neuropathol Appl Neurobiol. 2000;26:2-10
37. Allen IV, McQuaid S, Mirakhur M, Nevin G. Pathological abnormalities in the normal-appearing white matter in multiple sclerosis. Neurol Sci. 2001;22:141-144
38. Plumb J, McQuaid S, Mirakhur M, Kirk J. Abnormal endothelial tight junctions in active lesions and normal-appearing white matter in multiple sclerosis. Brain Pathol. 2002;12:154-169
39. Kirk J, Plumb J, Mirakhur M, McQuaid S. Tight junctional abnormality in multiple sclerosis white matter affects all calibres of vessel and is associated with blood-brain barrier leakage and active demyelination. J Pathol. 2003;201:319-327
40. Guseo A, Jellinger K. The significance of perivascular infiltrations in multiple sclerosis. J Neurol. 1975;211:51-60
41. Serafini B, Rosicarelli B, Magliozzi R et al. Detection of ectopic B-cell follicles with germinal centers in the meninges of patients with secondary progressive multiple sclerosis. Brain Pathol. 2004;14:164-174

42. Scolding NJ, Jones J, Compston DA, Morgan BP. Oligodendrocyte susceptibility to injury by T-cell perforin. Immunology. 1990;70:6-10
43. Selmaj K, Raine CS, Farooq M et al. Cytokine cytotoxicity against oligodendrocytes. Apoptosis induced by lymphotoxin. J Immunol. 1991;147:1522-1529
44. Selmaj K, Raine CS, Cannella B, Brosnan CF. Identification of lymphotoxin and tumor necrosis factor in multiple sclerosis lesions. J Clin Invest. 1991;87:949-954
45. Griot C, Vandevelde M, Richard A et al. Selective degeneration of oligodendrocytes mediated by reactive oxygen species. Free Radic Res Commun. 1990;11:181-193
46. Merrill JE, Ignarro LJ, Sherman MP et al. Microglial cell cytotoxicity of oligodendrocytes is mediated through nitric oxide. J Immunol. 1993;151:2132-2141
47. Mitrovic B, Ignarro LJ, Montestruque S et al. Nitric oxide as a potential pathological mechanism in demyelination: its differential effects on primary glial cells in vitro. Neuroscience. 1994;61:575-585
48. McDonald JW, Althomsons SP, Hyrc KL et al. Oligodendrocytes from forebrain are highly vulnerable to AMPA/kainate receptor-mediated excitotoxicity. Nat Med. 1998;4:291-297
49. Selmaj KW, Raine CS. Tumor necrosis factor mediates myelin and oligodendrocyte damage in vitro. Ann Neurol. 1988;23:339-346
50. Andrews T, Zhang P, Bhat NR. TNFalpha potentiates IFNgamma-induced cell death in oligodendrocyte progenitors. J Neurosci Res. 1998;54:574-583
51. D'Souza SD, Bonetti B, Balasingam V et al. Multiple sclerosis: Fas signaling in oligodendrocyte cell death. J Exp Med. 1996;184:2361-2370
52. Dowling P, Shang G, Raval S et al. Involvement of the CD95 (APO-1/Fas) receptor/ligand system in multiple sclerosis brain. J Exp Med. 1996;184:1513-1518
53. Trapp BD, Bo L, Mork S, Chang A. Pathogenesis of tissue injury in MS lesions. J Neuroimmunol. 1999;98:49-56
54. Archelos JJ, Storch MK, Hartung HP. The role of B cells and autoantibodies in multiple sclerosis. Ann Neurol. 2000;47:694-706
55. Genain CP, Nguyen MH, Letvin NL et al. Antibody facilitation of multiple sclerosis-like lesions in a nonhuman primate. J Clin Invest. 1995;96:2966-2974
56. Lucchinetti CF, Bruck W, Rodriguez M, Lassmann H. Distinct patterns of multiple sclerosis pathology indicates heterogeneity on pathogenesis. Brain Pathol. 1996;6:259-274

57. Lucchinetti C, Bruck W, Parisi J et al. Heterogeneity of multiple sclerosis lesions: implications for the pathogenesis of demyelination. Ann Neurol. 2000;47:707-717
58. Barnes D, Munro PM, Youl BD et al. The longstanding MS lesion. A quantitative MRI and electron microscopic study. Brain. 1991;114 (Pt 3):1271-1280
59. Ridet JL, Malhotra SK, Privat A, Gage FH. Reactive astrocytes: cellular and molecular cues to biological function. Trends Neurosci. 1997;20:570-577
60. Silver J, Miller JH. Regeneration beyond the glial scar. Nature reviews Neurosci. 2004;5:146-156
61. Fontana A, Fierz W, Wekerle H. Astrocytes present myelin basic protein to encephalitogenic T-cell lines. Nature. 1984;307:273-276
62. Minagar A, Shapshak P, Fujimura R et al. The role of macrophage/microglia and astrocytes in the pathogenesis of three neurologic disorders: HIV-associated dementia, Alzheimer disease, and multiple sclerosis. J Neurol Sci. 2002;202:13-23
63. Ozawa K, Suchanek G, Breitschopf H et al. Patterns of oligodendroglia pathology in multiple sclerosis. Brain. 1994;117 (Pt 6):1311-1322
64. Patrikios P, Stadelmann C, Kutzelnigg A et al. Remyelination is extensive in a subset of multiple sclerosis patients. Brain. 2006;129:3165-3172
65. Wolswijk G. Chronic stage multiple sclerosis lesions contain a relatively quiescent population of oligodendrocyte precursor cells. J Neurosci. 1998;18:601-609
66. Lucchinetti C, Bruck W, Parisi J et al. A quantitative analysis of oligodendrocytes in multiple sclerosis lesions. A study of 113 cases. Brain. 1999;122 (Pt 12):2279-2295
67. Targett MP, Sussman J, Scolding N et al. Failure to achieve remyelination of demyelinated rat axons following transplantation of glial cells obtained from the adult human brain. Neuropathol Appl Neurobiol. 1996;22:199-206
68. Gensert JM, Goldman JE. Endogenous progenitors remyelinate demyelinated axons in the adult CNS. Neuron. 1997;19:197-203
69. Chang A, Nishiyama A, Peterson J et al. NG2-positive oligodendrocyte progenitor cells in adult human brain and multiple sclerosis lesions. J Neurosci. 2000;20:6404-6412
70. Prineas JW, Connell F. Remyelination in multiple sclerosis. Ann Neurol. 1979;5:22-31
71. Kornek B, Storch MK, Weissert R et al. Multiple sclerosis and chronic autoimmune encephalomyelitis: a comparative quantitative study of axonal injury in active, inactive, and remyelinated lesions. Am J Pathol. 2000;157:267-276

72. Evangelou N, Konz D, Esiri MM et al. Regional axonal loss in the corpus callosum correlates with cerebral white matter lesion volume and distribution in multiple sclerosis. Brain. 2000;123 (Pt 9):1845-1849
73. Kuhlmann T, Lingfeld G, Bitsch A et al. Acute axonal damage in multiple sclerosis is most extensive in early disease stages and decreases over time. Brain. 2002;125:2202-2212
74. Davie CA, Hawkins CP, Barker GJ et al. Serial proton magnetic resonance spectroscopy in acute multiple sclerosis lesions. Brain. 1994;117 (Pt 1):49-58
75. Fu L, Matthews PM, De Stefano N et al. Imaging axonal damage of normal-appearing white matter in multiple sclerosis. Brain. 1998;121 (Pt 1):103-113
76. Bjartmar C, Kinkel RP, Kidd G et al. Axonal loss in normal-appearing white matter in a patient with acute MS. Neurology. 2001;57:1248-1252
77. Ganter P, Prince C, Esiri MM. Spinal cord axonal loss in multiple sclerosis: a post-mortem study. Neuropathol Appl Neurobiol. 1999;25:459-467
78. Lovas G, Szilagyi N, Majtenyi K et al. Axonal changes in chronic demyelinated cervical spinal cord plaques. Brain. 2000;123 (Pt 2):308-317
79. DeLuca GC, Ebers GC, Esiri MM. Axonal loss in multiple sclerosis: a pathological survey of the corticospinal and sensory tracts. Brain. 2004;127:1009-1018
80. Lassmann H. Axonal injury in multiple sclerosis. J Neurol Neurosurg Psychiatry. 2003;74:695-697
81. Ferguson B, Matyszak MK, Esiri MM, Perry VH. Axonal damage in acute multiple sclerosis lesions. Brain. 1997;120 (Pt 3):393-399
82. Trapp BD, Peterson J, Ransohoff RM et al. Axonal transection in the lesions of multiple sclerosis. N Engl J Med. 1998;338:278-285
83. Bitsch A, Schuchardt J, Bunkowski S et al. Acute axonal injury in multiple sclerosis. Correlation with demyelination and inflammation. Brain. 2000;123 (Pt 6):1174-1183
84. Gimsa U, Peter SV, Lehmann K et al. Axonal damage induced by invading T cells in organotypic central nervous system tissue in vitro: involvement of microglial cells. Brain Pathol. 2000;10:365-377
85. Medana I, Martinic MA, Wekerle H, Neumann H. Transection of major histocompatibility complex class I-induced neurites by cytotoxic T lymphocytes. Am J Pathol. 2001;159:809-815
86. Medana IM, Esiri MM. Axonal damage: a key predictor of outcome in human CNS diseases. Brain. 2003;126:515-530

87. Smith KJ, Lassmann H. The role of nitric oxide in multiple sclerosis. Lancet neurology. 2002;1:232-241
88. Madigan MC, Sadun AA, Rao NS et al. Tumor necrosis factor-alpha (TNF-alpha)-induced optic neuropathy in rabbits. Neurological research. 1996;18:176-184
89. Madigan MC, Rao NS, Tenhula WN, Sadun AA. Preliminary morphometric study of tumor necrosis factor-alpha (TNF alpha)-induced rabbit optic neuropathy. Neurological research. 1996;18:233-236
90. Newman TA, Woolley ST, Hughes PM et al. T-cell- and macrophage-mediated axon damage in the absence of a CNS-specific immune response: involvement of metalloproteinases. Brain. 2001;124:2203-2214
91. Rawes JA, Calabrese VP, Khan OA, DeVries GH. Antibodies to the axolemma-enriched fraction in the cerebrospinal fluid and serum of patients with multiple sclerosis and other neurological diseases. Multiple sclerosis. 1997;3:363-369
92. Sadatipour BT, Greer JM, Pender MP. Increased circulating antiganglioside antibodies in primary and secondary progressive multiple sclerosis. Ann Neurol. 1998;44:980-983
93. Silber E, Semra YK, Gregson NA, Sharief MK. Patients with progressive multiple sclerosis have elevated antibodies to neurofilament subunit. Neurology. 2002;58:1372-1381
94. Lily O, Palace J, Vincent A. Serum autoantibodies to cell surface determinants in multiple sclerosis: a flow cytometric study. Brain. 2004;127:269-279
95. Lassmann H, Bruck W, Lucchinetti C. Heterogeneity of multiple sclerosis pathogenesis: implications for diagnosis and therapy. Trends Mol Med. 2001;7:115-121
96. Bolanos JP, Almeida A, Stewart V et al. Nitric oxide-mediated mitochondrial damage in the brain: mechanisms and implications for neurodegenerative diseases. J Neurochem. 1997;68:2227-2240
97. Dutta R, McDonough J, Yin X et al. Mitochondrial dysfunction as a cause of axonal degeneration in multiple sclerosis patients. Ann Neurol. 2006;59:478-489
98. Griffiths I, Klugmann M, Anderson T et al. Axonal swellings and degeneration in mice lacking the major proteolipid of myelin. Science. 1998;280:1610-1613
99. Yin X, Crawford TO, Griffin JW et al. Myelin-associated glycoprotein is a myelin signal that modulates the caliber of myelinated axons. J Neurosci. 1998;18:1953-1962
100. Bruck W. The role of macrophages in Wallerian degeneration. Brain Pathol. 1997;7:741-752

101. DeLuca GC, Williams K, Evangelou N et al. The contribution of demyelination to axonal loss in multiple sclerosis. Brain. 2006;129:1507-1516
102. McDonald WI, Sears TA. Effect of demyelination on conduction in the central nervous system. Nature. 1969;221:182-183
103. Redford EJ, Kapoor R, Smith KJ. Nitric oxide donors reversibly block axonal conduction: demyelinated axons are especially susceptible. Brain. 1997;120 (Pt 12):2149-2157
104. Rovaris M, Gambini A, Gallo A et al. Axonal injury in early multiple sclerosis is irreversible and independent of the short-term disease evolution. Neurology 2005;65:1626-1630
105. De Stefano N, Matthews PM, Fu L et al. Axonal damage correlates with disability in patients with relapsing-remitting multiple sclerosis. Results of a longitudinal magnetic resonance spectroscopy study. Brain. 1998;121 (Pt 8):1469-1477
106. Lee MA, Blamire AM, Pendlebury S et al. Axonal injury or loss in the internal capsule and motor impairment in multiple sclerosis. Arch Neurol. 2000;57:65-70
107. Losseff NA, Wang L, Lai HM et al. Progressive cerebral atrophy in multiple sclerosis. A serial MRI study. Brain. 1996;119 (Pt 6):2009-2019
108. Edwards SG, Gong QY, Liu C et al. Infratentorial atrophy on magnetic resonance imaging and disability in multiple sclerosis. Brain. 1999;122 (Pt 2):291-301
109. Liu C, Edwards S, Gong Q et al. Three dimensional MRI estimates of brain and spinal cord atrophy in multiple sclerosis. J Neurol Neurosurg Psychiatry. 1999;66:323-330
110. Lin X, Tench CR, Turner B et al. Spinal cord atrophy and disability in multiple sclerosis over four years: application of a reproducible automated technique in monitoring disease progression in a cohort of the interferon beta-1a (Rebif) treatment trial. J Neurol Neurosurg Psychiatry. 2003;74:1090-1094
111. Brex PA, Jenkins R, Fox NC et al. Detection of ventricular enlargement in patients at the earliest clinical stage of MS. Neurology. 2000;54:1689-1691
112. Luks TL, Goodkin DE, Nelson SJ et al. A longitudinal study of ventricular volume in early relapsing-remitting multiple sclerosis. Multiple sclerosis. 2000;6:332-337
113. Dalton CM, Brex PA, Jenkins R et al. Progressive ventricular enlargement in patients with clinically isolated syndromes is associated with the early development of multiple sclerosis. J Neurol Neurosurg Psychiatry. 2002;73:141-147
114. Filippi M, Colombo B, Rovaris M et al. A longitudinal magnetic resonance imaging study of the cervical cord in multiple sclerosis. J Neuroimaging. 1997;7:78-80

115. Paolillo A, Coles AJ, Molyneux PD et al. Quantitative MRI in patients with secondary progressive MS treated with monoclonal antibody Campath 1H. Neurology. 1999;53:751-757
116. Simon JH, Jacobs LD, Campion MK et al. A longitudinal study of brain atrophy in relapsing multiple sclerosis. The Multiple Sclerosis Collaborative Research Group (MSCRG). Neurology. 1999;53:139-148
117. Fisher E, Rudick RA, Cutter G et al. Relationship between brain atrophy and disability: an 8-year follow-up study of multiple sclerosis patients. Multiple sclerosis. 2000;6:373-377
118. Ge Y, Grossman RI, Udupa JK et al. Brain atrophy in relapsing-remitting multiple sclerosis: fractional volumetric analysis of gray matter and white matter. Radiology. 2001;220:606-610
119. Zivadinov R, Rudick RA, De Masi R et al. Effects of IV methylprednisolone on brain atrophy in relapsing-remitting MS. Neurology. 2001;57:1239-1247
120. Zivadinov R, Sepcic J, Nasuelli D et al. A longitudinal study of brain atrophy and cognitive disturbances in the early phase of relapsing-remitting multiple sclerosis. J Neurol Neurosurg Psychiatry. 2001;70:773-780
121. Moll C, Mourre C, Lazdunski M, Ulrich J. Increase of sodium channels in demyelinated lesions of multiple sclerosis. Brain research. 1991;556:311-316
122. Waxman SG, Ritchie JM. Molecular dissection of the myelinated axon. Ann Neurol. 1993;33:121-136
123. Reddy H, Narayanan S, Arnoutelis R et al. Evidence for adaptive functional changes in the cerebral cortex with axonal injury from multiple sclerosis. Brain. 2000;123 (Pt 11):2314-2320
124. Kerns JM, Frank MJ. Non-neuronal cells in the spinal cord of nude and heterozygous mice. I. Ventral horn neuroglia. Journal of neurocytology. 1981;10:805-818
125. Skoff R. In: Herndon RM, ed. Multiple Sclerosis: Immunology, Pathology, and Pathophysiology. New York: Demos, 2003:7-24
126. Ludwin SK. The function of perineuronal satellite oligodendrocytes: an immunohistochemical study. Neuropathol Appl Neurobiol. 1984;10:143-149
127. Bo L, Vedeler CA, Nyland HI et al. Subpial demyelination in the cerebral cortex of multiple sclerosis patients. J Neuropathol Exp Neurol. 2003;62:723-732

128. Geurts JJ, Bo L, Pouwels PJ et al. Cortical lesions in multiple sclerosis: combined postmortem MR imaging and histopathology. AJNR Am J Neuroradiol. 2005;26:572-577
129. Bo L, Geurts JJ, van der Valk P et al. Lack of correlation between cortical demyelination and white matter pathologic changes in multiple sclerosis. Arch Neurol. 2007;64:76-80
130. Peterson JW, Bo L, Mork S et al. Transected neurites, apoptotic neurons, and reduced inflammation in cortical multiple sclerosis lesions. Ann Neurol. 2001;50:389-400
131. Wegner C, Esiri MM, Chance SA et al. Neocortical neuronal, synaptic, and glial loss in multiple sclerosis. Neurology. 2006;67:960-967
132. Vercellino M, Plano F, Votta B et al. Grey matter pathology in multiple sclerosis. J Neuropathol Exp Neurol. 2005;64:1101-1107
133. Kutzelnigg A, Lucchinetti CF, Stadelmann C et al. Cortical demyelination and diffuse white matter injury in multiple sclerosis. Brain. 2005;128:2705-2712
134. Kutzelnigg A, Lassmann H. Cortical demyelination in multiple sclerosis: A substrate for cognitive deficits? J Neurol Sci. 2006;245:123-126
135. Bo L, Vedeler CA, Nyland H et al. Intracortical multiple sclerosis lesions are not associated with increased lymphocyte infiltration. Multiple sclerosis. 2003;9:323-331
136. Brink BP, van Horssen J, de Vries HE et al. Absence of fibrinogen and IgG leakage in cortical MS lesions. Multiple Sclerosis. 2004;10:S154
137. Brink BP, Veerhuis R, Breij EC et al. The pathology of multiple sclerosis is location-dependent: no significant complement activation is detected in purely cortical lesions. J Neuropathol Exp Neurol. 2005;64:147-155
138. Dalton CM, Chard DT, Davies GR et al. Early development of multiple sclerosis is associated with progressive grey matter atrophy in patients presenting with clinically isolated syndromes. Brain. 2004
139. Tiberio M, Chard DT, Altmann DR et al. Gray and white matter volume changes in early RRMS: a 2-year longitudinal study. Neurology. 2005;64:1001-1007
140. Valsasina P, Benedetti B, Rovaris M et al. Evidence for progressive gray matter loss in patients with relapsing-remitting MS. Neurology. 2005;65:1126-1128
141. Ge Y, Grossman RI, Udupa JK et al. Magnetization transfer ratio histogram analysis of gray matter in relapsing-remitting multiple sclerosis. AJNR Am J Neuroradiol. 2001;22:470-475

142. Codella M, Rocca MA, Colombo B et al. Cerebral grey matter pathology and fatigue in patients with multiple sclerosis: a preliminary study. J Neurol Sci. 2002;194:71-74
143. Davies GR, Ramio-Torrenta L, Hadjiprocopis A et al. Evidence for grey matter MTR abnormality in minimally disabled patients with early relapsing-remitting multiple sclerosis. J Neurol Neurosurg Psychiatry. 2004;75:998-1002
144. Cercignani M, Bozzali M, Iannucci G et al. Magnetisation transfer ratio and mean diffusivity of normal appearing white and grey matter from patients with multiple sclerosis. J Neurol Neurosurg Psychiatry. 2001;70:311-317
145. Bozzali M, Cercignani M, Sormani MP et al. Quantification of brain gray matter damage in different MS phenotypes by use of diffusion tensor MR imaging. AJNR Am J Neuroradiol. 2002;23:985-988
146. Rovaris M, Bozzali M, Iannucci G et al. Assessment of normal-appearing white and gray matter in patients with primary progressive multiple sclerosis: a diffusion-tensor magnetic resonance imaging study. Arch Neurol. 2002;59:1406-1412
147. Fabiano AJ, Sharma J, Weinstock-Guttman B et al. Thalamic involvement in multiple sclerosis: a diffusion-weighted magnetic resonance imaging study. J Neuroimaging. 2003;13:307-314
148. Ciccarelli O, Werring DJ, Wheeler-Kingshott CA et al. Investigation of MS normal-appearing brain using diffusion tensor MRI with clinical correlations. Neurology. 2001;56:926-933
149. Oreja-Guevara C, Rovaris M, Iannucci G et al. Progressive gray matter damage in patients with relapsing-remitting multiple sclerosis: a longitudinal diffusion tensor magnetic resonance imaging study. Arch Neurol. 2005;62:578-584
150. Griffin CM, Chard DT, Parker GJ et al. The relationship between lesion and normal appearing brain tissue abnormalities in early relapsing remitting multiple sclerosis. J Neurol. 2002;249:193-199
151. Parry A, Clare S, Jenkinson M et al. MRI brain T1 relaxation time changes in MS patients increase over time in both the white matter and the cortex. J Neuroimaging. 2003;13:234-239
152. Niepel G, Tench CR, Morgan PS et al. Deep gray matter and fatigue in MS : A T1 relaxation time study. J Neurol. 2006;253:896-902
153. Kapeller P, McLean MA, Griffin CM et al. Preliminary evidence for neuronal damage in cortical grey matter and normal appearing white matter in short duration relapsing-

remitting multiple sclerosis: a quantitative MR spectroscopic imaging study. J Neurol. 2001;248:131-138

154. Chard DT, Griffin CM, McLean MA et al. Brain metabolite changes in cortical grey and normal-appearing white matter in clinically early relapsing-remitting multiple sclerosis. Brain. 2002;125:2342-2352
155. Sarchielli P, Presciutti O, Tarducci R et al. Localized (1)H magnetic resonance spectroscopy in mainly cortical gray matter of patients with multiple sclerosis. J Neurol. 2002;249:902-910
156. Sastre-Garriga J, Ingle GT, Chard DT et al. Metabolite changes in normal-appearing gray and white matter are linked with disability in early primary progressive multiple sclerosis. Arch Neurol. 2005;62:569-573
157. Cifelli A, Arridge M, Jezzard P et al. Thalamic neurodegeneration in multiple sclerosis. Ann Neurol. 2002;52:650-653
158. Wylezinska M, Cifelli A, Jezzard P et al. Thalamic neurodegeneration in relapsing-remitting multiple sclerosis. Neurology. 2003;60:1949-1954
159. Geurts JJ, Reuling IE, Vrenken H et al. MR spectroscopic evidence for thalamic and hippocampal, but not cortical, damage in multiple sclerosis. Magn Reson Med. 2006;55:478-483
160. Pirko I, Lucchinetti CF, Sriram S, Bakshi R. Gray matter involvement in multiple sclerosis. Neurology. 2007;68:634-642
161. Matthews B. Symptoms and signs of Multiple Sclerosis. In: Compston A, Ebers G, McDonald I et al., eds. McAlpines Multiple Sclerosis. 3rd ed. London: Churchill Livingstone, 1998:145-190
162. Freal JE, Kraft GH, Coryell JK. Symptomatic fatigue in multiple sclerosis. Archives of physical medicine and rehabilitation. 1984;65:135-138
163. Krupp LB, Alvarez LA, LaRocca NG, Scheinberg LC. Fatigue in multiple sclerosis. Arch Neurol. 1988;45:435-437
164. Minden SL, Schiffer RB. Affective disorders in multiple sclerosis. Review and recommendations for clinical research. Arch Neurol. 1990;47:98-104
165. Patten SB, Beck CA, Williams JV et al. Major depression in multiple sclerosis: a population-based perspective. Neurology. 2003;61:1524-1527
166. Fisk JD, Pontefract A, Ritvo PG et al. The impact of fatigue on patients with multiple sclerosis. The Canadian journal of neurological sciences. 1994;21:9-14

167. Janardhan V, Bakshi R. Quality of life in patients with multiple sclerosis: the impact of fatigue and depression. J Neurol Sci. 2002;205:51-58
168. Feinstein A. Mood disorders in multiple sclerosis and the effects on cognition. J Neurol Sci. 2006;245:63-66
169. Jongen PJ. Psychiatric onset of multiple sclerosis. J Neurol Sci. 2006;245:59-62
170. Rao SM, Leo GJ, Bernardin L, Unverzagt F. Cognitive dysfunction in multiple sclerosis. I. Frequency, patterns, and prediction. Neurology. 1991;41:685-691
171. Zarei M, Chandran S, Compston A, Hodges J. Cognitive presentation of multiple sclerosis: evidence for a cortical variant. J Neurol Neurosurg Psychiatry. 2003;74:872-877
172. Zarei M. Clinical characteristics of cortical multiple sclerosis. J Neurol Sci. 2006;245:53-58
173. Poser CM, Brinar VV. Epilepsy and multiple sclerosis. Epilepsy Behav. 2003;4:6-12
174. Moreau T, Sochurkova D, Lemesle M et al. Epilepsy in patients with multiple sclerosis: radiological-clinical correlations. Epilepsia. 1998;39:893-896
175. Miki Y, Grossman RI, Udupa JK et al. Isolated U-fiber involvement in MS: preliminary observations. Neurology. 1998;50:1301-1306
176. Moriarty DM, Blackshaw AJ, Talbot PR et al. Memory dysfunction in multiple sclerosis corresponds to juxtacortical lesion load on fast fluid-attenuated inversion-recovery MR images. AJNR Am J Neuroradiol. 1999;20:1956-1962
177. Rovaris M, Filippi M, Minicucci L et al. Cortical/subcortical disease burden and cognitive impairment in patients with multiple sclerosis. AJNR Am J Neuroradiol. 2000;21:402-408
178. Lazeron RH, Langdon DW, Filippi M et al. Neuropsychological impairment in multiple sclerosis patients: the role of (juxta)cortical lesion on FLAIR. Multiple sclerosis. 2000;6:280-285
179. Sokic DV, Stojsavljevic N, Drulovic J et al. Seizures in multiple sclerosis. Epilepsia. 2001;42:72-79
180. Feinstein A, Roy P, Lobaugh N et al. Structural brain abnormalities in multiple sclerosis patients with major depression. Neurology. 2004;62:586-590
181. Amato MP, Bartolozzi ML, Zipoli V et al. Neocortical volume decrease in relapsing-remitting MS patients with mild cognitive impairment. Neurology. 2004;63:89-93

182. Benedict RH, Weinstock-Guttman B, Fishman I et al. Prediction of neuropsychological impairment in multiple sclerosis: comparison of conventional magnetic resonance imaging measures of atrophy and lesion burden. Arch Neurol. 2004;61:226-230
183. Morgen K, Sammer G, Courtney SM et al. Evidence for a direct association between cortical atrophy and cognitive impairment in relapsing-remitting MS. NeuroImage. 2006;30:891-898
184. Sanfilipo MP, Benedict RH, Weinstock-Guttman B, Bakshi R. Gray and white matter brain atrophy and neuropsychological impairment in multiple sclerosis. Neurology. 2006;66:685-692
185. Portaccio E, Amato MP, Bartolozzi ML et al. Neocortical volume decrease in relapsing-remitting multiple sclerosis with mild cognitive impairment. J Neurol Sci. 2006;245:195-199
186. Roelcke U, Kappos L, Lechner-Scott J et al. Reduced glucose metabolism in the frontal cortex and basal ganglia of multiple sclerosis patients with fatigue: a 18F-fluorodeoxyglucose positron emission tomography study. Neurology. 1997;48:1566-1571
187. Filippi M, Rocca MA, Colombo B et al. Functional magnetic resonance imaging correlates of fatigue in multiple sclerosis. NeuroImage. 2002;15:559-567
188. Bakshi R, Czarnecki D, Shaikh ZA et al. Brain MRI lesions and atrophy are related to depression in multiple sclerosis. Neuroreport. 2000;11:1153-1158
189. Tartaglia MC, Narayanan S, Francis SJ et al. The relationship between diffuse axonal damage and fatigue in multiple sclerosis. Arch Neurol. 2004;61:201-207
190. Rovaris M, Comi G, Filippi M. MRI markers of destructive pathology in multiple sclerosis-related cognitive dysfunction. J Neurol Sci. 2006;245:111-116
191. De Stefano N, Matthews PM, Filippi M et al. Evidence of early cortical atrophy in MS: relevance to white matter changes and disability. Neurology. 2003;60:1157-1162
192. Sastre-Garriga J, Ingle GT, Chard DT et al. Grey and white matter atrophy in early clinical stages of primary progressive multiple sclerosis. NeuroImage. 2004;22:353-359
193. Chen JT, Narayanan S, Collins DL et al. Relating neocortical pathology to disability progression in multiple sclerosis using MRI. NeuroImage. 2004;23:1168-1175
194. Tedeschi G, Lavorgna L, Russo P et al. Brain atrophy and lesion load in a large population of patients with multiple sclerosis. Neurology. 2005;65:280-285

195. Sanfilipo MP, Benedict RH, Sharma J et al. The relationship between whole brain volume and disability in multiple sclerosis: a comparison of normalized gray vs. white matter with misclassification correction. NeuroImage. 2005;26:1068-1077

196. Pagani E, Rocca MA, Gallo A et al. Regional brain atrophy evolves differently in patients with multiple sclerosis according to clinical phenotype. AJNR Am J Neuroradiol. 2005;26:341-346

197. Davies GR, Altmann DR, Rashid W et al. Emergence of thalamic magnetization transfer ratio abnormality in early relapsing-remitting multiple sclerosis. Multiple Sclerosis. 2005;11:276-281

198. Oreja-Guevara C, Charil A, Caputo D et al. Magnetization transfer magnetic resonance imaging and clinical changes in patients with relapsing-remitting multiple sclerosis. Arch Neurol. 2006;63:736-740

199. Rovaris M, Judica E, Gallo A et al. Grey matter damage predicts the evolution of primary progressive multiple sclerosis at 5 years. Brain. 2006;129:2628-2634

200. Altman J, Bayer SA. Chapter 1 - an overview of spinal cord organisation. Development of the human spinal cord: An interpretation based on experimental studies in animals. New York: Oxford, 2001:1-87

201. Rexed B. The cytoarchitectonic organization of the spinal cord in the cat. J Comp Neurol. 1952;96:415-419

202. Larsen JO, Voneuler M, Janson AM. Virtual test systems for estimation of orientation-dependent parameters in thick, arbitarily orientated sections exemplified by length quantification of regenerating axons in spinal cord lesions using isotropic, virtual planes. In: Evans SM, Janson AM, Nyengaard JR, eds. Quantitative methods in neuroscience - a neuroanatomical approach. Oxford: Oxford University Press, 2004:265-284

203. Evangelou N, DeLuca GC, Owens T, Esiri MM. Pathological study of spinal cord atrophy in multiple sclerosis suggests limited role of local lesions. Brain. 2005;128:29-34

204. Raine CS. The neuropathology of multiple sclerosis. In: Raine CS, McFarland HF, Tourtellotte WM, eds. Multiple Sclerosis. London: Chapman & Hall Medical, 1997:151-172

205. Kidd D, Thorpe JW, Thompson AJ et al. Spinal cord MRI using multi-array coils and fast spin echo. II. Findings in multiple sclerosis. Neurology. 1993;43:2632-2637

206. Thorpe JW, Kidd D, Moseley IF et al. Serial gadolinium-enhanced MRI of the brain and spinal cord in early relapsing-remitting multiple sclerosis. Neurology. 1996;46:373-378
207. Miller D. Imaging in multiple sclerosis. In: Raine CS, McFarland HF, Tourtellotte WM, eds. Multiple Sclerosis. London: Chapman & Hall Medical, 1997:31-42
208. Swingler RJ, Compston DA. The morbidity of multiple sclerosis. The Quarterly journal of medicine. 1992;83:325-337
209. McDonald I, Compston A. The symptoms and signs of Multiple Sclerosis. In: Compston A, McDonald I, Noseworthy J et al., eds. McAlpine's Multiple Sclerosis. 4th ed. London: Churchill Livingstone, 2005:287- 346
210. Bjartmar C, Kidd G, Mork S et al. Neurological disability correlates with spinal cord axonal loss and reduced N-acetyl aspartate in chronic multiple sclerosis patients. Ann Neurol. 2000;48:893-901
211. Filippi M, Campi A, Colombo B et al. A spinal cord MRI study of benign and secondary progressive multiple sclerosis. J Neurol. 1996;243:502-505
212. Losseff NA, Webb SL, O'Riordan JI et al. Spinal cord atrophy and disability in multiple sclerosis. A new reproducible and sensitive MRI method with potential to monitor disease progression. Brain. 1996;119 (Pt 3):701-708
213. Vaithianathar L, Tench CR, Morgan PS, Constantinescu CS. Magnetic resonance imaging of the cervical spinal cord in multiple sclerosis--a quantitative T1 relaxation time mapping approach. J Neurol. 2003;250:307-315
214. Lin X, Blumhardt LD, Constantinescu CS. The relationship of brain and cervical cord volume to disability in clinical subtypes of multiple sclerosis: a three-dimensional MRI study. Acta Neurol Scand. 2003;108:401-406
215. Kidd D, Thorpe JW, Kendall BE et al. MRI dynamics of brain and spinal cord in progressive multiple sclerosis. J Neurol Neurosurg Psychiatry. 1996;60:15-19
216. Stevenson VL, Leary SM, Losseff NA et al. Spinal cord atrophy and disability in MS: a longitudinal study. Neurology. 1998;51:234-238
217. Stevenson VL, Miller DH, Leary SM et al. One year follow up study of primary and transitional progressive multiple sclerosis. J Neurol Neurosurg Psychiatry. 2000;68:713-718
218. Rashid W, Davies GR, Chard DT et al. Increasing cord atrophy in early relapsing-remitting multiple sclerosis: a 3 year study. J Neurol Neurosurg Psychiatry. 2006;77:51-55

219. Dow RS, Berglund G. Vascular pattern of lesions of multiple sclerosis. Arc Neurol Psychiat. 1942;47:1-18
220. Dawson JW. The histology of disseminated sclerosis. Trans R Soc Edinb. 1916;50:517–740
221. Fog T. The topography of plaques in multiple sclerosis with special reference to cerebral plaques. Acta Neurol Scand Suppl. 1965;15:1-161
222. Kidd D, Barkhof F, McConnell R et al. Cortical lesions in multiple sclerosis. Brain. 1999;122 (Pt 1):17-26
223. Tan IL, van Schijndel RA, Pouwels PJ et al. MR venography of multiple sclerosis. AJNR Am J Neuroradiol. 2000;21:1039-1042
224. Adams CW, Abdulla YH, Torres EM, Poston RN. Periventricular lesions in multiple sclerosis: their perivenous origin and relationship to granular ependymitis. Neuropathol Appl Neurobiol. 1987;13:141-152
225. Prineas JW, McDonald I. Demyelinating diseases. In: Graham DI, Lantos PL, eds. Greenfield's Neuropathology. 6th ed. London: Edward Arnold, 1997:813-896
226. Esiri MM, Gay D. Immunological and neuropathological significance of the Virchow-Robin space. J Neurol Sci. 1990;100:3-8
227. Barnard RO, Scott T. Patterns of proliferation in cerebral lymphoreticular tumours. Acta Neuropathol Suppl (Berl). 1975;Suppl 6:125-130
228. Horton JC, Hocking DR. Myelin patterns in V1 and V2 of normal and monocularly enucleated monkeys. Cereb Cortex. 1997;7:166-177
229. Clasen RA, Simon GR, Ayer JP et al. A chemical basis for the staining of myelin sheaths by luxol dye techniques; further observations. J Neuropathol Exp Neurol. 1967;26:153-154
230. Clark SL, Ward JW. A variation of the Pal-Weigert method for staining myelin sheaths. Stain Technol. 1934;43:13-16
231. Weil A. A rapid method for staining myelin sheaths. Arch Neurol Psychiatry. 1928;20:392-393
232. Hutchins B, Weber JT. A rapid myelin stain for frozen sections: modification of the Heidenhain procedure. Journal of neuroscience methods. 1983;7:289-294
233. Klüver H, Barrera E. A method for the combined staining of cells and fibers in the nervous system. J Neuropathol Exp Neurol. 1953;12:400-403
234. Wolman M. The mechanism of the Marchi type of methods for visualizing degenerating myelin. Model experiments with pure compounds. Vol. 4, 1956:195-199

235. Lillie RD, Ashburn LL. Supersaturated solutions of fat stains in dilute isopropanol for demonstration of acute fatty degeneration not shown by Herxheimer's technique. Archs.Path. . 1943;36:432

236. Herndon RM. Mechanisms of Repair, Adaptation, and Recovery of Function in Multiple Sclerosis. In: Herndon RM, ed. Multiple Sclerosis: Immunology, Pathology, and Pathophysiology. New York: Demos, 2003

237. Itoyama Y, Sternberger NH, Kies MW et al. Immunocytochemical method to identify myelin basic protein in oligodendroglia and myelin sheaths of the human nervous system. Ann Neurol. 1980;7:157-166

238. Itoyama Y, Sternberger NH, Webster HD et al. Immunocytochemical observations on the distribution of myelin-associated glycoprotein and myelin basic protein in multiple sclerosis lesions. Ann Neurol. 1980;7:167-177

239. Pomeroy IM, Matthews PM, Frank JA et al. Demyelinated neocortical lesions in marmoset autoimmune encephalomyelitis mimic those in multiple sclerosis. Brain. 2005;128:2713-2721

240. Merkler D, Ernsting T, Kerschensteiner M et al. A new focal EAE model of cortical demyelination: multiple sclerosis-like lesions with rapid resolution of inflammation and extensive remyelination. Brain. 2006

241. Huitinga I, Erkut ZA, van Beurden D, Swaab DF. Impaired hypothalamus-pituitary-adrenal axis activity and more severe multiple sclerosis with hypothalamic lesions. Ann Neurol. 2004;55:37-45

242. Kutzelnigg A, Faber-Rod JC, Bauer J et al. Widespread Demyelination in the Cerebellar Cortex in Multiple Sclerosis. Vol. 17, 2007:38-44

243. Ikuta F, Zimmerman HM. Distribution of plaques in seventy autopsy cases of multiple sclerosis in the United States. Neurology. 1976;26:26-28

244. McNally KJ, Peters A. A new method for intense staining of myelin. J Histochem Cytochem. 1998;46:541-545

245. Bo L, Brink BP, Breij EC et al. Homogenous MS lesion pathology in unselected autopsy material. Multiple Sclerosis. 2005;11:S42

246. Wekerle H. Immunology of multiple sclerosis. In: Compston A, Ebers G, McDonald I et al., eds. McAlpines Multiple Sclerosis. 3rd ed. London: Churchill Livingstone, 1998:379-407

247. Olsson T, Zhi WW, Hojeberg B et al. Autoreactive T lymphocytes in multiple sclerosis determined by antigen-induced secretion of interferon-gamma. J Clin Invest. 1990;86:981-985
248. Sun JB, Olsson T, Wang WZ et al. Autoreactive T and B cells responding to myelin proteolipid protein in multiple sclerosis and controls. Eur J Immunol. 1991;21:1461-1468
249. Sun J, Link H, Olsson T et al. T and B cell responses to myelin-oligodendrocyte glycoprotein in multiple sclerosis. J Immunol. 1991;146:1490-1495
250. Zhang J, Markovic-Plese S, Lacet B et al. Increased frequency of interleukin 2-responsive T cells specific for myelin basic protein and proteolipid protein in peripheral blood and cerebrospinal fluid of patients with multiple sclerosis. J Exp Med. 1994;179:973-984
251. Xiao BG, Linington C, Link H. Antibodies to myelin-oligodendrocyte glycoprotein in cerebrospinal fluid from patients with multiple sclerosis and controls. J Neuroimmunol. 1991;31:91-96
252. Sellebjerg FT, Frederiksen JL, Olsson T. Anti-myelin basic protein and anti-proteolipid protein antibody-secreting cells in the cerebrospinal fluid of patients with acute optic neuritis. Arch Neurol. 1994;51:1032-1036
253. Olsson T, Baig S, Hojeberg B, Link H. Antimyelin basic protein and antimyelin antibody-producing cells in multiple sclerosis. Ann Neurol. 1990;27:132-136
254. Link H, Baig S, Olsson O et al. Persistent anti-myelin basic protein IgG antibody response in multiple sclerosis cerebrospinal fluid. J Neuroimmunol. 1990;28:237-248
255. Baig S, Olsson T, Yu-Ping J et al. Multiple sclerosis: cells secreting antibodies against myelin-associated glycoprotein are present in cerebrospinal fluid. Scand J Immunol. 1991;33:73-79
256. Genain CP, Cannella B, Hauser SL, Raine CS. Identification of autoantibodies associated with myelin damage in multiple sclerosis. Nat Med. 1999;5:170-175
257. Vass K, Heininger K, Schafer B et al. Interferon-gamma potentiates antibody-mediated demyelination in vivo. Ann Neurol. 1992;32:198-206
258. Hirsch RL, Panitch HS, Johnson KP. Lymphocytes from multiple sclerosis patients produce elevated levels of gamma interferon in vitro. J Clin Immunol. 1985;5:386-389
259. Sharief MK, Hentges R. Association between tumor necrosis factor-alpha and disease progression in patients with multiple sclerosis. N Engl J Med. 1991;325:467-472

260. D'Souza S, Alinauskas K, McCrea E et al. Differential susceptibility of human CNS-derived cell populations to TNF-dependent and independent immune-mediated injury. J Neurosci. 1995;15:7293-7300

261. Magliozzi R, Columba-Cabezas S, Serafini B, Aloisi F. Intracerebral expression of CXCL13 and BAFF is accompanied by formation of lymphoid follicle-like structures in the meninges of mice with relapsing experimental autoimmune encephalomyelitis. J Neuroimmunol. 2004;148:11-23

262. Corcione A, Casazza S, Ferretti E et al. Recapitulation of B cell differentiation in the central nervous system of patients with multiple sclerosis. Proc Natl Acad Sci U S A. 2004;101:11064-11069

263. Voogd J, Feirabend HKP, Schoen JHR. Cerebellum and Precerebellar Nuclei. In: Paxinos G, Mai JK, eds. The Human Nervous System. London: Elsevier Academic Press, 2004:321-388

264. Schnell L, Fearn S, Klassen H et al. Acute inflammatory responses to mechanical lesions in the CNS: differences between brain and spinal cord. Eur J Neurosci. 1999;11:3648-3658

265. Schnell L, Fearn S, Schwab ME et al. Cytokine-induced acute inflammation in the brain and spinal cord. J Neuropathol Exp Neurol. 1999;58:245-254

266. Raine CS. The lesion in multiple sclerosis and chronic relapsing experimental allergic encephalomyelitis: a structural comparison. In: Raine CS, McFarland HF, Tourtellotte WM, eds. Multiple Sclerosis. London: Chapman & Hall Medical, 1997:243-286

267. Yasui K, Hashizume Y, Yoshida M et al. Age-related morphologic changes of the central canal of the human spinal cord. Acta Neuropathol (Berl). 1999;97:253-259

268. Lassmann H, Kitz K, Wisniewksi HM. The development of periventricular lesions in chronic relapsing experimental allergic encephalomyelitis in guinea-pigs: a light and scanning electron microscopic study. Neuropathol Appl Neurobiol. 1981;7:1-11

269. Cserr HF, Harling-Berg CJ, Knopf PM. Drainage of brain extracellular fluid into blood and deep cervical lymph and its immunological significance. Brain Pathol. 1992;2:269-276

270. Abbott NJ. Evidence for bulk flow of brain interstitial fluid: significance for physiology and pathology. Neurochem Int. 2004;45:545-552

271. Kutzelnigg A, Lassmann H. Cortical lesions and brain atrophy in MS. J Neurol Sci. 2005;233:55-59

272. Waxman SG. Cerebellar dysfunction in multiple sclerosis: evidence for an acquired channelopathy. Prog Brain Res. 2005;148:353-365

273. Lowe J, Cox G. Neuropathological techniques. In: Bancroft JD, Stevens A, eds. Theory and Practice of Histological Techniques. 3rd ed. Edinburgh: Churchill Livingstone, 1990:pages 348, 349 and 356

274. Schoenen J, Faull RLM. Spinal Cord: Cyto- and Chemoarchitecture. In: Paxinos G, Mai JK, eds. The Human Nervous System. 2nd ed. London: Elsevier Academic Press, 2004:190-232

275. Kameyama T, Hashizume Y, Sobue G. Morphologic features of the normal human cadaveric spinal cord. Spine. 1996;21:1285-1290

276. Magnuson DS, Trinder TC, Zhang YP et al. Comparing deficits following excitotoxic and contusion injuries in the thoracic and lumbar spinal cord of the adult rat. Experimental neurology. 1999;156:191-204

277. Yezierski RP, Liu S, Ruenes GL et al. Excitotoxic spinal cord injury: behavioral and morphological characteristics of a central pain model. Pain. 1998;75:141-155

278. Pistorio AL, Hendry SH, Wang X. A modified technique for high-resolution staining of myelin. Journal of neuroscience methods. 2005

279. Li DK, Zhao GJ, Paty DW. Randomized controlled trial of interferon-beta-1a in secondary progressive MS: MRI results. Neurology. 2001;56:1505-1513

280. Wynn DR, Rodriguez M, O'Fallon WM, Kurland LT. A reappraisal of the epidemiology of multiple sclerosis in Olmsted County, Minnesota. Neurology. 1990;40:780-786

281. Weinshenker BG, Rice GP, Noseworthy JH et al. The natural history of multiple sclerosis: a geographically based study. 3. Multivariate analysis of predictive factors and models of outcome. Brain. 1991;114 (Pt 2):1045-1056

282. Bronnum-Hansen H, Koch-Henriksen N, Hyllested K. Survival of patients with multiple sclerosis in Denmark: a nationwide, long-term epidemiologic survey. Neurology. 1994;44:1901-1907

283. Thompson AJ, Kermode AG, Wicks D et al. Major differences in the dynamics of primary and secondary progressive multiple sclerosis. Ann Neurol. 1991;29:53-62

284. Nijeholt GJ, van Walderveen MA, Castelijns JA et al. Brain and spinal cord abnormalities in multiple sclerosis. Correlation between MRI parameters, clinical subtypes and symptoms. Brain. 1998;121 (Pt 4):687-697

285. Stevenson VL, Miller DH, Rovaris M et al. Primary and transitional progressive MS: a clinical and MRI cross-sectional study. Neurology. 1999;52:839-845

286. van Walderveen MA, Lycklama ANGJ, Ader HJ et al. Hypointense lesions on T1-weighted spin-echo magnetic resonance imaging: relation to clinical characteristics in subgroups of patients with multiple sclerosis. Arch Neurol. 2001;58:76-81

287. Rovaris M, Bozzali M, Santuccio G et al. In vivo assessment of the brain and cervical cord pathology of patients with primary progressive multiple sclerosis. Brain. 2001;124:2540-2549

288. Lycklama a Nijeholt GJ, Barkhof F, Scheltens P et al. MR of the spinal cord in multiple sclerosis: relation to clinical subtype and disability. AJNR Am J Neuroradiol. 1997;18:1041-1048

289. Nijeholt GJ, Bergers E, Kamphorst W et al. Post-mortem high-resolution MRI of the spinal cord in multiple sclerosis: a correlative study with conventional MRI, histopathology and clinical phenotype. Brain. 2001;124:154-166

290. Chard DT, Brex PA, Ciccarelli O et al. The longitudinal relation between brain lesion load and atrophy in multiple sclerosis: a 14 year follow up study. J Neurol Neurosurg Psychiatry. 2003;74:1551-1554

291. Prineas JW, Barnard RO, Revesz T et al. Multiple sclerosis. Pathology of recurrent lesions. Brain. 1993;116 (Pt 3):681-693

292. Graeber MB, Blakemore WF, Kruetzberg GW. Cellular pathology of the central nervous system. In: Graham DI, Lantos PL, eds. Greenfield's Neuropathology. Vol. 1. 7th ed. London: Arnold, 2002:123-192

293. Pitt D, Nagelmeier IE, Wilson HC, Raine CS. Glutamate uptake by oligodendrocytes: Implications for excitotoxicity in multiple sclerosis. Neurology. 2003;61:1113-1120

294. Berger T, Weerth S, Kojima K et al. Experimental autoimmune encephalomyelitis: the antigen specificity of T lymphocytes determines the topography of lesions in the central and peripheral nervous system. Lab Invest. 1997;76:355-364

295. Kojima K, Berger T, Lassmann H et al. Experimental autoimmune panencephalitis and uveoretinitis transferred to the Lewis rat by T lymphocytes specific for the S100 beta molecule, a calcium binding protein of astroglia. J Exp Med. 1994;180:817-829

296. Weller RO, Kida S, Zhang ET. Pathways of fluid drainage from the brain--morphological aspects and immunological significance in rat and man. Brain Pathol. 1992;2:277-284

297. Reulen HJ, Graham R, Spatz M, Klatzo I. Role of pressure gradients and bulk flow in dynamics of vasogenic brain edema. Journal of neurosurgery. 1977;46:24-35

298. International Multiple Sclerosis Genetics Consortium - Hafler DA, Compston A, Sawcer S et al. Risk alleles for multiple sclerosis identified by a genomewide study. N Engl J Med. 2007 Aug 30;357(9):851-62.

299. Foote AK, Blakemore WF. Inflammation stimulates remyelination in areas of chronic demyelination. Brain. 2005;128:528-539

300. Bieber AJ, Kerr S, Rodriguez M. Efficient central nervous system remyelination requires T cells. Ann Neurol. 2003;53:680-684

301. Kotter MR, Setzu A, Sim FJ et al. Macrophage depletion impairs oligodendrocyte remyelination following lysolecithin-induced demyelination. Glia. 2001;35:204-212

302. Weerth SH, Rus H, Shin ML, Raine CS. Complement C5 in experimental autoimmune encephalomyelitis (EAE) facilitates remyelination and prevents gliosis. Am J Pathol. 2003;163:1069-1080

303. Bermel RA, Bakshi R. The measurement and clinical relevance of brain atrophy in multiple sclerosis. Lancet neurology. 2006;5:158-170

304. Carone DA, Benedict RH, Dwyer MG et al. Semi-automatic brain region extraction (SABRE) reveals superior cortical and deep gray matter atrophy in MS. NeuroImage. 2006;29:505-514

305. Horsfield MA, Rovaris M, Rocca MA et al. Whole-brain atrophy in multiple sclerosis measured by two segmentation processes from various MRI sequences. J Neurol Sci. 2003;216:169-177

306. Sanfilipo MP, Benedict RH, Zivadinov R, Bakshi R. Correction for intracranial volume in analysis of whole brain atrophy in multiple sclerosis: the proportion vs. residual method. NeuroImage. 2004;22:1732-1743

307. Zivadinov R, Grop A, Sharma J et al. Reproducibility and accuracy of quantitative magnetic resonance imaging techniques of whole-brain atrophy measurement in multiple sclerosis. J Neuroimaging. 2005;15:27-36

308. Zivadinov R, Locatelli L, Stival B et al. Normalized regional brain atrophy measurements in multiple sclerosis. Neuroradiology. 2003;45:793-798

309. Traboulsee A, Dehmeshki J, Brex PA et al. Normal-appearing brain tissue MTR histograms in clinically isolated syndromes suggestive of MS. Neurology. 2002;59:126-128

310. Chard DT, Griffin CM, Parker GJ et al. Brain atrophy in clinically early relapsing-remitting multiple sclerosis. Brain. 2002;125:327-337

311. Carone DA, Benedict RH, Dwyer MG et al. Semi-automatic brain region extraction (SABRE) reveals superior cortical and deep gray matter atrophy in MS. NeuroImage. 2005

312. Quarantelli M, Ciarmiello A, Morra VB et al. Brain tissue volume changes in relapsing-remitting multiple sclerosis: correlation with lesion load. NeuroImage. 2003;18:360-366

313. Prinster A, Quarantelli M, Orefice G et al. Grey matter loss in relapsing-remitting multiple sclerosis: A voxel-based morphometry study. NeuroImage. 2005

314. Sailer M, Fischl B, Salat D et al. Focal thinning of the cerebral cortex in multiple sclerosis. Brain. 2003;126:1734-1744

315. Bermel RA, Innus MD, Tjoa CW, Bakshi R. Selective caudate atrophy in multiple sclerosis: a 3D MRI parcellation study. Neuroreport. 2003;14:335-339

316. Sepulcre J, Sastre-Garriga J, Cercignani M et al. Regional gray matter atrophy in early primary progressive multiple sclerosis: a voxel-based morphometry study. Arch Neurol. 2006;63:1175-1180

317. Evangelou N, Konz D, Esiri MM et al. Size-selective neuronal changes in the anterior optic pathways suggest a differential susceptibility to injury in multiple sclerosis. Brain. 2001;124:1813-1820

318. Miller DH, Barkhof F, Frank JA et al. Measurement of atrophy in multiple sclerosis: pathological basis, methodological aspects and clinical relevance. Brain. 2002;125:1676-1695

319. Wegner C, Matthews PM. A new view of the cortex, new insights into multiple sclerosis. Brain. 2003;126:1719-1721

320. Inglese M, Liu S, Babb JS et al. Three-dimensional proton spectroscopy of deep gray matter nuclei in relapsing-remitting MS. Neurology. 2004;63:170-172

321. Charil A, Dagher A, Lerch JP et al. Focal cortical atrophy in multiple sclerosis: relation to lesion load and disability. NeuroImage. 2007;34:509-517

322. Chard DT, Griffin CM, Rashid W et al. Progressive grey matter atrophy in clinically early relapsing-remitting multiple sclerosis. Multiple sclerosis. 2004;10:387-391

323. Brex PA, Leary SM, O'Riordan JI et al. Measurement of spinal cord area in clinically isolated syndromes suggestive of multiple sclerosis. J Neurol Neurosurg Psychiatry. 2001;70:544-547

324. Highley JR, Esiri MM, McDonald B et al. The size and fibre composition of the corpus callosum with respect to gender and schizophrenia: a post-mortem study. Brain. 1999;122 (Pt 1):99-110

325. Pereira-Maxwell F. A-Z of Medical Statistics. London: Arnold, 1998:p70
326. Bland M. Clinical measurement. An introduction to medical statistics. 3rd ed. Oxford: Oxford University Press, 2000:268-293
327. Griffin JW, George R, Lobato C et al. Macrophage responses and myelin clearance during Wallerian degeneration: relevance to immune-mediated demyelination. J Neuroimmunol. 1992;40:153-165
328. Revesz T, Kidd D, Thompson AJ et al. A comparison of the pathology of primary and secondary progressive multiple sclerosis. Brain. 1994;117 (Pt 4):759-765
329. Rosas HD, Liu AK, Hersch S et al. Regional and progressive thinning of the cortical ribbon in Huntington's disease. Neurology. 2002;58:695-701
330. Dewulf A. Anatomy of the normal human thalamus. Topometry and standardized nomenclature. . Amsterdam: Elsevier, 1971
331. De Stefano N. Imaging Cerebral Grey Matter Volume in Multiple Sclerosis. In: Filippi M, Comi G, Rovaris M, eds. Normal-appearing White and Grey Matter Damage in Multiple Sclerosis. Milan: Springer, 2004:111-120
332. Adalsteinsson E, Langer-Gould A, Homer RJ et al. Gray matter N-acetyl aspartate deficits in secondary progressive but not relapsing-remitting multiple sclerosis. AJNR Am J Neuroradiol. 2003;24:1941-1945
333. Caramanos Z, Narayanan S, Arnold DL. 1H-MRS quantification of tNA and tCr in patients with multiple sclerosis: a meta-analytic review. Brain. 2005;128:2483-2506
334. Bjugn R, Nyengaard JR, Rosland JH. Spinal Cord Transection-No Loss of Distal Ventral Horn Neurons. Experimental neurology. 1997;148:179-186
335. Kameyama T, Hashizume Y, Ando T, Takahashi A. Morphometry of the normal cadaveric cervical spinal cord. Spine. 1994;19:2077-2081
336. Iwadare T, Mori H, Ishiguro K, Takeishi M. Dimensional changes of tissues in the course of processing. Journal of microscopy. 1984;136 (Pt 3):323-327
337. Pakkenberg B, Moller A, Gundersen HJ et al. The absolute number of nerve cells in substantia nigra in normal subjects and in patients with Parkinson's disease estimated with an unbiased stereological method. J Neurol Neurosurg Psychiatry. 1991;54:30-33
338. Nyengaard JR, Dorph-Petersen K, Tang Y. Number in electron microscopy: estimation of total number of synapses in the main regions of human neocortex. In: Evans SM, Janson AM, Nyengaard JR, eds. Quantitative methods in neuroscience - a neuroanatomical approach. Oxford: Oxford University Press, 2004:146-166

339. Guillery RW, August BK. Doubt and certainty in counting. Prog Brain Res. 2002;135:25-42

340. Rashid W, Davies GR, Chard DT et al. Upper cervical cord area in early relapsing-remitting multiple sclerosis: cross-sectional study of factors influencing cord size. J Magn Reson Imaging. 2006;23:473-476

341. Bieniek M, Altmann DR, Davies GR et al. Cord atrophy separates early primary progressive and relapsing remitting multiple sclerosis. J Neurol Neurosurg Psychiatry. 2006;77:1036-1039

342. Davison C, Goodhart S, Lander J. Multiple Sclerosis and Amyotrophies. Archives of Neurology and Psychiatry. 1934;31:270-289

343. Friedman AP, Davison C. Multiple Sclerosis with late onset of symptoms. Archives of Neurology and Psychiatry. 1945;54:348-360

344. Bannerman PG, Hahn A, Ramirez S et al. Motor neuron pathology in experimental autoimmune encephalomyelitis: studies in THY1-YFP transgenic mice. Brain. 2005;128:1877-1886

345. Giardino L, Giuliani A, Fernandez M, Calza L. Spinal motoneurone distress during experimental allergic encephalomyelitis. Neuropathol Appl Neurobiol. 2004;30:522-531

346. Byravan S, Foster LM, Phan T et al. Murine oligodendroglial cells express nerve growth factor. Proc Natl Acad Sci U S A. 1994;91:8812-8816

347. Kettenmann H, Sonnhof U, Schachner M. Exclusive potassium dependence of the membrane potential in cultured mouse oligodendrocytes. J Neurosci. 1983;3:500-505

348. Dai X, Lercher LD, Clinton PM et al. The trophic role of oligodendrocytes in the basal forebrain. J Neurosci. 2003;23:5846-5853

349. Du Y, Dreyfus CF. Oligodendrocytes as providers of growth factors. J Neurosci Res. 2002;68:647-654

350. Bien CG, Bauer J, Deckwerth TL et al. Destruction of neurons by cytotoxic T cells: a new pathogenic mechanism in Rasmussen's encephalitis. Ann Neurol. 2002;51:311-318

351. Dalmau J, Gultekin HS, Posner JB. Paraneoplastic neurologic syndromes: pathogenesis and physiopathology. Brain Pathol. 1999;9:275-284

352. Neumann H, Cavalie A, Jenne DE, Wekerle H. Induction of MHC class I genes in neurons. Science. 1995;269:549-552

353. Neumann H, Schmidt H, Cavalie A et al. Major histocompatibility complex (MHC) class I gene expression in single neurons of the central nervous system: differential

regulation by interferon (IFN)-gamma and tumor necrosis factor (TNF)-alpha. J Exp Med. 1997;185:305-316

354. Medana IM, Gallimore A, Oxenius A et al. MHC class I-restricted killing of neurons by virus-specific CD8+ T lymphocytes is effected through the Fas/FasL, but not the perforin pathway. Eur J Immunol. 2000;30:3623-3633

355. Giuliani F, Goodyer CG, Antel JP, Yong VW. Vulnerability of human neurons to T cell-mediated cytotoxicity. J Immunol. 2003;171:368-379

356. Nitsch R, Pohl EE, Smorodchenko A et al. Direct impact of T cells on neurons revealed by two-photon microscopy in living brain tissue. J Neurosci. 2004;24:2458-2464

357. Smith T, Groom A, Zhu B, Turski L. Autoimmune encephalomyelitis ameliorated by AMPA antagonists. Nat Med. 2000;6:62-66

358. Levin MC, Lee SM, Kalume F et al. Autoimmunity due to molecular mimicry as a cause of neurological disease. Nat Med. 2002;8:509-513

359. Gelbard HA, Dzenko KA, DiLoreto D et al. Neurotoxic effects of tumor necrosis factor alpha in primary human neuronal cultures are mediated by activation of the glutamate AMPA receptor subtype: implications for AIDS neuropathogenesis. Dev Neurosci. 1993;15:417-422

360. Downen M, Amaral TD, Hua LL et al. Neuronal death in cytokine-activated primary human brain cell culture: role of tumor necrosis factor-alpha. Glia. 1999;28:114-127

361. Sui Y, Potula R, Dhillon N et al. Neuronal apoptosis is mediated by CXCL10 overexpression in simian human immunodeficiency virus encephalitis. Am J Pathol. 2004;164:1557-1566

362. Sui Y, Stehno-Bittel L, Li S et al. CXCL10-induced cell death in neurons: role of calcium dysregulation. Eur J Neurosci. 2006;23:957-964

363. Simpson JE, Newcombe J, Cuzner ML, Woodroofe MN. Expression of the interferon-gamma-inducible chemokines IP-10 and Mig and their receptor, CXCR3, in multiple sclerosis lesions. Neuropathol Appl Neurobiol. 2000;26:133-142

364. Aktas O, Smorodchenko A, Brocke S et al. Neuronal damage in autoimmune neuroinflammation mediated by the death ligand TRAIL. Neuron. 2005;46:421-432

365. Krantic S, Mechawar N, Reix S, Quirion R. Molecular basis of programmed cell death involved in neurodegeneration. Trends Neurosci. 2005;28:670-676

366. Diestel A, Aktas O, Hackel D et al. Activation of microglial poly(ADP-ribose)-polymerase-1 by cholesterol breakdown products during neuroinflammation: a link between demyelination and neuronal damage. J Exp Med. 2003;198:1729-1740

367. Chang JY, Liu LZ. Neurotoxicity of cholesterol oxides on cultured cerebellar granule cells. Neurochem Int. 1998;32:317-323

368. Chang JY, Phelan KD, Chavis JA. Neurotoxicity of 25-OH-cholesterol on sympathetic neurons. Brain Res Bull. 1998;45:615-622

369. Chang JY, Phelan KD, Liu LZ. Neurotoxicity of 25-OH-cholesterol on NGF-differentiated PC12 cells. Neurochem Res. 1998;23:7-16

370. Tjoa CW, Benedict RH, Weinstock-Guttman B et al. MRI T2 hypointensity of the dentate nucleus is related to ambulatory impairment in multiple sclerosis. J Neurol Sci. 2005;234:17-24

371. Brass SD, Benedict RH, Weinstock-Guttman B et al. Cognitive impairment is associated with subcortical magnetic resonance imaging grey matter T2 hypointensity in multiple sclerosis. Multiple sclerosis. 2006;12:437-444

372. Cid C, Alvarez-Cermeno JC, Regidor I et al. Low concentrations of glutamate induce apoptosis in cultured neurons: implications for amyotrophic lateral sclerosis. J Neurol Sci. 2003;206:91-95

373. Groom AJ, Smith T, Turski L. Multiple sclerosis and glutamate. Ann N Y Acad Sci. 2003;993:229-275

374. Cuzner ML, Gveric D, Strand C et al. The expression of tissue-type plasminogen activator, matrix metalloproteases and endogenous inhibitors in the central nervous system in multiple sclerosis: comparison of stages in lesion evolution. J Neuropathol Exp Neurol. 1996;55:1194-1204

375. Leppert D, Ford J, Stabler G et al. Matrix metalloproteinase-9 (gelatinase B) is selectively elevated in CSF during relapses and stable phases of multiple sclerosis. Brain. 1998;121 (Pt 12):2327-2334

376. Maeda A, Sobel RA. Matrix metalloproteinases in the normal human central nervous system, microglial nodules, and multiple sclerosis lesions. J Neuropathol Exp Neurol. 1996;55:300-309

377. Cossins JA, Clements JM, Ford J et al. Enhanced expression of MMP-7 and MMP-9 in demyelinating multiple sclerosis lesions. Acta Neuropathol (Berl). 1997;94:590-598

378. Siao CJ, Tsirka SE. Extracellular proteases and neuronal cell death. Cell Mol Biol (Noisy-le-grand). 2002;48:151-161

379. Manabe S, Gu Z, Lipton SA. Activation of matrix metalloproteinase-9 via neuronal nitric oxide synthase contributes to NMDA-induced retinal ganglion cell death. Invest Ophthalmol Vis Sci. 2005;46:4747-4753

380. Alcazar A, Regidor I, Masjuan J et al. Induction of apoptosis by cerebrospinal fluid from patients with primary-progressive multiple sclerosis in cultured neurons. Neurosci Lett. 1998;255:75-78

381. Cid C, Alcazar A, Regidor I et al. Neuronal apoptosis induced by cerebrospinal fluid from multiple sclerosis patients correlates with hypointense lesions on T1 magnetic resonance imaging. J Neurol Sci. 2002;193:103-109

382. Cowan WM. Anterograde and retrograde transneuronal degeneration in the central and peripheral nervous system. In: Nauta WJH, Ebbesson SOE, eds. Contemporary research methods in neuroanatomy. Berlin: Springer-Verlag, 1970:217–251

383. Tuszynski MH, Armstrong DM, Gage FH. Basal forebrain cell loss following fimbria/fornix transection. Brain research. 1990;508:241-248

384. Sanner CA, Murray M, Goldberger ME. Removal of dorsal root afferents prevents retrograde death of axotomized Clarke's nucleus neurons in the cat. Experimental neurology. 1993;123:81-90

385. Al-Abdulla NA, Portera-Cailliau C, Martin LJ. Occipital cortex ablation in adult rat causes retrograde neuronal death in the lateral geniculate nucleus that resembles apoptosis. Neuroscience. 1998;86:191-209

386. Meyer R, Weissert R, Diem R et al. Acute neuronal apoptosis in a rat model of multiple sclerosis. J Neurosci. 2001;21:6214-6220

387. Hobom M, Storch MK, Weissert R et al. Mechanisms and time course of neuronal degeneration in experimental autoimmune encephalomyelitis. Brain Pathol. 2004;14:148-157

388. Lindholm D, Castren E, Berzaghi M et al. Activity-dependent and hormonal regulation of neurotrophin mRNA levels in the brain--implications for neuronal plasticity. J Neurobiol. 1994;25:1362-1372

389. Thoenen H. Neurotrophins and neuronal plasticity. Science. 1995;270:593-598

390. Meyer-Franke A, Wilkinson GA, Kruttgen A et al. Depolarization and cAMP elevation rapidly recruit TrkB to the plasma membrane of CNS neurons. Neuron. 1998;21:681-693

391. Shen S, Wiemelt AP, McMorris FA, Barres BA. Retinal ganglion cells lose trophic responsiveness after axotomy. Neuron. 1999;23:285-295

392. Hefti F. Nerve growth factor promotes survival of septal cholinergic neurons after fimbrial transections. J Neurosci. 1986;6:2155-2162

393. Johnson H, Cowey A. Transneuronal retrograde degeneration of retinal ganglion cells following restricted lesions of striate cortex in the monkey. Exp Brain Res. 2000;132:269-275
394. Goldby F. A note on transneuronal atrophy in the human lateral geniculate body. J Neurol Neurosurg Psychiatry. 1957;20:202-207
395. Beatty RM, Sadun AA, Smith L et al. Direct demonstration of transsynaptic degeneration in the human visual system: a comparison of retrograde and anterograde changes. J Neurol Neurosurg Psychiatry. 1982;45:143-146
396. Kupfer C. The distribution of cell size in the lateral geniculate nucleus of man following transneuronal cell atrophy. J Neuropathol Exp Neurol. 1965;24:653-661
397. Ciccarelli O, Toosy AT, Hickman SJ et al. Optic radiation changes after optic neuritis detected by tractography-based group mapping. Hum Brain Mapp. 2005;25:308-316
398. Audoin B, Fernando KT, Swanton JK et al. Selective magnetization transfer ratio decrease in the visual cortex following optic neuritis. Brain. 2006;129:1031-1039
399. Young IJ. Morphological and histochemical studies of partially and totally deafferented spinal cord segments. Experimental neurology. 1966;14:238-248
400. Eidelberg E, Nguyen LH, Polich R, Walden JG. Transsynaptic degeneration of motoneurones caudal to spinal cord lesions. Brain Res Bull. 1989;22:39-45
401. McBride RL, Feringa ER. Ventral horn motoneurons 10, 20 and 52 weeks after T-9 spinal cord transection. Brain Res Bull. 1992;28:57-60
402. Kaelan C, Jacobsen PF, Kakulas BA. An investigation of possible transynaptic neuronal degeneration in human spinal cord injury. J Neurol Sci. 1988;86:231-237
403. Terao S, Li M, Hashizume Y et al. No transneuronal degeneration between human cortical motor neurons and spinal motor neurons. J Neurol. 1999;246:61-62
404. Terao S, Li M, Hashizume Y et al. Upper motor neuron lesions in stroke patients do not induce anterograde transneuronal degeneration in spinal anterior horn cells. Stroke. 1997;28:2553-2556
405. Simmons ML, Frondoza CG, Coyle JT. Immunocytochemical localization of N-acetyl-aspartate with monoclonal antibodies. Neuroscience. 1991;45:37-45
406. De Stefano N, Matthews PM, Arnold DL. Reversible decreases in N-acetylaspartate after acute brain injury. Magn Reson Med. 1995;34:721-727
407. De Stefano N, Narayanan S, Matthews PM et al. In vivo evidence for axonal dysfunction remote from focal cerebral demyelination of the type seen in multiple sclerosis. Brain. 1999;122 (Pt 10):1933-1939

408. Bates TE, Strangward M, Keelan J et al. Inhibition of N-acetylaspartate production: implications for 1H MRS studies in vivo. Neuroreport. 1996;7:1397-1400
409. Bhakoo KK, Pearce D. In vitro expression of N-acetyl aspartate by oligodendrocytes: implications for proton magnetic resonance spectroscopy signal in vivo. J Neurochem. 2000;74:254-262
410. Gonen O, Inglese M, Grossman RI. MR Spectroscopy of the Normal-Appearing Grey Matter. In: Filippi M, Comi G, Rovaris M, eds. Normal-appearing White and Grey Matter Damage in Multiple Sclerosis. Milan: Springer-Verlag, 2004:129-143
411. Guillery RW. On counting and counting errors. J Comp Neurol. 2002;447:1-7
412. Abercromie M. Estimation of nuclear population from microtome sections. Anat Rec. 1946;94:239-247
413. Mullen RJ, Buck CR, Smith AM. NeuN, a neuronal specific nuclear protein in vertebrates. Development. 1992;116:201-211
414. Todd AJ, Spike RC, Polgar E. A quantitative study of neurons which express neurokinin-1 or somatostatin sst2a receptor in rat spinal dorsal horn. Neuroscience. 1998;85:459-473
415. Terao S, Sobue G, Li M et al. The lateral corticospinal tract and spinal ventral horn in X-linked recessive spinal and bulbar muscular atrophy: a quantitative study. Acta Neuropathol (Berl). 1997;93:1-6
416. Terao S, Sobue G, Hashizume Y et al. Age-related changes in human spinal ventral horn cells with special reference to the loss of small neurons in the intermediate zone: a quantitative analysis. Acta Neuropathol (Berl). 1996;92:109-114
417. Sobue G, Terao S, Kachi T et al. Somatic motor efferents in multiple system atrophy with autonomic failure: a clinico-pathological study. J Neurol Sci. 1992;112:113-125
418. Ishizawa K, Komori T, Okayama K et al. Large motor neuron involvement in Stiff-man syndrome: a qualitative and quantitative study. Acta Neuropathol (Berl). 1999;97:63-70
419. Swash M, Leader M, Brown A, Swettenham KW. Focal loss of anterior horn cells in the cervical cord in motor neuron disease. Brain. 1986;109 (Pt 5):939-952
420. Satoh K, Armstrong DM, Fibiger HC. A comparison of the distribution of central cholinergic neurons as demonstrated by acetylcholinesterase pharmacohistochemistry and choline acetyltransferase immunohistochemistry. Brain Res Bull. 1983;11:693-720
421. Tsang YM, Chiong F, Kuznetsov D et al. Motor neurons are rich in non-phosphorylated neurofilaments: cross-species comparison and alterations in ALS. Brain research. 2000;861:45-58

422. Nagata Y, Okuya M, Watanabe R, Honda M. Regional distribution of cholinergic neurons in human spinal cord transections in the patients with and without motor neuron disease. Brain research. 1982;244:223-229
423. Ince P, Stout N, Shaw P et al. Parvalbumin and calbindin D-28k in the human motor system and in motor neuron disease. Neuropathol Appl Neurobiol. 1993;19:291-299
424. Ren K, Ruda MA. A comparative study of the calcium-binding proteins calbindin-D28K, calretinin, calmodulin and parvalbumin in the rat spinal cord. Brain Res Brain Res Rev. 1994;19:163-179
425. Alexianu ME, Ho BK, Mohamed AH et al. The role of calcium-binding proteins in selective motoneuron vulnerability in amyotrophic lateral sclerosis. Ann Neurol. 1994;36:846-858
426. Megias M, Alvarez-Otero R, Pombal MA. Calbindin and calretinin immunoreactivities identify different types of neurons in the adult lamprey spinal cord. J Comp Neurol. 2003;455:72-85
427. Fahandejsaadi A, Leung E, Rahaii R et al. Calbindin-D28K, parvalbumin and calretinin in primate lower motor neurons. Neuroreport. 2004;15:443-448
428. Lim SM, Guiloff RJ, Navarrete R. Interneuronal survival and calbindin-D28k expression following motoneuron degeneration. J Neurol Sci. 2000;180:46-51
429. Oyanagi K, Ikuta F, Horikawa Y. Evidence for sequential degeneration of the neurons in the intermediate zone of the spinal cord in amyotrophic lateral sclerosis: a topographic and quantitative investigation. Acta Neuropathol (Berl). 1989;77:343-349
430. Tomlinson BE, Irving D, Rebeiz JJ. Total numbers of limb motor neurones in the human lumbosacral cord and an analysis of the accuracy of various sampling procedures. J Neurol Sci. 1973;20:313-327
431. Benes FM, Lange N. Reconciling theory and practice in cell counting. Trends Neurosci. 2001;24:378-380
432. West MJ. Stereological methods for estimating the total number of neurons and synapses: issues of precision and bias. Trends Neurosci. 1999;22:51-61
433. Benes FM, Lange N. Two-dimensional versus three-dimensional cell counting: a practical perspective. Trends Neurosci. 2001;24:11-17
434. Saper CB. Any way you cut it: a new journal policy for the use of unbiased counting methods. J Comp Neurol. 1996;364:5
435. West MJ. Reply. Trends Neurosci. 1999;22:346-347
436. West MJ. Reply. Trends Neurosci. 1999;22:345-346

437. Guillery RW, Herrup K. Quantification without pontification: choosing a method for counting objects in sectioned tissues. J Comp Neurol. 1997;386:2-7
438. West MJ, Slomanka L. 2-D versus 3-D cell counting--a debate. What is an optical disector? Trends Neurosci. 2001;24:374; author reply 378-380
439. Clarke PG, Oppenheim RW. Neuron death in vertebrate development: in vitro methods. Methods Cell Biol. 1995;46:277-321
440. Clarke PG. How inaccurate is the Abercrombie correction factor for cell counts? Trends Neurosci. 1992;15:211-212
441. Hedreen JC. Lost caps in histological counting methods. Anat Rec. 1998;250:366-372
442. Pover CM, Coggeshall RE. Verification of the disector method for counting neurons, with comments on the empirical method. Anat Rec. 1991;231:573-578
443. Popken GJ, Farel PB. Sensory neuron number in neonatal and adult rats estimated by means of stereologic and profile-based methods. J Comp Neurol. 1997;386:8-15
444. Hatton WJ, von Bartheld CS. Analysis of cell death in the trochlear nucleus of the chick embryo: calibration of the optical disector counting method reveals systematic bias. J Comp Neurol. 1999;409:169-186
445. von Bartheld CS. Systematic bias in an "unbiased" neuronal counting technique. Anat Rec. 1999;257:119-120
446. Coggeshall RE. Commentary of the paper by Benes and Lange. Trends Neurosci. 2001;24:376-377; author reply 378-380
447. Gundersen HJ, Bagger P, Bendtsen TF et al. The new stereological tools: disector, fractionator, nucleator and point sampled intercepts and their use in pathological research and diagnosis. Apmis. 1988;96:857-881
448. Sterio DC. The unbiased estimation of number and sizes of arbitrary particles using the disector. Journal of microscopy. 1984;134:127-136
449. West MJ. New stereological methods for counting neurons. Neurobiology of aging. 1993;14:275-285
450. Irving D, Rebeiz JJ, Tomlinson BE. The numbers of limb motor neurones in the individual segments of the human lumbosacral spinal cord. J Neurol Sci. 1974;21:203-212
451. Tomlinson BE, Irving D. The numbers of limb motor neurons in the human lumbosacral cord throughout life. J Neurol Sci. 1977;34:213-219
452. Ince PG. Neuropathology. In: Brown RH, Meininger V, Swash M, eds. Amyotrophic lateral sclerosis. London: Martin Dunitz, 2000:83-112

453. Fisher M, Long RR, Drachman DA. Hand muscle atrophy in multiple sclerosis. Arch Neurol. 1983;40:811-815
454. Kurtzke JF, Beebe GW, Nagler B et al. Studies on the natural history of multiple sclerosis. Acta Neurol Scand. 1972;48:19-46
455. Pollock M, Calder C, Allpress S. Peripheral nerve abnormality in multiple sclerosis. Ann Neurol. 1977;2:41-48
456. Petajan JH. Electromyographic findings in multiple sclerosis: remitting signs of denervation. Muscle Nerve. 1982;5:S157-160
457. Shefner JM, Mackin GA, Dawson DM. Lower motor neuron dysfunction in patients with multiple sclerosis. Muscle Nerve. 1992;15:1265-1270
458. Fry FJ, Cowan WM. A study of retrograde cell degeneration in the lateral mammillary nucleus of the cat, with special reference to the role of axonal branching in the preservation of the cell. J Comp Neurol. 1972;144:1-23
459. Lowrie MB, Lawson SJ. Cell death of spinal interneurones. Prog Neurobiol. 2000;61:543-555
460. Schoenen J. Dendritic organization of the human spinal cord: the motoneurons. J Comp Neurol. 1982;211:226-247
461. Zhu B, Luo L, Moore GR et al. Dendritic and synaptic pathology in experimental autoimmune encephalomyelitis. Am J Pathol. 2003;162:1639-1650
462. Moore KA, Kohno T, Karchewski LA et al. Partial peripheral nerve injury promotes a selective loss of GABAergic inhibition in the superficial dorsal horn of the spinal cord. J Neurosci. 2002;22:6724-6731
463. Newcombe J, Hawkins CP, Henderson CL et al. Histopathology of multiple sclerosis lesions detected by magnetic resonance imaging in unfixed postmortem central nervous system tissue. Brain. 1991;114 (Pt 2):1013-1023
464. Geurts JJ, Pouwels PJ, Uitdehaag BM et al. Intracortical lesions in multiple sclerosis: improved detection with 3D double inversion-recovery MR imaging. Radiology. 2005;236:254-260
465. Bagnato F, Butman JA, Gupta S et al. In vivo detection of cortical plaques by MR imaging in patients with multiple sclerosis. AJNR Am J Neuroradiol. 2006;27:2161-2167
466. Merkler D, Boscke R, Schmelting B et al. Differential macrophage/microglia activation in neocortical EAE lesions in the marmoset monkey. Brain Pathol. 2006;16:117-123

467. Neumann H, Misgeld T, Matsumuro K, Wekerle H. Neurotrophins inhibit major histocompatibility class II inducibility of microglia: involvement of the p75 neurotrophin receptor. Proc Natl Acad Sci U S A. 1998;95:5779-5784

468. Kerschensteiner M, Bareyre FM, Buddeberg BS et al. Remodeling of axonal connections contributes to recovery in an animal model of multiple sclerosis. J Exp Med. 2004;200:1027-1038

469. Bakshi R, Ariyaratana S, Benedict RH, Jacobs L. Fluid-attenuated inversion recovery magnetic resonance imaging detects cortical and juxtacortical multiple sclerosis lesions. Arch Neurol. 2001;58:742-748

470. Bot JC, Blezer EL, Kamphorst W et al. The spinal cord in multiple sclerosis: relationship of high-spatial-resolution quantitative MR imaging findings to histopathologic results. Radiology. 2004;233:531-540

471. Geurts JJG, Bo L, Blezer ELA et al. Imaging cortical lesions and NAGM at high and standard field-strength (4.7T and 1.5T): combined post-mortem MRI and histopathology. Multiple Sclerosis. 2005:S8

472. Campbell SJ, Wilcockson DC, Butchart AG et al. Altered chemokine expression in the spinal cord and brain contributes to differential interleukin-1beta-induced neutrophil recruitment. J Neurochem. 2002;83:432-441

473. Carvlin MJ, Asato R, Hackney DB et al. High-resolution MR of the spinal cord in humans and rats. AJNR Am J Neuroradiol. 1989;10:13-17

474. Pattany PM, Puckett WR, Klose KJ et al. High-resolution diffusion-weighted MR of fresh and fixed cat spinal cords: evaluation of diffusion coefficients and anisotropy. AJNR Am J Neuroradiol. 1997;18:1049-1056

475. Bergers E, Bot JC, van der Valk P et al. Diffuse signal abnormalities in the spinal cord in multiple sclerosis: direct postmortem in situ magnetic resonance imaging correlated with in vitro high-resolution magnetic resonance imaging and histopathology. Ann Neurol. 2002;51:652-656

476. Sospedra M, Martin R. Immunology of multiple sclerosis. Annual Reviews of Immunology. 2005;23:683-747.

477. Hickey WF.Basic principles of immunological surveillance of the normal central nervous system. Glia. 2001 Nov;36(2):118-24

478. Pachter JS, de Vries HE, Fabry Z. The blood-brain barrier and its role in immune privilege in the central nervous system. J Neuropathol Exp Neurol. 2003 Jun;62(6):593-604

479. Klawiter EC, Cross AH. B cells: no longer the nondominant arm of multiple sclerosis. Curr Neurology and Neuroscience Reports. 2007 May;7(3):231-8.

480. Tanuma N, Shin T, Matsumoto Y.Characterization of acute versus chronic relapsing autoimmune encephalomyelitis in DA rats. J Neuroimmunol. 2000 Aug 1;108(1-2):171-80

481. Smith K, McDonald I, Miller D et al. The pathophysiology of multiple sclerosis. In: Compston A, Confavreux C, Lassmann H et al., eds. McAlpine's Multiple Sclerosis. 3rd ed. London: Churchill Livingstone, 2005: 601-660